Event-triggered Control of Linear Systems

with Application to Embedded Control Systems

Ereignisbasierte Regelung linearer Systeme

mit Anwendung für eingebettete Regelungssysteme

Vom Fachbereich Elektrotechnik und Informationstechnik
der Technischen Universität Kaiserslautern
zur Verleihung des akademischen Grades
Doktor der Ingenieurwissenschaften (Dr.-Ing.)
genehmigte Dissertation

von

M.-Sc. Wei Wu
geboren in Nanjing, Jiangsu Provinz

D 386

Tag der mündlichen Prüfung:	31.07.2014
Dekan des Fachbereichs:	Prof. Dr.-Ing. Hans D. Schotten
Vorsitzender der Prüfungskommission:	Prof. Dr.-Ing. habil. Norbert Wehn
1. Berichterstatter:	Prof. Dr.-Ing. Steven Liu
2. Berichterstatter:	Prof. Dr.-Ing. habil. Lothar Litz

Contents

Preface

Motivation

Nowadays embedded control systems play a significant role in our society because of the wide application in many areas ranging from transportation (automobiles, trains, aircrafts, etc.) over industrial applications (manufacturing and process control) to infrastructure systems (power systems, building automation, etc) [Gör12]. Currently 98 % of computing devices in the world are embedded systems in all kinds of equipment. Based on conservative estimates by 2020 over 40 billion of embedded devices are worldwide available [Art06]. Economical and efficient utilizations of those embedded devices have a high demand.

Despite of the widely practical applications of embedded control systems theoretical foundations are still incomplete. In a long term control design and real-time scheduling design in control theory and computer science are developed in a decoupled manner. The rising issues about functionality, efficiency, reliability and safety are difficult to be handled in a unified frame with the rapid incremental complexity. The complexity in the progress of modern industrialization is especially aroused from the popularized wired and wireless networked systems, which ineluctably confronts the problems of energy, computation, and communication constraints. Therefore disciplines like mathematics, control theory, computer science and communications must be conjoined to complete the theoretical foundations of embedded control systems.

As pointed in [Cer03], traditionally the real-time scheduling community assumes that all control algorithms can be modeled as periodic tasks with hard deadlines. Control community assumes that the implementation is able to be accomplished by an equidistant sampling and actuation to ensure a fixed input output latency. This simple model has supplied an interface between the two communities so that each of both can focus on its own problems. From the control design standpoint periodic data abstraction is advantageous with the help of the well-developed theory on sampled-data systems [ÅW90]. However for many control systems keeping a constant sampling interval is unnecessary or redundant, for instance when no disturbance is acting on the system and the system is operating desirably yet. To relieve the probable over-provisioning of the communication and actuation from the traditional periodic manner the event-triggered control is a good alternative, in which the control actuation is performed only when some events happen. Furthermore the event-based nature of the sampling can be intrinsic to the measurement method used, or to the physical nature of the process being controlled [Lem10].

For a camera based sensor for instance it could be natural to read the signal when sufficient exposure is obtained [Åst08]. Dynamic resource allocation strategies and resource sharing can be supported by event-triggered architectures. The provision of resources in event-triggered systems can be accomplished by tolerating a certain loss of control performance in favor of more cost-effective solutions.

This thesis devotes to investigate the methods of event-triggered control and its applications in embedded control systems. From the control perspective the stability of controlled system is very often one of the main focuses. In safety-critical real-time control applications, such as X-by-wire systems in the automotive or avionic domain, the system's inability to fulfill its specified functions can result in catastrophical consequences [Obe05]. Therefore, the stability issue must be the baseline included in the considerations of controller design. Meanwhile, in order to serve different control objectives, the controller must be specifically designed to have a synthesis with the event-triggering condition. Concerning multiple embedded control systems with severely limited computation and communication, efficient and implementation-aware scheduling, i.e. the temporal assignment of resource to tasks, must be derived. Straightforward an orchestrating controller design is highly necessary in order to synergize the control performance.

Objectives

The objective of this thesis consists in developing systematic event-triggered control designs for specified event generators, which is an important alternative to the traditional periodic sampling control. Sporadic sampling inherently arising in event-triggered control is determined by the event-triggering conditions. This feature invokes the desire of finding new control theory as the traditional sampled-data theory in computer control. Developing controller coupling with the applied event-triggering condition to maximize the control performance is the essence for event-triggered control design. In the design the stability of the control system needs to be ensured with the first priority. Concerning variant control aims they should be clearly incorporated in the design procedures. Considering applications in embedded control systems efficient implementation requires a low complexity of embedded software architectures. The thesis targets at offering such a design to further complete the theory of event-triggered control designs.

Outlines

The research keynotes in this thesis are listed as follows:

Chapter 1 introduces the basic idea of event-triggered control in recent studies. Several intensively investigated event-triggering conditions are presented. Based on the control objectives, methodologies and applications the state of the art is given.

Chapter 2 concerns a suboptimal event-triggered controller design for time-delayed linear systems. The considered performance includes a linear quadratic cost function for quantifying the control performance and average event times for quantifying the transmission reductions. The controller synthesized with the event-triggering conditions is derived by solving an optimization problem in off-line. The derived controllers of low complexity are quite implementation-aware for embedded real-time systems, which is verified in the presented experiment.

Chapter 3 addresses the event-triggered control subject to actuator saturation for linear systems. In terms of an auxiliary feedback matrix a given ellipsoid is analyzed if it is contractively invariant. For maximizing the ellipsoidal contractive invariant set, an event-triggered synthesis approach is proposed. The search of the event-triggered controller in the end is formulated as an optimization problem of the geometrical size of an ellipsoid that is subject to the stability constraint of the controlled system in the sense of Lyapunov.

Chapter 4 addresses the event-triggering controller design for discrete-time linear systems subject to bounded disturbance. The main control objective is to diminish the influence aroused by the disturbance despite of a reduction of the communication of output or actuator signals. Criteria are given to design feedback controllers in order to guarantee that systems are uniformly ultimately bounded in an ellipsoidal positive invariant set, which is used as an estimate of control performance for disturbance rejection. A minimization of the ellipsoidal positive invariant set is achieved by synthesizing the feedback control gain and the event-triggering conditions in linear matrix inequalities (LMIs). The derived results are casted in the test of an experiment, where it vindicates the effectiveness postulated by the theoretical results.

Chapter 5 addresses the problem that a multiple of control systems are controlled by one single CPU platform. In a scarce computing resource scenario, all the control systems compete for the limited resource. By designing the scheduling strategy and the controllers jointly the given approach can present advantages at the control performance that is defined by the quadratic cost functions compared with the traditional periodic sampling control strategy in experiments. The event-triggered control strategy is used in the approach to allocate the computing resource. Meanwhile the controllers covering both the stability and the control performance are designed to orchestrate the strategy.

Chapter 6 concerns an approach of transforming multi-variable dependent time-varying systems into a polytopic representation with uncertain parameters for stability analysis. The approach is based on the over-approximation of Taylor Series expansion. By recursion the proposed approach can be extended to handle systems with any number of uncertain time-varying variables.

Chapter 7 provides conclusions and suggestions for future work.

Publications

Several articles on the event-triggered control for embedded control systems have been finished during the doctoral studies. A chronological list of these articles together with their topic and their relation to this thesis is given below.

W. Wu, and S. Liu. An approach to reduce complexity in stability analysis for time-varying systems with polytopic uncertainties. *In proceedings of IEEE Multi-conference on Systems and Control*, 1782–1787, 2009. (Chapter 6)

S. Reimann, W. Wu, and S. Liu. A novel control-schedule codesign method for embedded control. *In proceedings of American Control Conference*, 3766–3771, 2012. (Control and Scheduling Codesign)

W. Wu, S. Reimann, D. Görges, and S. Liu. Suboptimal event-triggered control for time-delayed linear systems. *IEEE Transactions on Automatic Control*, 2014. (Chapter 2 and Implementation-Aware Control)

W. Wu, S. Reimann, and S. Liu. Event-triggered control for linear systems subject to actuator saturation. *In proceedings of 19th IFAC World Congress*, 9492-9497, 2014. (Chapter 3)

W. Wu, S. Reimann, D. Görges, and S. Liu. Event-triggered control for discrete-time linear systems subject to bounded disturbance. *Submitted to International Journal of Control*, Under Review. (Chapter 4 and Implementation-Aware Control)

W. Wu, S. Reimann, D. Görges, and S. Liu. Scheduling and event-triggered control design for multiple embedded control systems. *Submitted to Control Engineering Practice*, Under Review. (Chapter 5 and Implementation-Aware Control)

S. Reimann, W. Wu, and S. Liu. PI control and scheduling design for embedded control systems. *In proceedings of 19th IFAC World Congress*, 11111-11116, 2014.

Notation

Throughout the thesis, scalars are denoted by lower- and upper-case non-bold letters ($a, b, \ldots, A, B, \ldots$), vectors by lower-case bold letters ($\boldsymbol{a}, \boldsymbol{b}, \ldots$), matrices by upper-case bold letters ($\boldsymbol{A}, \boldsymbol{B}, \ldots$) and sets by upper-case double-struck letters ($\mathbb{A}, \mathbb{B}, \ldots$).

Sets

$\mathbb{N}$	Set of positive integers
$\mathbb{N}_0$	Set of non-negative integers
$\mathbb{R}$	Set of real numbers
$\mathbb{R}_0^+$	Set of non-negative real numbers
$\mathbb{R}^-$	Set of negative real numbers
$\mathbb{C}$	Set of complex numbers

Operators

$\boldsymbol{A}^{-1}$	Inverse of matrix $\boldsymbol{A}$
$\boldsymbol{A}^T$	Transpose of matrix $\boldsymbol{A}$
$\boldsymbol{A} > \boldsymbol{0}$	Matrix $\boldsymbol{A} \in \mathbb{R}^{\mathrm{n}\times\mathrm{n}}$ positive definite, i.e. $\boldsymbol{x}^T\boldsymbol{A}\boldsymbol{x} > 0 \ \forall \boldsymbol{x} \in \mathbb{R}^{\mathrm{n}} \setminus \{\boldsymbol{0}\}$
$\boldsymbol{A} \geq \boldsymbol{0}$	Matrix $\boldsymbol{A} \in \mathbb{R}^{\mathrm{n}\times\mathrm{n}}$ positive semidefinite, i.e. $\boldsymbol{x}^T\boldsymbol{A}\boldsymbol{x} \geq 0 \ \forall \boldsymbol{x} \in \mathbb{R}^{\mathrm{n}}$
$\boldsymbol{A} < \boldsymbol{0}$	Matrix $\boldsymbol{A} \in \mathbb{R}^{\mathrm{n}\times\mathrm{n}}$ negative definite, i.e. $\boldsymbol{x}^T\boldsymbol{A}\boldsymbol{x} < 0 \ \forall \boldsymbol{x} \in \mathbb{R}^{\mathrm{n}} \setminus \{\boldsymbol{0}\}$
$\boldsymbol{A} \leq \boldsymbol{0}$	Matrix $\boldsymbol{A} \in \mathbb{R}^{\mathrm{n}\times\mathrm{n}}$ negative semidefinite, i.e. $\boldsymbol{x}^T\boldsymbol{A}\boldsymbol{x} \leq 0 \ \forall \boldsymbol{x} \in \mathbb{R}^{\mathrm{n}}$
$\mathrm{tr}(\boldsymbol{A})$	Trace of matrix $\boldsymbol{A}$
$\det(\boldsymbol{A})$	Determinant of matrix $\boldsymbol{A}$
$\lambda_{\mathrm{min}}(\boldsymbol{A})$	Minimum eigenvalue of matrix $\boldsymbol{A}$
$\lambda_{\mathrm{max}}(\boldsymbol{A})$	Maximum eigenvalue of matrix $\boldsymbol{A}$
$\mathrm{diag}(\boldsymbol{A}_1, \ldots)$	Block-diagonal matrix with blocks $\boldsymbol{A}_1, \ldots$
$\mathrm{col}_i(\boldsymbol{A})$	Denote the i-th column of matrix $\boldsymbol{A}$
$\boldsymbol{A}_{ij}$	Denote the entry at the i-th row and j-th column of matrix $\boldsymbol{A}$
$\|\|\boldsymbol{x}\|\|$	Arbitrary p-norm of vector $\boldsymbol{x} \in \mathbb{R}^{\mathrm{n}}$
$\|\|\boldsymbol{x}\|\|_2$	Euclidean norm of vector $\boldsymbol{x} \in \mathbb{R}^{\mathrm{n}}$, i.e. $\|\|\boldsymbol{x}\|\|_2 = \sqrt{\boldsymbol{x}^T\boldsymbol{x}} = \sqrt{x_1^2 + \ldots + x_{\mathrm{n}}^2}$
$N!$	Denote factorial $N! = N(N-1)(N-2)...(2)(1)$, $N \in \mathbb{N}$
$N!!$	Denote factorial $N!! = N(N-2)(N-4)...$, $N \in \mathbb{N}$

$\lim_{s \uparrow t} \boldsymbol{x}(s)$	The limit of $\boldsymbol{x}(s)$ as s increases in value approaching t from below
$\lfloor x \rfloor$	Floor, i.e. $\lfloor x \rfloor$ is the largest integer smaller than or equal to $x \in \mathbb{R}$
$\text{mod}\ (M, l)$	Modulo, i.e. $\text{mod}\ (M, l) = l - M \left\lfloor \frac{l}{M} \right\rfloor$ with $M, l \in \mathbb{R}$
$\otimes$	Denote the Kronecker product

Others

$\boldsymbol{I}$	Identity matrix
$\boldsymbol{0}$	Zero matrix
$\left(\begin{smallmatrix} \boldsymbol{A} & * \\ \boldsymbol{B} & \boldsymbol{C} \end{smallmatrix}\right)$	Symmetric matrix $\left(\begin{smallmatrix} \boldsymbol{A} & \boldsymbol{B}^T \\ \boldsymbol{B} & \boldsymbol{C} \end{smallmatrix}\right)$

Linear Matrix Inequalities

Linear matrix inequalities (LMIs) are utilized throughout the thesis. Introductions to LMIs are given in [BGFB94] and [SP05] where also related topics like the S-procedure [BGFB94, Section 2.6.3], [SP05, Section 12.3.4], the Schur complement [BGFB94, pages 7–8], [SP05, Section 12.3.3] and the congruence transformation [SP05, Section 12.3.2] are addressed.

1 Introduction

Event-triggered control has been applied in many situations from simple servo systems to large factory complexes and computer networks even though there has not been much development of theory for systems with event-triggered control [Åst08]. Early examples of event-triggered systems can be found in relay systems [Tsy84], systems with pulse-width of pulse-frequency modulation [Fri76, Fra79], delta-sigma modulator [NST96] and reaction-control systems in spacecraft such as reaction jets, solar sails and magnetic torquers. More recent examples with the event-triggered control strategy can be found in systems using motors [HGvZ+99, SHHvdB07, HSB08, HC09], robotic systems [TXB96] and chemical plants [LL11b].

The basic idea of event-triggered control for the recent studies in state-space can be introduced by considering the simplified work in [Tab07], which originally investigates nonlinear systems. Consider a linear system

$$\dot{\boldsymbol{x}}(t) = \boldsymbol{A}\boldsymbol{x}(t) + \boldsymbol{B}\boldsymbol{u}(t), \tag{1.1}$$

where $\boldsymbol{x} \in \mathbb{R}^n$ is the state vector and $\boldsymbol{u} \in \mathbb{R}^m$ is the control signal. And a linear feedback control law is assumed

$$\boldsymbol{u}(t) = \boldsymbol{K}\boldsymbol{x}(t), \tag{1.2}$$

where the feedback gain $\boldsymbol{K}$ makes the real part of the eigenvalue of $\boldsymbol{A} + \boldsymbol{B}\boldsymbol{K}$ negative. Regarding an implementation on an embedded digital platform the traditional periodic control necessitates a periodic computation of (1.2) and actuation of the computed control input value. Instead of the periodic manner the control tasks of computation and actuation can be executed only when a certain performance is not satisfactory. The way in the literature [Tab07, VMB09, PANT11, SP11, MMDGC13] to define performance is to employ a Lyapunov function for the ideal closed-loop system (1.1) (The definitions about Lyapunov function and stability can refer to Section A.1). The Lyapunov function is denoted by

$$V(\boldsymbol{x}(t)) = \boldsymbol{x}^T(t)\boldsymbol{P}\boldsymbol{x}(t), \tag{1.3}$$

where matrix $\boldsymbol{P} \in \mathbb{R}^{n \times n}$ is symmetric and positive definite. The used Lyapunov function needs to satisfy

$$\begin{aligned}\dot{V}(\boldsymbol{x}(t)) &= \boldsymbol{x}^T(t)(\boldsymbol{A} + \boldsymbol{B}\boldsymbol{K})^T\boldsymbol{P}\boldsymbol{x}(t) + \boldsymbol{x}^T(t)\boldsymbol{P}(\boldsymbol{A} + \boldsymbol{B}\boldsymbol{K})\boldsymbol{x}(t) \\ &= -\boldsymbol{x}^T(t)\boldsymbol{Q}\boldsymbol{x}(t) \\ &\leq -\alpha\boldsymbol{x}^T(t)\boldsymbol{Q}\boldsymbol{x}(t), \end{aligned} \tag{1.4}$$

where matrix $\boldsymbol{Q} \in \mathbb{R}^{n\times n}$ is symmetric and positive definite and $\alpha \in (0, 1]$. This negativeness of the derivative of $V(\boldsymbol{x})$ guarantees the decreasing of the Lyapunov function and parameter α can influence the convergent rate of $V(\boldsymbol{x})$. If a slow convergent rate can be tolerated, α can be specified small.

Since the event-triggered control intends to reduce the updates of the control input signal, the inputs are held constant in between the successive updates. This behavior is called as sample-and-hold in the literature [Tab07], where can be formalized as

$$\boldsymbol{u}(t) = \boldsymbol{u}(t_k), \quad \forall t \in [t_k, t_{k+1}), \quad k \in \mathbb{N}, \tag{1.5}$$

where the sequence $\{t_1, t_2, ..., t_k, ...\}, k \in \mathbb{N}$ represents the time instants at which control input signal (1.2) is computed and forwarded to the actuator. The event-triggering condition can be defined by using (1.4). Once the inequality (1.4) is about to be violated, i.e., when (1.4) becomes an equality then the actual control input signal needs to be calculated and forwarded to the actuator. By introducing an error variable

$$\boldsymbol{e}(t) = \boldsymbol{x}(t_k) - \boldsymbol{x}(t), \quad \forall t \in [t_k, t_{k+1}), \quad k \in \mathbb{N} \tag{1.6}$$

the closed-loop system during the time interval $[t_k, t_{k+1})$ can be rewritten as

$$\begin{aligned} \dot{\boldsymbol{x}}(t) &= \boldsymbol{A}\boldsymbol{x}(t) + \boldsymbol{B}\boldsymbol{K}\boldsymbol{x}(t_k) \\ &= (\boldsymbol{A} + \boldsymbol{B}\boldsymbol{K})\boldsymbol{x}(t) + \boldsymbol{B}\boldsymbol{K}\boldsymbol{e}(t). \end{aligned} \tag{1.7}$$

Consider (1.7) into the time derivative of $V(\boldsymbol{x})$

$$\dot{V}(\boldsymbol{x}(t)) = -\boldsymbol{x}^T(t)\boldsymbol{Q}\boldsymbol{x}(t) + 2\boldsymbol{x}^T(t)\boldsymbol{P}\boldsymbol{B}\boldsymbol{K}\boldsymbol{e}(t) \tag{1.8}$$

Finally the event-triggering condition can be formulated:

$$-(1-\alpha)\boldsymbol{x}^T(t)\boldsymbol{Q}\boldsymbol{x}(t) + 2\boldsymbol{x}^T(t)\boldsymbol{P}\boldsymbol{B}\boldsymbol{K}\boldsymbol{e}(t) \leq 0. \tag{1.9}$$

The event is triggered at the times t_k when the equality of (1.9) holds. Basically the event in the literature is defined by the convergence rate of a Lyapunov function. Once the desired convergence is lost, updates are made in order to regain it. Generally the triggering times determined by the condition (1.9) can not be kept equidistant. This characteristic, which occurs almost in all kinds of event-triggered control approach, proposes a challenging question how the controller design is synthesized for the event-triggering condition. The approach in the literature [Tab07] also raises the question of the existence of a lower bound $\underline{h}$, $t_{k+1} - t_k \geq \underline{h}$, $k \in \mathbb{N}$, which is called the minimal inter-event time. When the minimal inter-event time $\underline{h}$ too small, even $\underline{h} = 0$, it means that a very fast, even infinite fast update is required, which is impossible in a digital implementation. Therefore extra considerations are needed to exclude this behaviour (Zeno behaviour). This point is discussed in [Tab07, Proposition VI.1].

An alternative to this continuously monitoring approach is a periodic event-triggered control [HDT13], whose event-triggering condition is verified periodically and at every measuring time it is decided whether or not to compute and to transmit new measurements and new control signals. The periodic event-triggered strategy with the periodic measurement interval however makes the necessity of guaranteeing a non-zero minimal inter-event time obsolete. Additionally the periodic event-triggered control strategy fits well to practical implementations for the standard time-sliced embedded software architectures. The piecewise linear system approach as one part of the work in [HDT13] is to guarantee an exponential stability of the system given by

$$\dot{\boldsymbol{x}}(t) = \boldsymbol{A}\boldsymbol{x}(t) + \boldsymbol{B}\hat{\boldsymbol{u}}(t), \tag{1.10}$$

where $\boldsymbol{x} \in \mathbb{R}^n$ is the state vector and $\hat{\boldsymbol{u}} \in \mathbb{R}^m$ is the input applied to the plant. It is assumed that the state of the plant is measured periodically at time instants $t_k = kh, k \in \mathbb{N}$, with periodic measurement interval h. The controller is

$$\hat{\boldsymbol{u}}(t) = \boldsymbol{K}\hat{\boldsymbol{x}}(t),\ t \in \mathbb{R}_0^+, \tag{1.11}$$

where $\boldsymbol{K}$ is a predefined feedback control gain and $\hat{\boldsymbol{x}}(t)$ is a left-continuous signal[1], defined for $t \in (t_k, t_{k+1}]$, $k \in \mathbb{N}$ by

$$\hat{\boldsymbol{x}}(t) = \begin{cases} \boldsymbol{x}(t_k), & \text{when } \mathcal{C}(\boldsymbol{x}(t_k), \hat{\boldsymbol{x}}(t_k)) > 0 \\ \hat{\boldsymbol{x}}(t_k), & \text{when } \mathcal{C}(\boldsymbol{x}(t_k), \hat{\boldsymbol{x}}(t_k)) \leq 0. \end{cases} \tag{1.12}$$

The value $\hat{\boldsymbol{x}}(t)$ is interpreted as the most recently transmitted measurement of the state $\boldsymbol{x}$ to the controller at time t, and $\mathcal{C} : \mathbb{R}^{2n} \to \mathbb{R}$ is the event-triggering condition. If at time t_k it holds that $\mathcal{C}(\boldsymbol{x}(t_k), \hat{\boldsymbol{x}}(t_k)) > 0$, the state vector $\boldsymbol{x}(t_k)$ is transmitted to the controller and $\hat{\boldsymbol{x}}$ and the control input $\hat{\boldsymbol{u}}$ are updated accordingly. In case $\mathcal{C}(\boldsymbol{x}(t_k), \hat{\boldsymbol{x}}(t_k)) \leq 0$ it means no update for the control input and the previous value is held by the Zero-Order-Hold (ZOH) function. In the literature [HDT13] the event-triggering condition $\mathcal{C}$ is considered in a general quadratic form given by

$$\mathcal{C}(\boldsymbol{\xi}(t_k)) = \boldsymbol{\xi}^T(t_k)\boldsymbol{Q}\boldsymbol{\xi}(t_k) > 0, \tag{1.13}$$

where $\boldsymbol{\xi}(t_k) := \left(\boldsymbol{x}^T(t_k)\ \hat{\boldsymbol{x}}^T(t_k)\right)^T \in \mathbb{R}^{2n}$ and $\boldsymbol{Q} \in \mathbb{R}^{2n \times 2n}$ is a symmetric and indefinite matrix. With this form matrix $\boldsymbol{Q}$ can easily describe some important applied event-triggering conditions.

1) State Error Based Event-Triggering Conditions: This event-triggering conditions have been applied in [WL11, GA11], which is given by

$$\|\hat{\boldsymbol{x}}(t_k) - \boldsymbol{x}(t_k)\|_2 > \sigma\|\boldsymbol{x}(t_k)\|_2 \tag{1.14}$$

for $k \in \mathbb{N}$, where $\sigma > 0$. Eq. (1.14) can be represented in the form of Eq. (1.13) with

$$\boldsymbol{Q} = \begin{pmatrix} (1-\sigma^2)\boldsymbol{I} & -\boldsymbol{I} \\ -\boldsymbol{I} & \boldsymbol{I} \end{pmatrix}. \tag{1.15}$$

[1]A signal $\boldsymbol{x} : \mathbb{R}_0^+ \to \mathbb{R}^n$ is called left-continuous, if for all $t > 0$, $\lim_{s \uparrow t} \boldsymbol{x}(s) = \boldsymbol{x}(t)$

2) Control Input Error Based Event-Triggering Conditions: The event-triggering conditions is given by

$$\|\boldsymbol{K}\hat{\boldsymbol{x}}(t_k) - \boldsymbol{K}\boldsymbol{x}(t_k)\|_2 > \sigma\|\boldsymbol{K}\boldsymbol{x}(t_k)\|_2, \tag{1.16}$$

where $\sigma > 0$. Eq. (1.16) is equivalent to $\|\hat{\boldsymbol{u}}(t_k) - \boldsymbol{u}(t_k)\|_2 > \sigma\|\boldsymbol{u}(t_k)\|_2$, where $\boldsymbol{u}(t_k) = \boldsymbol{K}\boldsymbol{x}(t_k)$ is the control input value based on the periodic sampling control. This event-triggering condition has been applied in [DH12]. Eq. (1.16) can be represented in the form of Eq. (1.13) with

$$\boldsymbol{Q} = \begin{pmatrix} (1-\sigma^2)\boldsymbol{K}^T\boldsymbol{K} & -\boldsymbol{K}^T\boldsymbol{K} \\ -\boldsymbol{K}^T\boldsymbol{K} & \boldsymbol{K}^T\boldsymbol{K} \end{pmatrix}. \tag{1.17}$$

3) l_2-Gain Event-Triggering Conditions: The event-triggering conditions used in [WL09a] is

$$\|\hat{\boldsymbol{u}}(t_k) - \boldsymbol{u}(t_k)\|_2^2 > (1-\beta^2)\|\boldsymbol{x}(t_k)\|_2^2 + \|\hat{\boldsymbol{u}}(t_k)\|_2^2, \tag{1.18}$$

where $0 < \beta \leq 1$ and $\boldsymbol{u}(t_k) = \boldsymbol{K}\boldsymbol{x}(t_k)$. Eq. (1.13) can be adapted as

$$\boldsymbol{Q} = \begin{pmatrix} (\beta^2-1)\boldsymbol{I} + \boldsymbol{K}^T\boldsymbol{K} & -\boldsymbol{K}^T\boldsymbol{K} \\ -\boldsymbol{K}^T\boldsymbol{K} & \boldsymbol{0} \end{pmatrix}. \tag{1.19}$$

4) Lyapunov Function based Event-Triggering Conditions: Lyapunov function based event-triggering conditions have been applied in [WL08, VMB09, MAT10]. In order to formulate these event-triggering conditions in the frame of periodic event-triggered control a discretization of Eq. (1.10) is crucial. The discretized sampled-data system with respect to the sampling period h is

$$\boldsymbol{x}(k+1) = \boldsymbol{\Phi}\boldsymbol{x}(k) + \boldsymbol{\Gamma}\hat{\boldsymbol{u}}(k), \tag{1.20}$$

where $\boldsymbol{\Phi} = e^{\boldsymbol{A}h}$ and $\boldsymbol{\Gamma} = \int_0^h e^{\boldsymbol{A}s}\boldsymbol{B}ds$. Predefine a feedback gain $\boldsymbol{K}$ rendering $\boldsymbol{\Phi} + \boldsymbol{\Gamma}\boldsymbol{K}$ with all eigenvalues inside the unit circle such that there exists a quadratic Lyapunov function $V(\boldsymbol{x}) = \boldsymbol{x}^T\boldsymbol{P}\boldsymbol{x}$, $\boldsymbol{P} \in \mathbb{R}^{n\times n}$ being symmetric and positive definite. The stability condition in the sense of the Lyapunov function is

$$(\boldsymbol{\Phi} + \boldsymbol{\Gamma}\boldsymbol{K})^T\boldsymbol{P}(\boldsymbol{\Phi} + \boldsymbol{\Gamma}\boldsymbol{K}) \leq \lambda\boldsymbol{P} \tag{1.21}$$

for some $0 \leq \lambda < 1$. This implies the exponential convergence of the Lyapunov function $V(\boldsymbol{x}(k+1)) \leq \lambda V(\boldsymbol{x}(k))$ for all $k \in \mathbb{N}$. By considering the Lyapunov function along the trajectory determined by system (1.20) the event-triggering condition can be formulated

$$(\boldsymbol{\Phi}\boldsymbol{x}(k) + \boldsymbol{\Gamma}\boldsymbol{K}\hat{\boldsymbol{x}}(t_k))^T\boldsymbol{P}(\boldsymbol{\Phi}\boldsymbol{x}(k) + \boldsymbol{\Gamma}\boldsymbol{K}\hat{\boldsymbol{x}}(t_k)) > \lambda\boldsymbol{x}^T(k)\boldsymbol{P}\boldsymbol{x}(k). \tag{1.22}$$

Rewrite (1.22) in the form of Eq. (1.13)

$$\boldsymbol{Q} = \begin{pmatrix} \boldsymbol{\Phi}^T\boldsymbol{P}\boldsymbol{\Phi} - \lambda\boldsymbol{P} & \boldsymbol{\Phi}^T\boldsymbol{P}\boldsymbol{\Gamma}\boldsymbol{K} \\ \boldsymbol{K}^T\boldsymbol{\Gamma}^T\boldsymbol{P}\boldsymbol{\Phi} & \boldsymbol{K}^T\boldsymbol{\Gamma}^T\boldsymbol{P}\boldsymbol{\Gamma}\boldsymbol{K} \end{pmatrix}. \tag{1.23}$$

Generally the indefiniteness of matrix $\boldsymbol{Q}$ partitions the space $\mathbb{R}^{2n}$ into two divisions

$$\Omega_1 := \left\{\boldsymbol{\xi}|\boldsymbol{\xi}^T(t_k)\boldsymbol{Q}\boldsymbol{\xi}(t_k) > 0\right\} \quad \text{and} \quad \Omega_2 := \left\{\boldsymbol{\xi}|\boldsymbol{\xi}^T(t_k)\boldsymbol{Q}\boldsymbol{\xi}(t_k) \leq 0\right\}, \tag{1.24}$$

with $\Omega_1 \cup \Omega_2 = \mathbb{R}^{2n}$. In each division the dynamic of system (1.10) is influenced either by the feedback of the actual states $\hat{\boldsymbol{u}}(t) = \boldsymbol{K}\boldsymbol{x}(t_k)$ or by the control input held by ZOH $\hat{\boldsymbol{u}}(t) = \boldsymbol{K}\hat{\boldsymbol{x}}(t_k)$. Thus the dynamics of the system (1.10) can be analyzed by piecewise linear system approach [Joh99] in order to verify the exponential stability, about which the results are given as [HDT13, Theorem III.4]. However controller design jointly with the event-triggering conditions are still missing in the literature [HDT13] because the use of piecewise Lyapunov function makes the LMI formulation difficult. This thesis makes contributions in filling this gap, where the two classes of event-triggering conditions—state error based event-triggering conditions and control input error based event-triggering conditions are investigated. The selections of those two event-triggering conditions are motivated by 1) The physical meanings of the two event-triggering conditions are straightforward by considering the facts that the previous control input can be also effective if the state or the recomputed control input of the systems only has a minor change. 2) In the sense of state-feedback control complete state information are utilized in the determination whether an event should be triggered. 3) Manipulating parameter σ which can be defined by user has direct influence in the numbers of triggering an event. 4) Compared with l_2-gain event-triggering conditions and Lyapunov function based event-triggering conditions easy programming and little computation complexity are implementation-friendly.

Event-triggered control is integrated with Model Predictive Control (MPC) [SLH10, EDK11b, EDK11a, FOSS12, LHJ13], where [SLH10, LHJ13] consider linear systems and [EDK11b, EDK11a, FOSS12] consider nonlinear system. The basic idea for the event-triggered MPC control takes advantages of the predicted control input sequence generated from the MPC algorithm. When the difference between the actual system's state and predicted one by the MPC algorithm is bigger than a threshold, or the running steps are larger than the prediction horizon of MPC, the event of re-executing the MPC algorithm will be triggered. In an optimal control framework the design of transmission sequences is studied in [RJJ08, HJC08, Cog09, MH09, MH10, AHT12] for stochastic systems. The work in [RJJ08, HJC08] considers the continuous first-order linear stochastic systems. The focus is put on finding the inter-event duration so that the average frequency of control events and the state variance can be reduced simultaneously. However an open question is how the approaches in [RJJ08, HJC08] can be extended to high-order systems. Another consideration is that the approach requires continuous measurements, which may not be supported by common digital platform. Specific hardware could be needed. In [Cog09, MH09, MH10, AHT12] the controller designs jointly with the event-triggering conditions are investigated. The basic idea for the co-design is penalizing the control events by assigning a certain cost for them. Combining the cost from control events with the traditional quadratic cost function yields a new cost function. The consequent work in [Cog09, MH09, MH10, AHT12] is transformed to derive event-triggering conditions and controllers to minimize the new cost function. However in [Cog09, MH09, MH10] the convergence feature of the systems are not covered by the presented approaches. In [AHT12] the transmission sequence and controller co-design is based on dynamic programming at each scheduling time for a future time horizon, where an exhaustive search for the minimal cost associated with a transmission sequence is required. Additionally, [AHT12] discusses the method for a unitary decision horizon to reduce the computational complexity. Thereby, a triggering rule is provided and an upper bound on the costs can be given.

The event-triggered PI and PID control approaches are discussed in [Årz99, VK06, DM09, LL11b, LJ12, LKJ12]. The work in [Årz99] proposes a simple event-triggered control structure, where the event triggering conditions include two parts. One is that the absolute value of the difference between the current value of the error for set-point tracking and the value of the error when a control signal was calculated the last time is compared with a fixed threshold. When the absolute value of the difference bigger than the threshold, an event is triggered. The other condition to trigger an event is when the time elapsed since the last sample is bigger than a given maximum time. The event triggering condition is checked in a discrete-time way. Simulations on a double-tank process show large reductions in CPU utilization with only minor control performance degradation. The work in [DM09] extends the work in [Årz99] by eliminating the maximum time condition in the event-triggering conditions in [Årz99]. Another extension to the work in [Årz99] is to add a minimum time between two successive events in [VK06]. However in all the work [Årz99, VK06, DM09] the stability of the system is not explicitly considered. In the work [LL11b, LJ12, LKJ12] event-triggered PI controller is investigated by considering continuous measurement, where practical stability is addressed. However how to tune the PI controller is not deeply discussed in the work [LL11b, LJ12, LKJ12].

The constant threshold in the event-triggering conditions is studied in [OMT02, Mis06, KB06, LL10, LL11b, LL11a]. Event-triggering conditions with the constant threshold are an intuitive way to generate events, which is easy to implement without the requirement of precise plant models. However these event-triggering conditions could make it hard to guarantee the asymptotical stability of the controlled systems because of the constant threshold.

In the considerations of various control objectives and constraints event-triggered control is applied to system subject to actuator saturations [LKJ12, KLJ12, SPTZ13]. For the nonlinearity of actuator saturation estimating the domain of attraction and obtaining a bigger domain is always an interesting topic in control theory, where the absolute stability analysis tools, such as the circle and Popov criteria [Kha96] are widely used. In [LKJ12, KLJ12] the stability region under a constant threshold based event-triggered PI control is studied. In [SPTZ13] a local exponentially stability is guaranteed by a designed event-triggering condition concerning an LQ cost function. However none of the work in [LKJ12, KLJ12, SPTZ13] addresses the problem of deriving an as big as possible domain of attraction under event-triggered control.

Explicitly considering exogenous disturbance for the event-triggered control systems can be found in [HSB08, CS11, VGH13, LHJ13]. In [HSB08, CS11, VGH13] the controller are chosen a priori. For the chosen controller the effects of the disturbance on the system dynamics are investigated. In [LHJ13] the MPC controller is employed and the disturbance is used in determining the event-triggering condition. The controller design actually is separated from the event-triggering condition.

Conclusively one critical point also motivating this thesis is how to achieve controller design that is synthesized with event-triggering conditions such that a satisfactory control performance can be guaranteed even with control input update reductions. At the same time the stability of the system can also be ensured.

2 Suboptimal Event-Triggered Control

In this chapter synthesized controller design approaches with the event-triggering conditions are investigated aiming to minimize a quadratic cost function. The control design approach generates a unique control gain after solving an LMI optimization problem. By adjusting the weighting parameters of the quadratic cost function and the parameter of the event generator, it is tractable and easy to find suitably asymptotically stabilizing control parameters in real applications. The optimal controller is computed off-line such that the proposed control design will not consume additional computation resources, which is crucial for embedded control systems with limited computation resources. The proposed event-triggered control approach includes the optimization of the control performance, while transmission reductions can be configured by adapting a design parameter in the event generator. The delay that sometimes is not ignorable in control systems such as networked control systems is also considered in this work.

2.1 Problem Formulation

In this chaper the considered plant is described by the continuous-time state equation

$$\dot{\boldsymbol{x}}(t) = \boldsymbol{A}\boldsymbol{x}(t) + \boldsymbol{B}\boldsymbol{u}(t-\tau) \tag{2.1}$$

where $\boldsymbol{x}(t) \in \mathbb{R}^n$ is the state vector, $\boldsymbol{A} \in \mathbb{R}^{n\times n}$ is the system matrix, $\boldsymbol{B} \in \mathbb{R}^{n\times m}$ is the input matrix, and $\boldsymbol{u}(t-\tau) \in \mathbb{R}^m$ is the control signal with the constant input delay τ. In the following the plant is controlled in a periodic event-triggered way [HDT13], which is illustrated in Fig. 2.1. This means that at each measuring time instant, the state vector

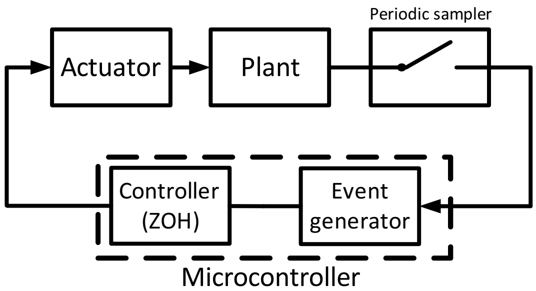

Figure 2.1: Diagram of periodic event-triggered control

$\boldsymbol{x}(t_k)$ of the plant is measured and forwarded to the event generator where an event-triggering condition is verified. If an event is triggered the required state is forwarded to the controller to compute the control signal $\boldsymbol{u}(t_k)$ and transmit it to the actuator. The measurement is made periodically with the time interval h at the time instances $t_k, k \in \mathbb{N}_0$ with $h = t_{k+1} - t_k$. After the input-delay $\tau \le h$ control task T is finished. The control input is updated using a zero-order-hold (ZOH). This behaviour is illustrated in Fig. 2.2. Note that between the control update and the next measurement there may be an idle time to account for non-control tasks. The goal is to design the fitting controller

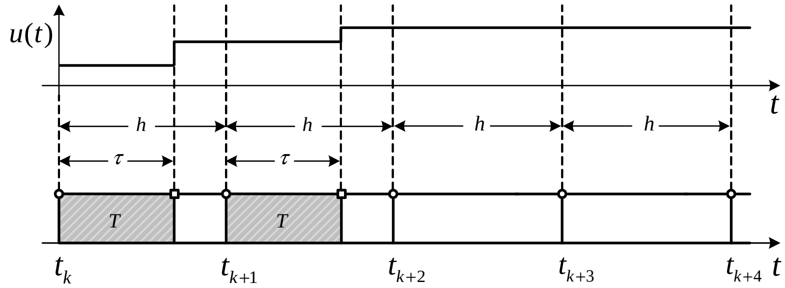

Figure 2.2: Timing diagram for event-triggered control where a new measurement is indicated by a circle, a control update by a square, and the execution of the control task T by the hatching

orchestrated by the event-generator to maintain satisfactory control performance and reduce the amount of control updates. First, discretizing the model (2.1) using ZOH to an augmented sampled-data system model with respect to the measurement interval h yields

$$\boldsymbol{z}(k+1) = \boldsymbol{\Phi}\boldsymbol{z}(k) + \boldsymbol{\Gamma}\boldsymbol{u}(k) \tag{2.2}$$

with

$$\boldsymbol{z}(k) = \begin{pmatrix} \boldsymbol{x}(k) \\ \boldsymbol{u}(k-1) \end{pmatrix}, \qquad \boldsymbol{\Phi} = \begin{pmatrix} e^{\boldsymbol{A}h} & \int_{h-\tau}^{h} e^{\boldsymbol{A}s} ds \boldsymbol{B} \\ \boldsymbol{0} & \boldsymbol{0} \end{pmatrix}, \qquad \boldsymbol{\Gamma} = \begin{pmatrix} \int_0^{h-\tau} e^{\boldsymbol{A}s} ds \boldsymbol{B} \\ \boldsymbol{I} \end{pmatrix}$$

where $\boldsymbol{x}(k)$ is the measured state vector at time instant t_k. A full state-feedback control law is considered

$$\boldsymbol{u}(k) = \boldsymbol{K}\hat{\boldsymbol{z}}^+(k), \tag{2.3}$$

where $\hat{\boldsymbol{z}}^+(k)$ is a signal defined with

$$\hat{\boldsymbol{z}}^+(k) = \begin{cases} \boldsymbol{z}(k) & \text{if } \boldsymbol{u}(k) \text{ is updated} \\ \hat{\boldsymbol{z}}^+(k-1) & \text{if } \boldsymbol{u}(k) \text{ is not updated.} \end{cases} \tag{2.4}$$

The decision for control updates is made by the event-triggering condition which is introduced in section 2.2.

In this chapter the considered control performance is measured by the classical quadratic cost function associated to the continuous-time system (2.1)

$$J_\infty = \int_0^\infty \begin{pmatrix} \boldsymbol{x}(s) \\ \boldsymbol{u}(s-\tau) \end{pmatrix}^T \begin{pmatrix} \boldsymbol{Q}_c & \boldsymbol{0} \\ \boldsymbol{0} & \boldsymbol{R}_c \end{pmatrix} \begin{pmatrix} \boldsymbol{x}(s) \\ \boldsymbol{u}(s-\tau) \end{pmatrix} ds \tag{2.5}$$

where $\boldsymbol{Q}_c \in \mathbb{R}^{n\times n}$ is symmetric and positive semi-definite and $\boldsymbol{R}_c \in \mathbb{R}^{m\times m}$ is symmetric and positive definite. This cost function can equivalently be written as

$$J = \sum_{k=0}^{\infty} \underbrace{\int_{t_k}^{t_k+h} \begin{pmatrix} \boldsymbol{x}(s) \\ \boldsymbol{u}(s-\tau) \end{pmatrix}^T \begin{pmatrix} \boldsymbol{Q}_c & \boldsymbol{0} \\ \boldsymbol{0} & \boldsymbol{R}_c \end{pmatrix} \begin{pmatrix} \boldsymbol{x}(s) \\ \boldsymbol{u}(s-\tau) \end{pmatrix} ds}_{\Delta J(k)} . \tag{2.6}$$

Considering the continuous-time state equation (2.1) over one measurement interval $(t_k, t_{k+1}]$ we obtain

$$\Delta J(k) = \begin{pmatrix} \boldsymbol{x}(k) \\ \boldsymbol{u}(k-1) \\ \boldsymbol{u}(k) \end{pmatrix}^T \boldsymbol{Q}_d \begin{pmatrix} \boldsymbol{x}(k) \\ \boldsymbol{u}(k-1) \\ \boldsymbol{u}(k) \end{pmatrix} = \begin{pmatrix} \boldsymbol{z}(k) \\ \boldsymbol{u}(k) \end{pmatrix}^T \boldsymbol{Q}_d \begin{pmatrix} \boldsymbol{z}(k) \\ \boldsymbol{u}(k) \end{pmatrix} \tag{2.7}$$

where the weighting matrix $\boldsymbol{Q}_d$ consists of two parts integrated over the time intervals $[0, \tau]$ and $[\tau, h]$

$$\boldsymbol{Q}_d = \boldsymbol{Q}_{d_0} + \boldsymbol{Q}_{d_1} = \left(\begin{array}{c|c} \boldsymbol{Q}_{d,11} & \boldsymbol{Q}_{d,12} \\ \hline \boldsymbol{Q}_{d,12}^T & \boldsymbol{Q}_{d,22} \end{array}\right) \tag{2.8a}$$

$$\boldsymbol{Q}_{d_0} = \int_0^{\tau} \left(\begin{array}{cc|c} \hat{\boldsymbol{A}}^T \boldsymbol{Q}_c \hat{\boldsymbol{A}} & \hat{\boldsymbol{A}}^T \boldsymbol{Q}_c \hat{\boldsymbol{B}}_1 & \boldsymbol{0} \\ \hat{\boldsymbol{B}}_1^T \boldsymbol{Q}_c \hat{\boldsymbol{A}} & \hat{\boldsymbol{B}}_1^T \boldsymbol{Q}_c \hat{\boldsymbol{B}}_1 + \boldsymbol{R}_c & \boldsymbol{0} \\ \hline \boldsymbol{0} & \boldsymbol{0} & \boldsymbol{0} \end{array}\right) dt \tag{2.8b}$$

$$\boldsymbol{Q}_{d_1} = \int_{\tau}^{h} \left(\begin{array}{cc|c} \hat{\boldsymbol{A}}^T \boldsymbol{Q}_c \hat{\boldsymbol{A}} & \boldsymbol{0} & \hat{\boldsymbol{A}}^T \boldsymbol{Q}_c \hat{\boldsymbol{B}}_0 \\ \boldsymbol{0} & \boldsymbol{0} & \boldsymbol{0} \\ \hline \hat{\boldsymbol{B}}_0^T \boldsymbol{Q}_c \hat{\boldsymbol{A}} & \boldsymbol{0} & \hat{\boldsymbol{B}}_0^T \boldsymbol{Q}_c \hat{\boldsymbol{B}}_0 + \boldsymbol{R}_c \end{array}\right) dt \tag{2.8c}$$

where $\hat{\boldsymbol{A}} = e^{\boldsymbol{A}h}$, $\hat{\boldsymbol{B}}_0 = e^{\boldsymbol{A}(h-\tau)} \int_0^{h-\tau} e^{\boldsymbol{A}s} ds \boldsymbol{B}$ and $\hat{\boldsymbol{B}}_1 = e^{\boldsymbol{A}(h-\tau)} \int_0^{\tau} e^{\boldsymbol{A}s} ds \boldsymbol{B}$. Thus the discretized cost function of (2.5) is given by

$$J_\infty = \sum_{k=0}^{\infty} \begin{pmatrix} \boldsymbol{z}(k) \\ \boldsymbol{u}(k) \end{pmatrix}^T \boldsymbol{Q}_d \begin{pmatrix} \boldsymbol{z}(k) \\ \boldsymbol{u}(k) \end{pmatrix} . \tag{2.9}$$

For a detailed discussion on deriving the discretized weighting matrices (2.8) one can refer to section A.2.

Problem 2.1 *For the discrete-time system* (2.2) *find an event-triggered controller* (2.3) *such that the cost function* (2.9) *is minimized.*

2.2 Main Result

In this section the synthesis approach of the event-generator and the controller is presented. Two different event-triggering conditions are studied based on the state error and the control input error, respectively, which are important classes of event-triggering conditions already applied in [HDT13, Tab07, WL09b]. With respect to those event-triggering conditions a state feedback controller is designed in order to optimize the cost function (2.5).

2.2.1 Controller Synthesis Based on State Error

Consider the event-triggering condition

$$\|\hat{\boldsymbol{z}}^{+}(k-1)-\boldsymbol{z}(k)\|_2 > \sigma\|\boldsymbol{z}(k)\|_2 \tag{2.10}$$

where $\sigma \in \mathbb{R}^{+}$. Based on (2.10), (2.4) can be rewritten as

$$\hat{\boldsymbol{z}}^{+}(k) = \begin{cases} \boldsymbol{z}(k) & \text{if } \|\hat{\boldsymbol{z}}^{+}(k-1)-\boldsymbol{z}(k)\|_2 > \sigma\|\boldsymbol{z}(k)\|_2 \\ \hat{\boldsymbol{z}}^{+}(k-1) & \text{if } \|\hat{\boldsymbol{z}}^{+}(k-1)-\boldsymbol{z}(k)\|_2 \leq \sigma\|\boldsymbol{z}(k)\|_2 \end{cases} \tag{2.11}$$

Now the problem 2.1 can be formulated as follows

Problem 2.2 *For the discrete-time system* (2.2) *find an event-triggered controller* (2.3) *under the event-triggering condition* (2.11) *for a given* σ *such that cost function* (2.9) *is minimized, i.e.*

$$\min_{\boldsymbol{K}} J_{\infty} \textit{ subject to } (2.2), (2.3) \textit{ and } (2.11). \tag{2.12}$$

Define the error variable

$$\boldsymbol{e}^{+}(k) = \hat{\boldsymbol{z}}^{+}(k) - \boldsymbol{z}(k). \tag{2.13}$$

Based on the definition (2.11) the inequality

$$\|\boldsymbol{e}^{+}(k)\|_2 \leq \sigma\|\boldsymbol{z}(k)\|_2 \tag{2.14}$$

is always satisfied. With the control input $\boldsymbol{u}(k) = \boldsymbol{K}\hat{\boldsymbol{z}}^{+}(k)$ and $\hat{\boldsymbol{z}}^{+}(k) = \boldsymbol{e}^{+}(k) + \boldsymbol{z}(k)$ the closed-loop system of (2.2) is given by

$$\boldsymbol{z}(k+1) = (\boldsymbol{\Phi} + \boldsymbol{\Gamma}\boldsymbol{K})\boldsymbol{z}(k) + \boldsymbol{\Gamma}\boldsymbol{K}\boldsymbol{e}^{+}(k) \tag{2.15}$$

with the denotation $\boldsymbol{\Phi}_c = \boldsymbol{\Phi} + \boldsymbol{\Gamma}\boldsymbol{K}$. This model (2.15) enables a closed-loop system with a control input error.

For designing the controller introduce the quadratic Lyapunov function

$$V(k) = \boldsymbol{z}(k)^T\boldsymbol{P}\boldsymbol{z}(k) \tag{2.16}$$

with $\boldsymbol{P} \in \mathbb{R}^{(n+m)\times(n+m)}$ symmetric and positive definite. Now search for a controller such that the difference of the Lyapunov function $\Delta V = V(k+1) - V(k)$ along the trajectories of the closed-loop system (2.15) satisfies

$$\Delta V = \boldsymbol{z}(k+1)^T\boldsymbol{P}\boldsymbol{z}(k+1) - \boldsymbol{z}(k)^T\boldsymbol{P}\boldsymbol{z}(k) < -\Delta J(k). \tag{2.17}$$

Under the satisfaction of (2.17) the asymptotic stability of the equilibrium point for system (2.15) can be guaranteed, which implies $\lim_{k\to\infty} \boldsymbol{z}(k) = \boldsymbol{0}$. Therefore $\lim_{k\to\infty} V(k) = 0$ holds. By summing (2.17) up from $k = 0$ to $k = \infty$ it yields

$$J_\infty < \boldsymbol{z}(0)^T \boldsymbol{P} \boldsymbol{z}(0) < \mathrm{tr}\,(\boldsymbol{P})\,\|\boldsymbol{z}(0)\|^2 . \tag{2.18}$$

This implies that the cost function J_∞ is upper-bounded by $\boldsymbol{z}(0)^T \boldsymbol{P} \boldsymbol{z}(0)$. The closed-loop system (2.15) with the event-triggering condition (2.11) and state error (2.13) lead to a hybrid system as shown in [HDT13] where the event-triggering condition (2.11) indicates the switching law of the hybrid system. As the switching is state dependent and thus not known before runtime, a suboptimal solution of Problem 2.2 is sought in order to allow an LMI formulation. Consequently, the control gain can be determined off-line. Problem 2.2 with a relaxation can be reformulated as follows

Problem 2.3 *For the closed-loop system* (2.15) *find an event-triggered controller* (2.3) *such that for a given σ the upper bound of the cost function* (2.9) *is minimized subject to condition* (2.14), *i.e.*

$$\min_{\boldsymbol{K}} tr\,(\boldsymbol{P}) \;\; \textit{subject to } (2.15) \textit{ and } (2.14). \tag{2.19}$$

Theorem 2.1 *A solution to Problem 2.3 is obtained from the LMI optimization problem*

$$\min tr(\boldsymbol{S}^{-1}) \quad \textit{subject to} \tag{2.20a}$$

$$\begin{pmatrix} \boldsymbol{G}^T + \boldsymbol{G} - \boldsymbol{S} & * & * & * & * \\ \boldsymbol{0} & \boldsymbol{G}^T + \boldsymbol{G} - \alpha \boldsymbol{I} & * & * & * \\ \boldsymbol{\Phi G} + \boldsymbol{\Gamma W} & \boldsymbol{\Gamma W} & \boldsymbol{S} & * & * \\ \boldsymbol{G} & \boldsymbol{0} & \boldsymbol{0} & \frac{\alpha}{\sigma^2}\boldsymbol{I} & * \\ \begin{pmatrix} \boldsymbol{G} \\ \boldsymbol{W} \end{pmatrix} & \begin{pmatrix} \boldsymbol{0} \\ \boldsymbol{W} \end{pmatrix} & \boldsymbol{0} & \boldsymbol{0} & \boldsymbol{Q}_d^{-1} \end{pmatrix} > \boldsymbol{0} \tag{2.20b}$$

with the LMI variables $\boldsymbol{S} \in \mathbb{R}^{(n+m)\times(n+m)}$ symmetric and positive definite, $\boldsymbol{W} \in \mathbb{R}^{m\times(n+m)}$ unrestricted, $\boldsymbol{G} \in \mathbb{R}^{(n+m)\times(n+m)}$ invertible and $\alpha > 0$. The control gain and the Lyapunov matrix result from

$$\boldsymbol{K} = \boldsymbol{W}\boldsymbol{G}^{-1}, \quad \boldsymbol{P} = \boldsymbol{S}^{-1}.$$

Proof. Substituting (2.15) into (2.17) results in

$$\begin{aligned} &\boldsymbol{z}(k)^T \boldsymbol{P} \boldsymbol{z}(k) - \boldsymbol{z}(k)^T \boldsymbol{\Phi}_c^T \boldsymbol{P} \boldsymbol{\Phi}_c \boldsymbol{z}(k) - 2\boldsymbol{z}(k)^T \boldsymbol{\Phi}_c^T \boldsymbol{P} \boldsymbol{\Gamma} \boldsymbol{K} \boldsymbol{e}^+(k) \\ &- \boldsymbol{e}^+(k)^T \boldsymbol{K}^T \boldsymbol{\Gamma}^T \boldsymbol{P} \boldsymbol{\Gamma} \boldsymbol{K} \boldsymbol{e}^+(k) > \Delta J(k) \end{aligned} \tag{2.21}$$

The inequality (2.21) is equivalent to

$$\begin{pmatrix} \boldsymbol{z}(k) \\ \boldsymbol{e}^+(k) \end{pmatrix}^T \hat{\boldsymbol{P}}_1 \begin{pmatrix} \boldsymbol{z}(k) \\ \boldsymbol{e}^+(k) \end{pmatrix} > \Delta J(k) \tag{2.22}$$

with

$$\hat{\boldsymbol{P}}_1 = \begin{pmatrix} \boldsymbol{P} - \boldsymbol{\Phi}_c^T \boldsymbol{P} \boldsymbol{\Phi}_c & * \\ -\boldsymbol{K}^T \boldsymbol{\Gamma}^T \boldsymbol{P} \boldsymbol{\Phi}_c & -\boldsymbol{K}^T \boldsymbol{\Gamma}^T \boldsymbol{P} \boldsymbol{\Gamma} \boldsymbol{K} \end{pmatrix}. \tag{2.23}$$

By substituting (2.3) and (2.13) into (2.7) it yields

$$\begin{aligned} \Delta J(k) &= \begin{pmatrix} \boldsymbol{z}(k) \\ \boldsymbol{K}(\boldsymbol{e}^+(k) + \boldsymbol{z}(k)) \end{pmatrix}^T \boldsymbol{Q}_d \begin{pmatrix} \boldsymbol{z}(k) \\ \boldsymbol{K}(\boldsymbol{e}^+(k) + \boldsymbol{z}(k)) \end{pmatrix} \\ &= \begin{pmatrix} \boldsymbol{z}(k) \\ \boldsymbol{e}^+(k) \end{pmatrix}^T \begin{pmatrix} \hat{\boldsymbol{Q}}_{11} & \hat{\boldsymbol{Q}}_{12} \\ \hat{\boldsymbol{Q}}_{12}^T & \hat{\boldsymbol{Q}}_{22} \end{pmatrix} \begin{pmatrix} \boldsymbol{z}(k) \\ \boldsymbol{e}^+(k) \end{pmatrix} \end{aligned} \tag{2.24}$$

where

$$\begin{aligned} \hat{\boldsymbol{Q}}_{11} &= \boldsymbol{Q}_{d,11} + \boldsymbol{Q}_{d,12} \boldsymbol{K} + \boldsymbol{K}^T \boldsymbol{Q}_{d,12}^T + \boldsymbol{K}^T \boldsymbol{Q}_{d,22} \boldsymbol{K}, \\ \hat{\boldsymbol{Q}}_{12} &= \boldsymbol{Q}_{d,12} \boldsymbol{K} + \boldsymbol{K}^T \boldsymbol{Q}_{d,22} \boldsymbol{K}, \\ \hat{\boldsymbol{Q}}_{22} &= \boldsymbol{K}^T \boldsymbol{Q}_{d,22} \boldsymbol{K}. \end{aligned}$$

Combining (2.22) and (2.24) leads to

$$\begin{pmatrix} \boldsymbol{z}(k) \\ \boldsymbol{e}^+(k) \end{pmatrix}^T \hat{\boldsymbol{P}}_2 \begin{pmatrix} \boldsymbol{z}(k) \\ \boldsymbol{e}^+(k) \end{pmatrix} > 0 \tag{2.25}$$

with

$$\hat{\boldsymbol{P}}_2 = \begin{pmatrix} \boldsymbol{P} - \boldsymbol{\Phi}_c^T \boldsymbol{P} \boldsymbol{\Phi}_c - \hat{\boldsymbol{Q}}_{11} & * \\ -\boldsymbol{K}^T \boldsymbol{\Gamma}^T \boldsymbol{P} \boldsymbol{\Phi}_c - \hat{\boldsymbol{Q}}_{12}^T & -\boldsymbol{K}^T \boldsymbol{\Gamma}^T \boldsymbol{P} \boldsymbol{\Gamma} \boldsymbol{K} - \hat{\boldsymbol{Q}}_{22} \end{pmatrix}. \tag{2.26}$$

The constraint (2.14) can be rewritten as

$$\begin{pmatrix} \boldsymbol{z}(k) \\ \boldsymbol{e}^+(k) \end{pmatrix}^T \begin{pmatrix} \sigma^2 \boldsymbol{I} & \boldsymbol{0} \\ \boldsymbol{0} & -\boldsymbol{I} \end{pmatrix} \begin{pmatrix} \boldsymbol{z}(k) \\ \boldsymbol{e}^+(k) \end{pmatrix} \geq 0 \tag{2.27}$$

Applying the lossless S-procedure [BV04, pp. 653-654] allows to combine the inequalities (2.25) and (2.27) to

$$\begin{pmatrix} \boldsymbol{P} - \boldsymbol{\Phi}_c^T \boldsymbol{P} \boldsymbol{\Phi}_c - \hat{\boldsymbol{Q}}_{11} - \kappa \sigma^2 \boldsymbol{I} & -\boldsymbol{\Phi}_c^T \boldsymbol{P} \boldsymbol{\Gamma} \boldsymbol{K} - \hat{\boldsymbol{Q}}_{12} \\ -\boldsymbol{K}^T \boldsymbol{\Gamma}^T \boldsymbol{P} \boldsymbol{\Phi}_c - \hat{\boldsymbol{Q}}_{12}^T & -\boldsymbol{K}^T \boldsymbol{\Gamma}^T \boldsymbol{P} \boldsymbol{\Gamma} \boldsymbol{K} - \hat{\boldsymbol{Q}}_{22} + \kappa \boldsymbol{I} \end{pmatrix} > \boldsymbol{0} \tag{2.28}$$

with the scalar $\kappa \geq 0$. The remaining problem is to obtain κ, $\boldsymbol{P}$ and $\boldsymbol{K}$ such that (2.28) is satisfied. For transforming (2.28) from a bilinear matrix inequality to an LMI use the Schur complement which results in

$$\begin{pmatrix} \boldsymbol{P} - \hat{\boldsymbol{Q}}_{11} - \kappa \sigma^2 \boldsymbol{I} & * & * \\ -\hat{\boldsymbol{Q}}_{12}^T & \kappa \boldsymbol{I} - \hat{\boldsymbol{Q}}_{22} & * \\ \boldsymbol{\Phi}_c & \boldsymbol{\Gamma} \boldsymbol{K} & \boldsymbol{P}^{-1} \end{pmatrix} > 0. \tag{2.29}$$

Applying the Schur complement again leads to

$$\begin{pmatrix} \boldsymbol{P}-\hat{\boldsymbol{Q}}_{11} & * & * & * \\ -\hat{\boldsymbol{Q}}_{12}^T & \kappa\boldsymbol{I}-\hat{\boldsymbol{Q}}_{22} & * & * \\ \boldsymbol{\Phi}_c & \boldsymbol{\Gamma K} & \boldsymbol{P}^{-1} & * \\ \boldsymbol{I} & \boldsymbol{0} & \boldsymbol{0} & \frac{1}{\kappa\sigma^2}\boldsymbol{I} \end{pmatrix} \geq 0. \tag{2.30}$$

Note that

$$\begin{pmatrix} \hat{\boldsymbol{Q}}_{11} & \hat{\boldsymbol{Q}}_{12} \\ \hat{\boldsymbol{Q}}_{12}^T & \hat{\boldsymbol{Q}}_{22} \end{pmatrix} = \begin{pmatrix} \boldsymbol{I} & \boldsymbol{K}^T \\ \boldsymbol{0} & \boldsymbol{K}^T \end{pmatrix} \boldsymbol{Q}_d \begin{pmatrix} \boldsymbol{I} & \boldsymbol{0} \\ \boldsymbol{K} & \boldsymbol{K} \end{pmatrix}. \tag{2.31}$$

By using the Schur complement again inequality (2.30) equals

$$\begin{pmatrix} \boldsymbol{P} & * & * & * & * \\ \boldsymbol{0} & \kappa\boldsymbol{I} & * & * & * \\ \boldsymbol{\Phi}_c & \boldsymbol{\Gamma K} & \boldsymbol{P}^{-1} & * & * \\ \boldsymbol{I} & \boldsymbol{0} & \boldsymbol{0} & \frac{1}{\kappa\sigma^2}\boldsymbol{I} & * \\ \begin{pmatrix} \boldsymbol{I} \\ \boldsymbol{K} \end{pmatrix} & \begin{pmatrix} \boldsymbol{0} \\ \boldsymbol{K} \end{pmatrix} & \boldsymbol{0} & \boldsymbol{0} & \boldsymbol{Q}_d^{-1} \end{pmatrix} > \boldsymbol{0}. \tag{2.32}$$

Pre-/post-multiplying (2.32) by diag $\left(\boldsymbol{G}^T, \boldsymbol{G}^T, \boldsymbol{I}, \boldsymbol{I}, \boldsymbol{I}\right)$ and its transposed one results in

$$\begin{pmatrix} \boldsymbol{G}^T\boldsymbol{P}\boldsymbol{G} & * & * & * & * \\ \boldsymbol{0} & \kappa\boldsymbol{G}^T\boldsymbol{G} & * & * & * \\ \boldsymbol{\Phi}_c\boldsymbol{G} & \boldsymbol{\Gamma K G} & \boldsymbol{P}^{-1} & * & * \\ \boldsymbol{G} & \boldsymbol{0} & \boldsymbol{0} & \frac{1}{\kappa\sigma^2}\boldsymbol{I} & * \\ \begin{pmatrix} \boldsymbol{G} \\ \boldsymbol{KG} \end{pmatrix} & \begin{pmatrix} \boldsymbol{0} \\ \boldsymbol{KG} \end{pmatrix} & \boldsymbol{0} & \boldsymbol{0} & \boldsymbol{Q}_d^{-1} \end{pmatrix} > \boldsymbol{0}. \tag{2.33}$$

Since the identity matrix $\boldsymbol{I}$ and $\boldsymbol{P}$ are symmetric and positive definite, also

$$\left(\kappa^{-1}\boldsymbol{I}-\boldsymbol{G}\right)^T \kappa\boldsymbol{I}\left(\kappa^{-1}\boldsymbol{I}-\boldsymbol{G}\right) \geq \boldsymbol{0} \tag{2.34}$$

$$\left(\boldsymbol{P}^{-1}-\boldsymbol{G}\right)^T \boldsymbol{P}\left(\boldsymbol{P}^{-1}-\boldsymbol{G}\right) \geq \boldsymbol{0} \tag{2.35}$$

hold as inversion and congruence transformation do not affect definiteness. The inequalities (2.34) and (2.56) are equivalent to

$$\kappa\boldsymbol{G}^T\boldsymbol{G} \geq \boldsymbol{G}^T + \boldsymbol{G} - \kappa^{-1}\boldsymbol{I} \tag{2.36}$$

$$\boldsymbol{G}^T\boldsymbol{P}\boldsymbol{G} \geq \boldsymbol{G}^T + \boldsymbol{G} - \boldsymbol{P}^{-1} \tag{2.37}$$

Therefore, a sufficient condition for (2.33) is given by (2.20b) by substituting $\boldsymbol{S} = \boldsymbol{P}^{-1}$, $\boldsymbol{W} = \boldsymbol{KG}$ and $\alpha = 1/\kappa$.

For solving the minimization problem (2.19) the matrix substitution $\boldsymbol{S} = \boldsymbol{P}^{-1}$ in the stability constraint (2.20b) needs to be considered. Thus, $\mathrm{tr}(\boldsymbol{S}^{-1})$ represents an equivalent objective function to (2.19). Since trace of the inverse $\mathrm{tr}(\boldsymbol{S}^{-1})$ is a convex function [BV04, p.118], the problem can be numerically efficiently solved in MATLAB by using toolbox CVX, a package for specifying and solving convex programs [GB13,GB08]. This completes the proof. □

The synthesis procedure produces a control gain $\boldsymbol{K}$ minimizing the upper-bound of the cost function (2.5) for a given σ in (2.14) and measurement interval h. In the examples shown in Section 2.3 it can be seen that the costs can be kept low by adapting $\boldsymbol{K}$ according to the synthesis procedure even when σ increases. When σ is chosen very small, the generated control gain $\boldsymbol{K}$ is very close to the LQR control gain under periodic control.

2.2.2 Controller Synthesis Based on Control Input Error

In this subsection sufficient conditions for the controller synthesis based on the control input error that is often used as event-triggering conditions [DH12, HDT13] are given. Consider the event-triggering condition

$$\|\boldsymbol{K}(\hat{\boldsymbol{z}}^+(k-1) - \boldsymbol{z}(k))\|_2 > \sigma\|\boldsymbol{K}\boldsymbol{z}(k)\|_2 \tag{2.38}$$

where $\boldsymbol{K}$ is obtained after the controller synthesis and $\sigma \in \mathbb{R}^+$. Correspondingly, (2.4) can be rewritten as

$$\hat{\boldsymbol{z}}^+(k) = \begin{cases} \boldsymbol{z}(k) & \text{if } \|\boldsymbol{K}(\hat{\boldsymbol{z}}^+(k-1)-\boldsymbol{z}(k))\|_2 > \sigma\|\boldsymbol{K}\boldsymbol{z}(k)\|_2 \\ \hat{\boldsymbol{z}}^+(k-1) & \text{if } \|\boldsymbol{K}(\hat{\boldsymbol{z}}^+(k-1)-\boldsymbol{z}(k))\|_2 \le \sigma\|\boldsymbol{K}\boldsymbol{z}(k)\|_2 \end{cases} \tag{2.39}$$

Based on (2.39) now define the error variable

$$\boldsymbol{e}^+(k) = \boldsymbol{K}\hat{\boldsymbol{z}}^+(k) - \boldsymbol{K}\boldsymbol{z}(k). \tag{2.40}$$

Equivalently

$$\|\boldsymbol{e}^+(k)\|_2 \le \sigma\|\boldsymbol{K}\boldsymbol{z}(k)\|_2 \tag{2.41}$$

is always satisfied in the time interval $(t_k, t_{k+1}]$. The equivalent expression for (2.41) is

$$\begin{pmatrix} \boldsymbol{z}(k) \\ \boldsymbol{e}^+(k) \end{pmatrix}^T \begin{pmatrix} \sigma^2\boldsymbol{K}^T\boldsymbol{K} & \boldsymbol{0} \\ \boldsymbol{0} & -\boldsymbol{I} \end{pmatrix} \begin{pmatrix} \boldsymbol{z}(k) \\ \boldsymbol{e}^+(k) \end{pmatrix} \ge 0. \tag{2.42}$$

The closed-loop system (2.2) can be rewritten as

$$\boldsymbol{z}(k+1) = (\boldsymbol{\Phi} + \boldsymbol{\Gamma}\boldsymbol{K})\boldsymbol{z}(k) + \boldsymbol{\Gamma}\boldsymbol{e}^+(k). \tag{2.43}$$

Based on the same Lyapunov function (2.16), stability constraint (2.17), and the resulting upper bound of the cost function (2.18) as in the previous subsection the problem for designing the event-triggering law and the control law can be formulated as follows

Problem 2.4 *For the closed-loop system* (2.43) *find an event-triggered controller* (2.3) *such that for a given σ the upper bound of the cost function* (2.9) *is minimized subject to condition* (2.41), *i.e.*

$$\min_{\boldsymbol{K}} tr(\boldsymbol{P}) \;\; \textit{subject to } (2.2) \textit{ and } (2.41). \tag{2.44}$$

Theorem 2.2 *A solution to Problem 2.4 is obtained from the LMI optimization problem*

$$\min tr(\boldsymbol{S}^{-1}) \quad \textit{subject to} \tag{2.45a}$$

$$\begin{pmatrix} \boldsymbol{G}^T+\boldsymbol{G}-\boldsymbol{S} & * & * & * & * \\ \boldsymbol{0} & (2-\alpha)\boldsymbol{I} & * & * & * \\ \boldsymbol{\Phi G}+\boldsymbol{\Gamma W} & \boldsymbol{\Gamma} & \boldsymbol{S} & * & * \\ \boldsymbol{W} & \boldsymbol{0} & \boldsymbol{0} & \frac{\alpha}{\sigma^2}\boldsymbol{I} & * \\ \begin{pmatrix}\boldsymbol{G}\\ \boldsymbol{W}\end{pmatrix} & \begin{pmatrix}\boldsymbol{0}\\ \boldsymbol{I}\end{pmatrix} & \boldsymbol{0} & \boldsymbol{0} & \boldsymbol{Q}_d^{-1} \end{pmatrix} > \boldsymbol{0} \tag{2.45b}$$

with the LMI variables $\boldsymbol{S}\in\mathbb{R}^{(n+m)\times(n+m)}$ *symmetric and positive definite,* $\boldsymbol{W}\in\mathbb{R}^{m\times(n+m)}$ *unrestricted,* $\boldsymbol{G}\in\mathbb{R}^{(n+m)\times(n+m)}$ *invertible and* $\alpha>0$*. The control gain and the Lyapunov matrix result from*

$$\boldsymbol{K}=\boldsymbol{W}\boldsymbol{G}^{-1}, \quad \boldsymbol{P}=\boldsymbol{S}^{-1}.$$

Proof. Search similarly for a Lyapunov function $\boldsymbol{z}(k)^T\boldsymbol{P}\boldsymbol{z}(k)$, $\boldsymbol{P}\in\mathbb{R}^{(n+m)\times(n+m)}$ is symmetric positive definite and control gain $\boldsymbol{K}$ under the constraint (2.41) which is stepwise penalized

$$\boldsymbol{z}(k)^T\boldsymbol{P}\boldsymbol{z}(k)-\boldsymbol{z}(k+1)^T\boldsymbol{P}\boldsymbol{z}(k+1)\geq\Delta J(h). \tag{2.46}$$

Consider $\Delta J(h)$ in (2.7)

$$\begin{aligned} J(h) &= \begin{pmatrix}\boldsymbol{z}(k)\\ \boldsymbol{u}(k)\end{pmatrix}^T \boldsymbol{Q}_{dc}\begin{pmatrix}\boldsymbol{z}(k)\\ \boldsymbol{u}(k)\end{pmatrix} \\ &= \begin{pmatrix}\boldsymbol{z}(k)\\ \boldsymbol{e}^+(k)+\boldsymbol{K}\boldsymbol{z}(k)\end{pmatrix}^T \boldsymbol{Q}_{dc}\begin{pmatrix}\boldsymbol{z}(k)\\ \boldsymbol{e}^+(k)+\boldsymbol{K}\boldsymbol{z}(k)\end{pmatrix} \\ &= \begin{pmatrix}\boldsymbol{z}(k)\\ \boldsymbol{e}^+(k)\end{pmatrix}^T \begin{pmatrix}\hat{\boldsymbol{Q}}_{11} & \hat{\boldsymbol{Q}}_{12}\\ \hat{\boldsymbol{Q}}_{12}^T & \hat{\boldsymbol{Q}}_{22}\end{pmatrix}\begin{pmatrix}\boldsymbol{z}(k)\\ \boldsymbol{e}^+(k)\end{pmatrix}, \end{aligned} \tag{2.47}$$

where

$$\begin{aligned} \hat{\boldsymbol{Q}}_{11} &= \boldsymbol{Q}_{dc,11}+\boldsymbol{Q}_{dc,12}\boldsymbol{K}+\boldsymbol{K}^T\boldsymbol{Q}_{dc,12}^T+\boldsymbol{K}^T\boldsymbol{Q}_{dc,22}\boldsymbol{K}, \\ \hat{\boldsymbol{Q}}_{12} &= \boldsymbol{Q}_{dc,12}+\boldsymbol{K}^T\boldsymbol{Q}_{dc,22}\boldsymbol{K}, \\ \hat{\boldsymbol{Q}}_{22} &= \boldsymbol{Q}_{dc,22} \end{aligned}$$

And further it can be written

$$\begin{pmatrix}\hat{\boldsymbol{Q}}_{11} & \hat{\boldsymbol{Q}}_{12}\\ \hat{\boldsymbol{Q}}_{12}^T & \hat{\boldsymbol{Q}}_{22}\end{pmatrix} = \begin{pmatrix}\boldsymbol{I} & \boldsymbol{K}^T\\ \boldsymbol{0} & \boldsymbol{I}\end{pmatrix}\boldsymbol{Q}_{dc}\begin{pmatrix}\boldsymbol{I} & \boldsymbol{0}\\ \boldsymbol{K} & \boldsymbol{I}\end{pmatrix} \tag{2.48}$$

Substitute the model (2.43) and $\Delta J(h)$ from (2.47) into (2.46)

$$\begin{pmatrix}\boldsymbol{z}(k)\\ \boldsymbol{e}^+(k)\end{pmatrix}^T \hat{\boldsymbol{P}}_3\begin{pmatrix}\boldsymbol{z}(k)\\ \boldsymbol{e}^+(k)\end{pmatrix} > 0 \tag{2.49}$$

with

$$\hat{\boldsymbol{P}}_3 = \begin{pmatrix} \boldsymbol{P} - \boldsymbol{\Phi}_c^T \boldsymbol{P} \boldsymbol{\Phi}_c - \hat{\boldsymbol{Q}}_{11} & -\boldsymbol{\Phi}_c^T \boldsymbol{P} \boldsymbol{\Gamma} - \hat{\boldsymbol{Q}}_{12} \\ -\boldsymbol{\Gamma}^T \boldsymbol{P} \boldsymbol{\Phi}_c - \hat{\boldsymbol{Q}}_{12}^T & -\boldsymbol{\Gamma}^T \boldsymbol{P} \boldsymbol{\Gamma} - \hat{\boldsymbol{Q}}_{22} \end{pmatrix} \tag{2.50}$$

Applying the lossless S-procedure allows to combine the inequalities (2.49) and (2.42) to

$$\begin{pmatrix} \boldsymbol{P} - \boldsymbol{\Phi}_c^T \boldsymbol{P} \boldsymbol{\Phi}_c - \hat{\boldsymbol{Q}}_{11} - \kappa\sigma^2 \boldsymbol{K}^T \boldsymbol{K} & -\boldsymbol{\Phi}_c^T \boldsymbol{P} \boldsymbol{\Gamma} - \hat{\boldsymbol{Q}}_{12} \\ -\boldsymbol{\Gamma}^T \boldsymbol{P} \boldsymbol{\Phi}_c - \hat{\boldsymbol{Q}}_{12}^T & \kappa \boldsymbol{I} - \boldsymbol{\Gamma}^T \boldsymbol{P} \boldsymbol{\Gamma} - \hat{\boldsymbol{Q}}_{22} \end{pmatrix} > 0 \tag{2.51}$$

By using Schur complement (2.51) can be transformed into

$$\begin{pmatrix} \boldsymbol{P} - \hat{\boldsymbol{Q}}_{11} - \kappa\sigma^2 \boldsymbol{K}^T \boldsymbol{K} & * & * \\ -\hat{\boldsymbol{Q}}_{12}^T & \kappa \boldsymbol{I} - \hat{\boldsymbol{Q}}_{22} & * \\ \boldsymbol{\Phi}_c & \boldsymbol{\Gamma} & \boldsymbol{P}^{-1} \end{pmatrix} > 0 \tag{2.52}$$

Using Schur complement again (2.52) gives

$$\begin{pmatrix} \boldsymbol{P} - \hat{\boldsymbol{Q}}_{11} & * & * & * \\ -\hat{\boldsymbol{Q}}_{12}^T & \kappa \boldsymbol{I} - \hat{\boldsymbol{Q}}_{22} & * & * \\ \boldsymbol{\Phi}_c & \boldsymbol{\Gamma} & \boldsymbol{P}^{-1} & * \\ \boldsymbol{K} & \boldsymbol{0} & \boldsymbol{0} & \frac{1}{\kappa\sigma^2} \boldsymbol{I} \end{pmatrix} > 0 \tag{2.53}$$

Considering (2.48) in the application of Schur complement (2.53) yields

$$\begin{pmatrix} \boldsymbol{P} & * & * & * & * \\ \boldsymbol{0} & \kappa \boldsymbol{I} & * & * & * \\ \boldsymbol{\Phi}_c & \boldsymbol{\Gamma} & \boldsymbol{P}^{-1} & * & * \\ \boldsymbol{K} & \boldsymbol{0} & \boldsymbol{0} & \frac{1}{\kappa\sigma^2} \boldsymbol{I} & * \\ \begin{pmatrix} \boldsymbol{I} \\ \boldsymbol{K} \end{pmatrix} & \begin{pmatrix} \boldsymbol{0} \\ \boldsymbol{I} \end{pmatrix} & \boldsymbol{0} & \boldsymbol{0} & \boldsymbol{Q}_{dc}^{-1} \end{pmatrix} > 0 \tag{2.54}$$

Pre-/post-multiplying (2.54) by $\operatorname{diag}(\boldsymbol{G}, \boldsymbol{I}, \boldsymbol{I}, \boldsymbol{I}, \boldsymbol{I})$ results in

$$\begin{pmatrix} \boldsymbol{G}^T \boldsymbol{P} \boldsymbol{G} & * & * & * & * \\ \boldsymbol{0} & \kappa \boldsymbol{I} & * & * & * \\ \boldsymbol{\Phi}_c \boldsymbol{G} & \boldsymbol{\Gamma} & \boldsymbol{P}^{-1} & * & * \\ \boldsymbol{K} \boldsymbol{G} & \boldsymbol{0} & \boldsymbol{0} & \frac{1}{\kappa\sigma^2} \boldsymbol{I} & * \\ \begin{pmatrix} \boldsymbol{G} \\ \boldsymbol{K} \boldsymbol{G} \end{pmatrix} & \begin{pmatrix} \boldsymbol{0} \\ \boldsymbol{I} \end{pmatrix} & \boldsymbol{0} & \boldsymbol{0} & \boldsymbol{Q}_{dc}^{-1} \end{pmatrix} > 0 \tag{2.55}$$

Since the identity matrix $\boldsymbol{I}$ is symmetric and positive definite, also

$$\left(\kappa^{-1} \boldsymbol{I} - \boldsymbol{I}\right)^T \kappa \boldsymbol{I} \left(\kappa^{-1} \boldsymbol{I} - \boldsymbol{I}\right) \geq \boldsymbol{0} \tag{2.56}$$

holds as inversion and congruence transformation do not affect definiteness. The inequality (2.56) is equivalent to

$$\kappa \boldsymbol{I} \geq (2 - \kappa^{-1}) \boldsymbol{I}. \tag{2.57}$$

Therefore, a sufficient condition for (2.55) is given by (2.45b) by substituting $\boldsymbol{S} = \boldsymbol{P}^{-1}$, $\boldsymbol{W} = \boldsymbol{K}\boldsymbol{G}$ and $\alpha = 1/\kappa$. The proof is finished. □

2.3 Simulations and Comparisons

In this section several comparisons between the approaches proposed in this chapter and the ones in [HDT13, EDK10, LX11] are made. Because the delay issue is not considered in the work [HDT13, EDK10, LX11], $\tau = 0$ is set, which is only a special case of the approaches presented in this chapter. The focus of the comparisons includes the control performance and transmission reductions at the same measurement frequency. Generally, increasing σ in (2.14) and (2.41) means increasing the tolerance with respect to the errors, which plays a role in degrading control performance. However, the tolerance with respect to the errors enables the possibility of reducing the control input updates so that the transmission of control input signals is reduced. Since the two indices are contradictory, usually a compromise needs to be made. The design of controller and event-triggering condition can be biased to one of the two indices by tuning the design parameter σ. The transmission reduction is measured by the following ratio for the whole evaluation time. The evaluation time should last until the state of controlled system is very close to the equilibrium point.

$$R_{\text{event}} = \frac{\text{the number of control input updates}}{\text{the number of measurements}}. \tag{2.58}$$

Example 2.1 Consider the example used in [HDT13, Tab07] with the plant given by

$$\dot{\boldsymbol{x}}(t) = \begin{pmatrix} 0 & 1 \\ -2 & 3 \end{pmatrix} \boldsymbol{x}(t) + \begin{pmatrix} 0 \\ 1 \end{pmatrix} \boldsymbol{u}(t) + \begin{pmatrix} 1 \\ 0 \end{pmatrix} \boldsymbol{w}(t) \tag{2.59}$$

with input delay $\tau = 0$ and the state-feedback controller (2.3) with measurement interval $h = 0.05\,\text{s}$. In [HDT13] the control gain is given as $\boldsymbol{K} = \begin{pmatrix} 1 & 4 \end{pmatrix}$ and the event generator is given by (2.38). The whole simulation time is set to 50 s. The disturbance is set equivalent to [HDT13] as $\boldsymbol{w}(t) = \sin(0.8\pi t)$ from time instant $t = 10\,\text{s}$ to $t = 20\,\text{s}$. Additionally, $\boldsymbol{Q}_c = \text{diag}(100, 1)$ and $\boldsymbol{R}_c = 10$ are taken for the control input error based approach. The resulting costs with the initial state vector $\boldsymbol{x}(0) = \begin{pmatrix} 1 & 0 \end{pmatrix}^T$ and different values of σ are listed in Table 2.1 for the Control Input Error (CIE) based method presented in this chapter and the method from [HDT13].

σ	method from [HDT13]		CIE based method	
	R_{event}	J_∞	R_{event}	J_∞
0.01	92.66%	454	94.54%	385.85
0.1	55.06%	455.1	66.07%	384.25
0.24	36.41%	494.56	30.65%	384.1
0.34	27.28%	527.2	19.15%	393.95

Table 2.1: Comparison with method from [HDT13]

Based on the observation of the comparisons results, the cost for the results from [HDT13] increases with σ. However, the synthesized CIE based method is specified to minimize the cost function with adapted controllers so that the cost does not change

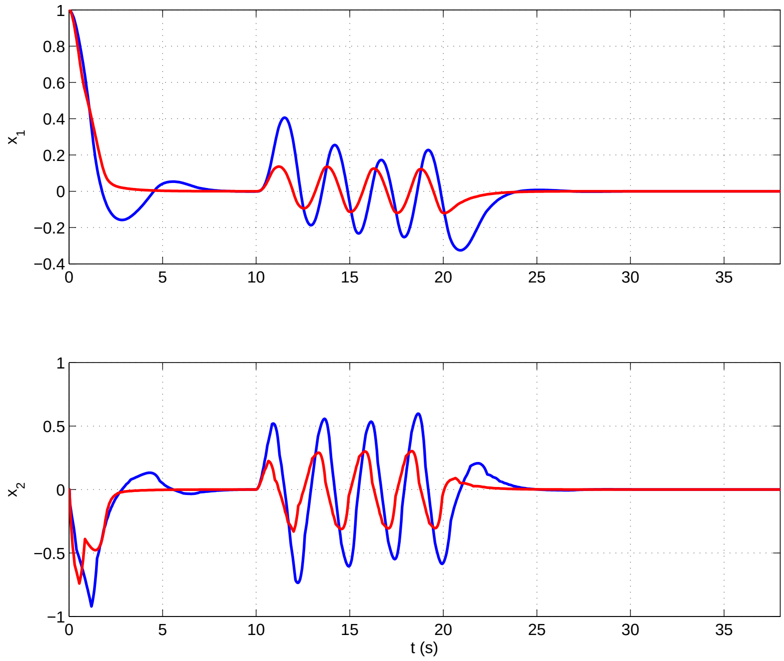

Figure 2.3: Transient dynamics under the control strategy from [HDT13] (blue) and the CIE based method (red) for $\sigma = 0.34$

too much comparatively. When σ is 0.1 or 0.01, the control input is updated more often in the CIE based method, but the costs are smaller. When σ is 0.24 or 0.34, the CIE based method gives a better result for both control performance and transmission reduction. The non-monotonic changes of the costs in the CIE based method with the increase of σ come from the adaption of the controller and their different reactions to the certain disturbance. When $\sigma = 0.34$ is picked, the transient dynamics are shown in Fig. 2.3. It clearly shows the CIE based method generates smaller oscillations in the amplitude of states.

Example 2.2 Consider the linearized fourth-order inverted pendulum system

$$\dot{\boldsymbol{x}}(t) = \begin{pmatrix} 0 & 1 & 0 & 0 \\ 0 & -1.001 & -0.5117 & 0 \\ 0 & 0 & 0 & 1 \\ 0 & 2.916 & 30.05 & 0 \end{pmatrix} \boldsymbol{x}(t) + \begin{pmatrix} 0 \\ 0.8455 \\ 0 \\ -2.461 \end{pmatrix} \boldsymbol{u}(t) \tag{2.60}$$

where the state vector $\boldsymbol{x} = \begin{pmatrix} x_1 & x_2 & x_3 & x_4 \end{pmatrix}^T$ consists of the cart position x_1, cart velocity x_2, angle of the pendulum x_3, and angular velocity of the pendulum x_4. This linear model is based on the real cart-pendulum system in Fig. 2.4. Now the State Error (SE) based method presented in this chapter is compared to the approaches in [EDK10] and [LX11]. In [EDK10, LX11] input-to-state stability of the controlled system

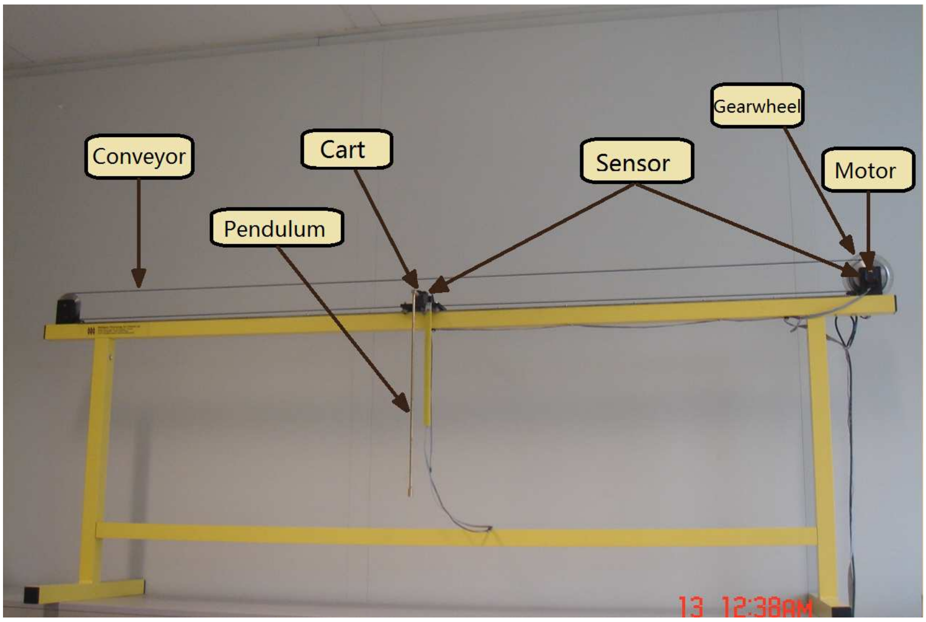

Figure 2.4: Cart-pendulum system

is considered. The parameter in event-triggering condition is determined by the derived criteria for input-to-state stability. In [LX11] additionally the controller is co-designed simultaneously with the event-triggering condition by letting the parameter in event-triggering condition be determined through solving LMIs. The measurement interval is taken as 12.5 ms and the simulation time is 20 s. The initial state vector is $\boldsymbol{x}(0) = \begin{pmatrix} 0 & 0 & 1 & 0 \end{pmatrix}^T$. The weighting matrices are $\boldsymbol{Q}_c = \text{diag}(35, 1, 80, 2)$ and $\boldsymbol{R}_c = 1$. The SE based event-generator (2.10) is used.

For the approach [EDK10] the control gain is calculated based on an LQR problem for the input-to-state stability as proposed in the example [EDK10, Section VI] which results in $\boldsymbol{K} = (5.417\ 7.212\ 43.351\ \ 7.959)$. The event triggering condition is computed independently from the control gain based on equation (16) in [EDK10] and leads to $\sigma = 1.13 \cdot 10^{-7}$. [LX11] proposes an extension of [EDK10] where the controller and event-triggering condition are designed jointly in a co-design scheme. Thereby the co-design is derived based on the input-to-state stability (ISS) condition. This results in $\boldsymbol{K} = \begin{pmatrix} 26.385 & 41.591 & 185.166 & 41.701 \end{pmatrix}$ and $\sigma = 5.22 \cdot 10^{-4}$. All the LMIs are solved by CVX. For the SE based approach presented in this chapter σ is chosen as 0.035 and correspondingly $\boldsymbol{K} = (6.868\ 10.352\ 56.531\ \ 11.335)$.

	R_{event}	cost
method from [EDK10]	100%	225.4
method from [LX11]	100%	597.3
SE based method	64.12%	235.1

Table 2.2: Comparison with methods from [EDK10] and [LX11]

With the given setup, for the approaches from [EDK10] and [LX11] a control update is required for each measurement interval. In contrast, the result from the SE based method requires control updates only for 64.12% of the measurement intervals. The reason for the low transmission reduction in [EDK10] and [LX11] can be found in the small value of σ. The control performances of [EDK10] and the SE based approach measured by the cost function (2.5) are close to each other. Please note that by adapting the control gain in [EDK10] a smaller transmission rate can be achieved. However this may result in a performance degradation and it is not clear how to design the controller to reduce the transmission rate. The result of [LX11] shows a high value of the cost function compared to the other approaches. This is due to the fact that [LX11] only considers ISS stability and does not optimize the costs. Further the codesign approach in [LX11] does not contain any design parameters in order to affect the transmission rate.

Since two event-triggered control design approaches are proposed it's interesting to make comparisons between them. With the same weighting matrices in the example the comparison results based on a variety of setups are given in Table. 2.3 and 2.4. In this example when there is no disturbance imposed on control input CIE based approach is always better for the two indices. When a disturbance $\sin(100t)$ is imposed on control input, for the index R_{event} SE based approach can achieve better performance as $\sigma = 0.02$ and $\sigma = 0.03$. But for the cost CIE based approach is always better. However a general conclusion that one approach outperforms the other can not be made. The results may vary with respect to different systems, initial state and disturbance.

σ	Performance	CIE	SE
0.01	Cost	225.4581	225.4959
	R_{event}	86.77%	99.88%
0.02	Cost	225.4727	226.267
	R_{event}	73.91%	83.9%
0.03	Cost	225.4967	229.956
	R_{event}	62.8%	69.1%

Table 2.3: Comparison between CIE based event-triggered control and SE based event-triggered control with initial state $\boldsymbol{x}(0) = (0\ 0\ 1\ 0)^T$ without disturbance

2.4 Experimental Implementation

In this section experimental results on the inverted pendulum system, whose model is already given in Example 2.2, are presented. The experiment uses microcontroller NXP LPC2294 as the computing unit (see Fig. 2.5). The ZOH function is implemented automatically by the pulse width modulator. The control structure is illustrated in Fig. 2.6. The states of the pendulum system are measured by encoders. The measured information is transmitted to the NXP LPC2294. Then, it is first processed by the

σ	Performance	CIE	SE
0.01	Cost	359.7561	359.8415
	R_{event}	97.38%	99.9%
0.02	Cost	359.7663	361.3853
	R_{event}	94.51%	93.51%
0.03	Cost	359.8125	368.7319
	R_{event}	93.13%	89.89%

Table 2.4: Comparison between CIE based event-triggered control and SE based event-triggered control with initial state $\boldsymbol{x}(0) = (0\ 0\ 1\ 0)^T$ with disturbance $\sin(100t)$ on control input

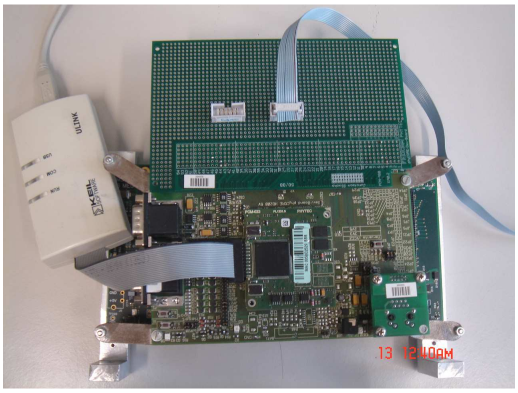

Figure 2.5: ARM LPC2294

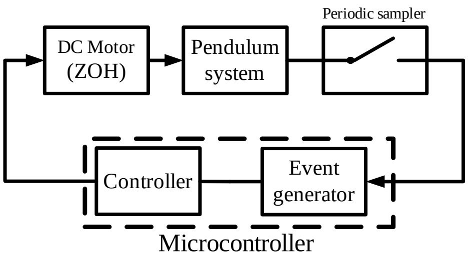

Figure 2.6: Control structure

event generator in the software level. If no events are triggered, the controller holds the previous control input value. New control inputs will not be calculated. The measurement interval is chosen as 12.5 ms. The whole experiment lasts 62.5 s. The weighting parameters $\boldsymbol{Q}_c = \text{diag}(55000, 1, 8000, 200)$ and $\boldsymbol{R}_c = 1$ are picked in order to generate a suitable control gain fitting the physical properties. The event-generator uses the condition (2.10) with $\sigma = 0.01$. The corresponding control gain is generated as $\boldsymbol{K} = \begin{pmatrix} 162.148 & 94.073 & 270.532 & 50.98 \end{pmatrix}$. One result is shown in Fig. 2.7 to demonstrate the applicability and effectiveness of the approach presented in this chapter. The events are recorded in the last sub-figure, where one means that the control input is updated

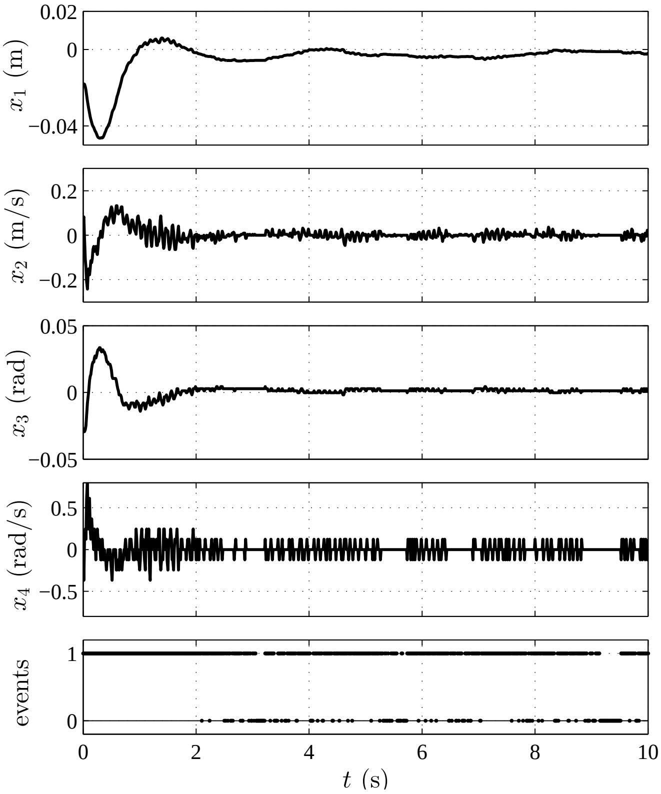

Figure 2.7: Experiment results

and zero otherwise. The ratio for events is $R_{\text{event}} = 74.35\%$. The other states can be stabilized very well around zero. The vibration of the pendulum is quite small. It implies that the control strategy is able to supply smooth transient control dynamics, which is good for the lifetime of mechanical systems.

2.5 Conclusion

In this chapter event-triggered synthesis approaches are studied. By synthesizing the feedback control gain and the event-triggering conditions in LMIs the upper bound of quadratic cost functions is minimized. The advantages of the presented approaches lie in: 1) The designed controller advocates to guarantee the optimal control performance despite the transmissions are reduced. 2) The stability is guaranteed in optimizing procedures. 3) The convenient implementation is important for real applications because of the low complexity in the control tasks and intuitive tuning parameters for obtaining a suitable control gain.

3 Event-Triggered Control Subject to Actuator Saturations

Basically in all practical systems the control input is constrained. If it is ignored in the control design the performance of the control system designed will seriously deteriorate, even render instability. Therefore this nonlinear characteristic demands specific stability analysis. This chapter first presents a criterion to analyse if a given ellipsoid is contractively invariant under an event-triggered control. Then by introducing an auxiliary feedback matrix an event-triggering condition and controller synthesis approach is presented aiming to maximize the contractive invariant set. The control design approach generates a unique control gain after solving an LMI optimization problem. The simulation results show that the selected design parameter of the event-triggering condition has large influence on the size of the contractive invariant ellipsoid.

3.1 Problem Formulation

In this chapter the considered plant is described by the continuous-time state equation subject to actuator saturation

$$\dot{\boldsymbol{x}}(t) = \boldsymbol{A}\boldsymbol{x}(t) + \boldsymbol{B}\mathrm{sat}(\boldsymbol{u}(t)), \tag{3.1}$$

where $\boldsymbol{x}(t) \in \mathbb{R}^n$ is the state vector, $\boldsymbol{A} \in \mathbb{R}^{n\times n}$ is the system matrix, $\boldsymbol{B} \in \mathbb{R}^{n\times m}$ is the input matrix, and $\boldsymbol{u}(t) \in \mathbb{R}^m$ is the control signal. $\mathrm{sat}(\cdot)$ is the standard saturation function, sat: $\mathbb{R}^m \to \mathbb{R}^m$ and $\mathrm{sat}(\boldsymbol{u}) = \big(\mathrm{sat}(u_1) \quad \cdots \quad \mathrm{sat}(u_m)\big)^T$, where $\mathrm{sat}(u_j) = \mathrm{sgn}(u_j)\min\{1, |u_j|\}$. The plant will be controlled in a periodic event-triggered way. The measurement is made periodically with the time interval h at the time instances $t_k, k \in \mathbb{N}_0$ with $h = t_{k+1} - t_k$. The control input is updated using ZOH.

Remark 3.1. If the control input is not saturated by one but another value, i.e. $\mathrm{sat}^*(u_j) = \mathrm{sgn}(u_j)\min\{u_{j\max}, |u_j|\}$, the model can be transformed to the form of (3.1) with an input saturation of one for all inputs. Assume the model is given by

$$\dot{\boldsymbol{x}}(t) = \boldsymbol{A}\boldsymbol{x}(t) + \boldsymbol{B}^*\mathrm{sat}^*(\boldsymbol{u}(t)) \tag{3.2}$$

with $\mathrm{sat}^*(\boldsymbol{u}) = \big(\mathrm{sat}^*(u_1) \quad \cdots \quad \mathrm{sat}^*(u_m)\big)^T$ which is equivalent to

$$\dot{\boldsymbol{x}}(t) = \boldsymbol{A}\boldsymbol{x}(t) + \boldsymbol{b}_1^*\mathrm{sat}^*(u_1) + ... + \boldsymbol{b}_m^*\mathrm{sat}^*(u_m) \tag{3.3}$$

where $\boldsymbol{B}^* = \begin{pmatrix} \boldsymbol{b}_1^* & \cdots & \boldsymbol{b}_m^* \end{pmatrix}$. The model (3.3) can also be written as

$$\dot{\boldsymbol{x}}(t) = \boldsymbol{A}\boldsymbol{x}(t) + \sum_{j=1}^{m} \left(\boldsymbol{b}_j^* u_{j\max}\right) \frac{\mathrm{sat}^*(u_j)}{u_{j\max}}. \tag{3.4}$$

Obviously $\frac{\mathrm{sat}^*(u_j)}{u_{j\max}}$ is saturated by one, i.e. $\mathrm{sat}(u_j) = \frac{\mathrm{sat}^*(u_j)}{u_{j\max}}$. Therefore, the model (3.1) and (3.2) are equivalent defining $\boldsymbol{B} = \begin{pmatrix} \boldsymbol{b}_1 & \cdots & \boldsymbol{b}_m \end{pmatrix}$ with $\boldsymbol{b}_j = \boldsymbol{b}_j^* u_{i\max}$ for all $j = \{1, ..., m\}$. Consequently, any linear plant (3.2) with arbitrary saturation bounds can be transformed into a model (3.1) with saturation bounds equal one.

The objective first is to obtain the estimate of the domain of attraction of the system (3.1) under periodic event-triggered control. To maximize the domain of attraction an event-generator and controller synthesis is to be investigated. The discretization of the model (3.1) using ZOH to a sampled-data system model with respect to the measurement interval h yields

$$\boldsymbol{x}(k+1) = \boldsymbol{\Phi}\boldsymbol{x}(k) + \boldsymbol{\Gamma}\mathrm{sat}\left(\boldsymbol{u}(k)\right) \tag{3.5}$$

with

$$\boldsymbol{\Phi} = e^{\boldsymbol{A}h}, \qquad \boldsymbol{\Gamma} = \int_0^h e^{\boldsymbol{A}s} ds \boldsymbol{B}$$

where $\boldsymbol{x}(k)$ is the measured state vector at the time instant t_k. In this chapter a full state-feedback control law is considered

$$\boldsymbol{u}(k) = \boldsymbol{K}\hat{\boldsymbol{x}}^+(k), \tag{3.6}$$

where $\hat{\boldsymbol{x}}^+(k)$ is a signal defined with

$$\hat{\boldsymbol{x}}^+(k) = \begin{cases} \boldsymbol{x}(k) & \text{if } \boldsymbol{u}(k) \text{ is updated} \\ \hat{\boldsymbol{x}}^+(k-1) & \text{if } \boldsymbol{u}(k) \text{ is not updated.} \end{cases} \tag{3.7}$$

and $\hat{\boldsymbol{x}}^+(k) = \boldsymbol{0}$ for $k \leq 0$ with the initial time $k_0 = 0$. The decision for control updates is made by the event-triggering condition which is

$$\|\hat{\boldsymbol{x}}^+(k-1) - \boldsymbol{x}(k)\|_2 > \sigma \|\boldsymbol{x}(k)\|_2 \tag{3.8}$$

where $\sigma \in \mathbb{R}^+$, i.e. the control input $\boldsymbol{u}(k)$ is updated if condition (3.8) holds. Based on the event-triggering condition (3.8), (3.7) can be rewritten as

$$\hat{\boldsymbol{x}}^+(k) = \begin{cases} \boldsymbol{x}(k) & \text{if } \|\hat{\boldsymbol{x}}^+(k-1) - \boldsymbol{x}(k)\|_2 > \sigma \|\boldsymbol{x}(k)\|_2 \\ \hat{\boldsymbol{x}}^+(k-1) & \text{if } \|\hat{\boldsymbol{x}}^+(k-1) - \boldsymbol{x}(k)\|_2 \leq \sigma \|\boldsymbol{x}(k)\|_2 \end{cases} \tag{3.9}$$

To investigate the attraction domain of system (3.5) the following definitions and Lemmas are introduced.

Notation 3.1 *Given a matrix $\boldsymbol{H} \in \mathbb{R}^{m \times n}$, denote the j-th row of $\boldsymbol{H}$ as $\boldsymbol{h}_j$ and a symmetric polyhedron is defined*

$$\mathcal{L}(\boldsymbol{H}) := \left\{\boldsymbol{x} \in \mathbb{R}^n : |\boldsymbol{h}_j \boldsymbol{x}| \leq 1, j \in \mathbb{J} = \{1, ..., m\}\right\}. \tag{3.10}$$

Notation 3.2 *Given a symmetric and positive definite matrix $\boldsymbol{P}$ and a positive scalar ρ, $\mathcal{E}(\boldsymbol{P}, \rho)$ represents the following ellipsoid*

$$\mathcal{E}(\boldsymbol{P}, \rho) = \left\{\boldsymbol{x} \in \mathbb{R}^n : \boldsymbol{x}^T \boldsymbol{P} \boldsymbol{x} \leq \rho\right\}. \tag{3.11}$$

Definition 3.1 *A set $\mathcal{M}$ is said to be an invariant set with respect to a dynamic system if all the trajectories starting from it will remain in it, i.e.*

$$\boldsymbol{x}(0) \in \mathcal{M} \quad \Rightarrow \quad \boldsymbol{x}(k) \in \mathcal{M} \;\; \forall k > 0.$$

Definition 3.2 *Given a Lyapunov function*

$$V(k) = \boldsymbol{x}^T(k) \boldsymbol{P} \boldsymbol{x}(k)$$

with $\boldsymbol{P}$ symmetric and positive definite the set $\mathcal{E}(\boldsymbol{P}, \rho)$ is called to be contractively invariant with respect to a dynamic system if

$$\Delta V(k) = \boldsymbol{x}(k+1)^T \boldsymbol{P} \boldsymbol{x}(k+1) - \boldsymbol{x}^T(k) \boldsymbol{P} \boldsymbol{x}(k) < 0 \tag{3.12}$$

for all $\boldsymbol{x} \in \mathcal{E}(\boldsymbol{P}, \rho) \backslash \{0\}$, i.e. the trajectories starting in the set $\mathcal{E}(\boldsymbol{P}, \rho)$ converge to the origin.

Notation 3.3 *Let $\mathcal{D}$ be the set of all combinations of $m \times m$ diagonal matrices whose diagonal elements are either 1 or 0. Then there are 2^m elements in $\mathcal{D}$. Denote each element of $\mathcal{D}$ as $\boldsymbol{D}_i, i = 1, 2, ..., 2^m$. Then $\mathcal{D} = \left\{\boldsymbol{D}_i : i \in \{1, ..., 2^m\}\right\}$. Denote $\boldsymbol{D}_i^- = \boldsymbol{I} - \boldsymbol{D}_i$ and define the set $\mathbb{I} = \{1, ..., 2^m\}$.*

Lemma 3.1 *[HLC02] Let $\boldsymbol{u}$, $\boldsymbol{\nu} \in \mathbb{R}^m$. Suppose $\|\boldsymbol{\nu}\|_\infty \leq 1$. Then*

$$sat(\boldsymbol{u}) \in co\left\{\boldsymbol{D}_i \boldsymbol{u} + \boldsymbol{D}_i^- \boldsymbol{\nu} : i \in \mathbb{I}\right\},$$

where $co\{\cdot\}$ denotes the convex hull of a set.

Proof. The proof is appended in section A.3.1. □

Lemma 3.2 *Given an ellipsoid $\mathcal{E}(\boldsymbol{P}, \rho)$ and a polyhedron $\mathcal{L}(\boldsymbol{H})$, if*

$$\begin{pmatrix} 1 & * \\ \boldsymbol{h}_j^T & \boldsymbol{P}/\rho \end{pmatrix} \geq 0, \quad j \in \mathbb{J}, \tag{3.13}$$

then $\mathcal{E}(\boldsymbol{P}, \rho) \subset \mathcal{L}(\boldsymbol{H})$.

Proof. The proof can be found in section A.3.2. □

3.2 Main Result

Define the error variable

$$\boldsymbol{e}^{+}(k) = \hat{\boldsymbol{x}}^{+}(k) - \boldsymbol{x}(k) \tag{3.14}$$

in the time interval $(t_k, t_{k+1}]$. Based on the definition (3.9) the inequality

$$\|\boldsymbol{e}^{+}(k)\| \leq \sigma \|\boldsymbol{x}(k)\| \tag{3.15}$$

is always satisfied. With the control input $\boldsymbol{u}(k) = \boldsymbol{K}\hat{\boldsymbol{x}}^{+}(k)$ the closed-loop system of (3.5) is given by

$$\boldsymbol{x}(k+1) = \boldsymbol{\Phi}\boldsymbol{x}(k) + \boldsymbol{\Gamma}\mathrm{sat}\left(\boldsymbol{K}\hat{\boldsymbol{x}}^{+}(k)\right). \tag{3.16}$$

3.2.1 Contractive Invariant Set

In the first part of this section a method is proposed for proving that a given ellipsoid is a contractively invariant set for a linear system with actuator saturation (3.5) which is controlled by the event-triggered control method (3.6), (3.9).

Theorem 3.1 *Given an ellipsoid $\mathcal{E}(\boldsymbol{P}, \rho)$, a control gain $\boldsymbol{K}$ and a positive scalar σ, if there exist a matrix $\boldsymbol{H} \in \mathbb{R}^{m \times n}$ and a scalar $\kappa \geq 0$ such that*

$$\begin{pmatrix} \boldsymbol{P} - \hat{\boldsymbol{\Phi}}_i^T \boldsymbol{P} \hat{\boldsymbol{\Phi}}_i - \kappa\sigma^2 \boldsymbol{I} & * \\ -\boldsymbol{\Theta}_i^T \boldsymbol{\Gamma}^T \boldsymbol{P} \hat{\boldsymbol{\Phi}}_i & \kappa \boldsymbol{I} - \boldsymbol{\Theta}_i^T \boldsymbol{\Gamma}^T \boldsymbol{P} \boldsymbol{\Gamma} \boldsymbol{\Theta}_i \end{pmatrix} > 0 \tag{3.17}$$

for all $i \in \mathbb{I}$ with $\hat{\boldsymbol{\Phi}}_i = \boldsymbol{\Phi} + \boldsymbol{\Gamma}(\boldsymbol{D}_i \boldsymbol{K} + \boldsymbol{D}_i^{-} \boldsymbol{H})$, $\boldsymbol{\Theta}_i = \boldsymbol{D}_i \boldsymbol{K} + \boldsymbol{D}_i^{-} \boldsymbol{H}$ and $\mathcal{E}(\boldsymbol{P}, \rho) \subset \mathcal{L}(\boldsymbol{H})$ i.e.

$$\begin{pmatrix} 1 & * \\ \boldsymbol{h}_j^T & \boldsymbol{P}/\rho \end{pmatrix} \geq 0 \quad \forall j \in \mathbb{J}, \tag{3.18}$$

then $\mathcal{E}(\boldsymbol{P}, \rho)$ is a contractively invariant set for the closed-loop system (3.16).

Proof. For a given ellipsoid $\mathcal{E}(\boldsymbol{P}, \rho)$, a corresponding quadratic Lyapunov function can be constructed by

$$V(k) = \boldsymbol{x}(k)^T \boldsymbol{P} \boldsymbol{x}(k). \tag{3.19}$$

Assume that the difference of the Lyapunov function $\Delta V(k) = V(k+1) - V(k)$ along the trajectories of the closed-loop system (3.16) satisfies

$$\boldsymbol{x}(k+1)^T \boldsymbol{P} \boldsymbol{x}(k+1) - \boldsymbol{x}(k)^T \boldsymbol{P} \boldsymbol{x}(k) < 0. \tag{3.20}$$

Substituting (3.16) in (3.20) results in

$$\begin{aligned} &\left(\boldsymbol{\Phi}\boldsymbol{x}(k) + \boldsymbol{\Gamma}\mathrm{sat}\left(\boldsymbol{K}\hat{\boldsymbol{x}}^{+}(k)\right)\right)^T \boldsymbol{P} \left(\boldsymbol{\Phi}\boldsymbol{x}(k) + \boldsymbol{\Gamma}\mathrm{sat}\left(\boldsymbol{K}\hat{\boldsymbol{x}}^{+}(k)\right)\right) \\ &- \boldsymbol{x}(k)^T \boldsymbol{P} \boldsymbol{x}(k) < 0, \end{aligned} \tag{3.21}$$

$\forall \boldsymbol{x}(k) \in \mathcal{E}(\boldsymbol{P}, \rho) \setminus \{0\}$. According to the constraint $\mathcal{E}(\boldsymbol{P}, \rho) \subset \mathcal{L}(\boldsymbol{H})$ it yields

$$|\boldsymbol{h}_j \boldsymbol{x}(k)| \leq 1, \quad \forall \boldsymbol{x}(k) \in \mathcal{E}(\boldsymbol{P}, \rho), \quad j \in \mathbb{J}. \tag{3.22}$$

The definition of the variable $\hat{\boldsymbol{x}}^+(k)$ in (3.7) yields

$$\hat{\boldsymbol{x}}^+(k) \in \mathcal{E}(\boldsymbol{P}, \rho), \quad \forall \boldsymbol{x}(k) \in \mathcal{E}(\boldsymbol{P}, \rho).$$

Thus $\|\boldsymbol{H}\hat{\boldsymbol{x}}^+(k)\|_\infty \leq 1$. Based on Lemma 3.1

$$\text{sat}\left(\boldsymbol{K}\hat{\boldsymbol{x}}^+(k)\right) \in \text{co}\left\{\boldsymbol{D}_i \boldsymbol{K}\hat{\boldsymbol{x}}^+(k) + \boldsymbol{D}_i^- \boldsymbol{H}\hat{\boldsymbol{x}}^+(k) : i \in \mathbb{I}\right\}. \tag{3.23}$$

It follows that

$$\boldsymbol{\Phi}\boldsymbol{x}(k) + \boldsymbol{\Gamma}\text{sat}\left(\boldsymbol{K}\hat{\boldsymbol{x}}^+(k)\right) \in \text{co}\left\{\boldsymbol{\Phi}\boldsymbol{x}(k) + \boldsymbol{\Gamma}\boldsymbol{\Theta}_i \hat{\boldsymbol{x}}^+(k) : i \in \mathbb{I}\right\}. \tag{3.24}$$

with $\boldsymbol{\Theta}_i = (\boldsymbol{D}_i \boldsymbol{K} + \boldsymbol{D}_i^- \boldsymbol{H})$. The convexity of the quadratic function (3.19) gives

$$\begin{aligned}
&\left(\boldsymbol{\Phi}\boldsymbol{x}(k) + \boldsymbol{\Gamma}\text{sat}\left(\boldsymbol{K}\hat{\boldsymbol{x}}^+(k)\right)\right)^T \boldsymbol{P} \left(\boldsymbol{\Phi}\boldsymbol{x}(k) + \boldsymbol{\Gamma}\text{sat}\left(\boldsymbol{K}\hat{\boldsymbol{x}}^+(k)\right)\right) \\
&\leq \max_{i \in \mathbb{I}} \left(\boldsymbol{\Phi}\boldsymbol{x}(k) + \boldsymbol{\Gamma}\boldsymbol{\Theta}_i \hat{\boldsymbol{x}}^+(k)\right)^T \boldsymbol{P} \left(\boldsymbol{\Phi}\boldsymbol{x}(k) + \boldsymbol{\Gamma}\boldsymbol{\Theta}_i \hat{\boldsymbol{x}}^+(k)\right).
\end{aligned} \tag{3.25}$$

Therefore a sufficient condition satisfying (3.21) is

$$\begin{aligned}
&\left(\boldsymbol{\Phi}\boldsymbol{x}(k) + \boldsymbol{\Theta}_i \hat{\boldsymbol{x}}^+(k)\right)^T \boldsymbol{P} \left(\boldsymbol{\Phi}\boldsymbol{x}(k) + \boldsymbol{\Theta}_i \hat{\boldsymbol{x}}^+(k)\right) \\
&- \boldsymbol{x}(k)^T \boldsymbol{P} \boldsymbol{x}(k) < 0, \quad \forall i \in \mathbb{I}.
\end{aligned} \tag{3.26}$$

By substituting (3.14) into (3.26) we have

$$\boldsymbol{\Phi}\boldsymbol{x}(k) + \boldsymbol{\Gamma}\boldsymbol{\Theta}_i \hat{\boldsymbol{x}}^+(k) = (\boldsymbol{\Phi} + \boldsymbol{\Gamma}\boldsymbol{\Theta}_i)\, \boldsymbol{x}(k) + \boldsymbol{\Gamma}\boldsymbol{\Theta}_i \boldsymbol{e}^+(k). \tag{3.27}$$

Defining $\hat{\boldsymbol{\Phi}}_i = \boldsymbol{\Phi} + \boldsymbol{\Gamma}(\boldsymbol{D}_i \boldsymbol{K} + \boldsymbol{D}_i^- \boldsymbol{H})$ and substituting (3.27) into (3.26) yields

$$\begin{pmatrix} \boldsymbol{x}(k) \\ \boldsymbol{e}^+(k) \end{pmatrix}^T \hat{\boldsymbol{P}}_1 \begin{pmatrix} \boldsymbol{x}(k) \\ \boldsymbol{e}^+(k) \end{pmatrix} > 0 \tag{3.28}$$

with

$$\hat{\boldsymbol{P}}_1 = \begin{pmatrix} \boldsymbol{P} - \hat{\boldsymbol{\Phi}}_i^T \boldsymbol{P} \hat{\boldsymbol{\Phi}}_i & * \\ -\boldsymbol{\Theta}_i^T \boldsymbol{\Gamma}^T \boldsymbol{P} \hat{\boldsymbol{\Phi}}_i & -\boldsymbol{\Theta}_i^T \boldsymbol{\Gamma}^T \boldsymbol{P} \boldsymbol{\Gamma} \boldsymbol{\Theta}_{\boldsymbol{i}} \end{pmatrix}. \tag{3.29}$$

The constraint (3.15) can be rewritten as

$$\begin{pmatrix} \boldsymbol{x}(k) \\ \boldsymbol{e}^+(k) \end{pmatrix}^T \begin{pmatrix} \sigma^2 \boldsymbol{I} & \boldsymbol{0} \\ \boldsymbol{0} & -\boldsymbol{I} \end{pmatrix} \begin{pmatrix} \boldsymbol{x}(k) \\ \boldsymbol{e}^+(k) \end{pmatrix} \geq 0 \tag{3.30}$$

Applying the lossless S-procedure allows to combine the inequalities (3.28) and (3.30) to (3.17). The constraint $\mathcal{E}(\boldsymbol{P}, \rho) \subset \mathcal{L}(\boldsymbol{H})$ can be expressed as the LMI (3.18) via Lemma 3.2. This completes the proof. □

Theorem 3.1 can be extended to maximize the volume of the ellipsoid by maximizing the level value ρ for a given matrix $\boldsymbol{P}$.

Corollary 3.1 *A maximization of the level value ρ is obtained for a given $\sigma > 0$ by the LMI optimization problem*

$$\max \rho \text{ subject to } (3.17) \text{ and } (3.18) \tag{3.31}$$

with the LMI variables $\boldsymbol{H} \in \mathbb{R}^{m \times n}$ and $\kappa \geq 0$.

Simulation Example

The result about contractive region can be illustrated by the following example

Example 3.1 Consider the inverted pendulum as shown in Fig. 3.1. The relationship between σ in event-triggering condition (3.8) and the level value ρ of the ellipsoidal contractive invariant set is to be investigated. The linearized dynamic model of the inverted pendulum is given by

$$\begin{pmatrix} \dot{\phi}(t) \\ \ddot{\phi}(t) \end{pmatrix} = \begin{pmatrix} 0 & 1 \\ \frac{(m+M)g}{M\ell} & 0 \end{pmatrix} \begin{pmatrix} \phi(t) \\ \dot{\phi}(t) \end{pmatrix} + \begin{pmatrix} 0 \\ \frac{-1}{M\ell} \end{pmatrix} \text{sat}(u(t)).$$

where ϕ is the pendulum angle, u is the force acting on the cart with the pendulum mass $m = 0.1\,\text{kg}$, the cart mass $M = 0.1\,\text{kg}$, and the pendulum length $\ell = 0.136\,\text{m}$. Gravitational acceleration is considered here equal to $g = 9.81\,\text{m/s}^2$. The saturation bound is $u_{\max} = 1$ and the discretization interval is $h = 10\,\text{ms}$ such that the sampled-data system is

$$\boldsymbol{x}(k+1) = \begin{pmatrix} 1.0018 & 0.01 \\ 0.36 & 1.0018 \end{pmatrix} \boldsymbol{x}(k) + \begin{pmatrix} -0.001 \\ -0.184 \end{pmatrix} \text{sat}(u(k)). \tag{3.32}$$

Further consider the given matrices for the analysis of contractive set

$$\boldsymbol{P} = \begin{pmatrix} 68.341 & 2.785 \\ 2.785 & 3.12 \end{pmatrix}, \quad \boldsymbol{K} = \begin{pmatrix} 5.394 & 5.024 \end{pmatrix}.$$

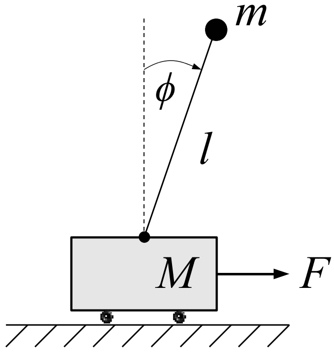

Figure 3.1: An inverted pendulum

The numerical results applying Corollary 3.1 are shown in Table 3.1 for a set of values of σ. In the last column the resulting update rate of a simulation lasting 10 seconds with an initial value $\boldsymbol{x}(0) = \begin{pmatrix}0.2 & 0.8\end{pmatrix}^T$ for each case is shown. The update rate is defined as ratio of number of events and number of samples in the simulation time.

σ	maximal ρ	$\boldsymbol{H}$	update rate
0.1	7.53	$\begin{pmatrix}2.638 & 0.413\end{pmatrix}$	15.2 %
0.06	8.92	$\begin{pmatrix}2.55 & 0.33\end{pmatrix}$	17.9 %
0.02	10.32	$\begin{pmatrix}2.443 & 0.269\end{pmatrix}$	37.0 %

Table 3.1

The visualization of the invariant ellipsoids and polyhedrons is shown in Fig. 3.2 for the linear system (3.32). The nonlinear behaviour of the pendulum system for large angles is not taken into account as the approach only considers linear systems. The results show an inverse relationship between σ and ρ, i.e. increasing σ in the event-triggering condition (3.8) decreases the volume of the contractive invariant set of system (3.16). This also shows that the size of contractive invariant set and the update rate are correlated, i.e. for achieving a smaller update rate the size of the contractive invariant set is reduced. In applications a compromise between the size of the contractive invariant set and the update rate needs to be found.

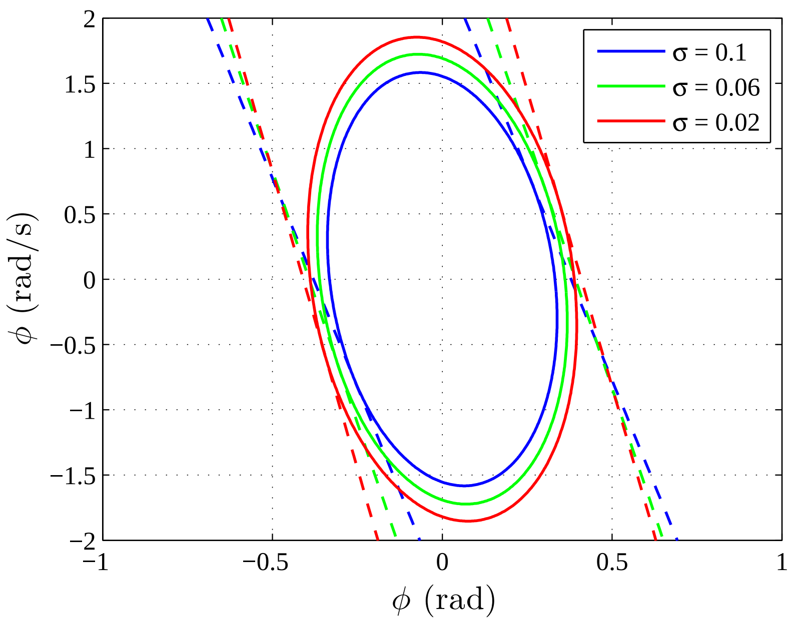

Figure 3.2: Invariant ellipsoids determined with different σ in the event-triggering condition (3.15)

In Fig. 3.3-3.4 the simulation results are shown for the event-triggered control approach with $\sigma = 0.1$. Fig. 3.3 shows the performance of the states and Fig. 3.4 shows the control input, the force on the cart in Newton. Especially in Fig. 3.4 it can be seen that in the beginning the control input is saturated and at every time instant t_k an event occurs. From $t = 0.09\,\mathrm{s}$ the control input is not saturated anymore as the state vector approaches the origin and events only occur sparsely.

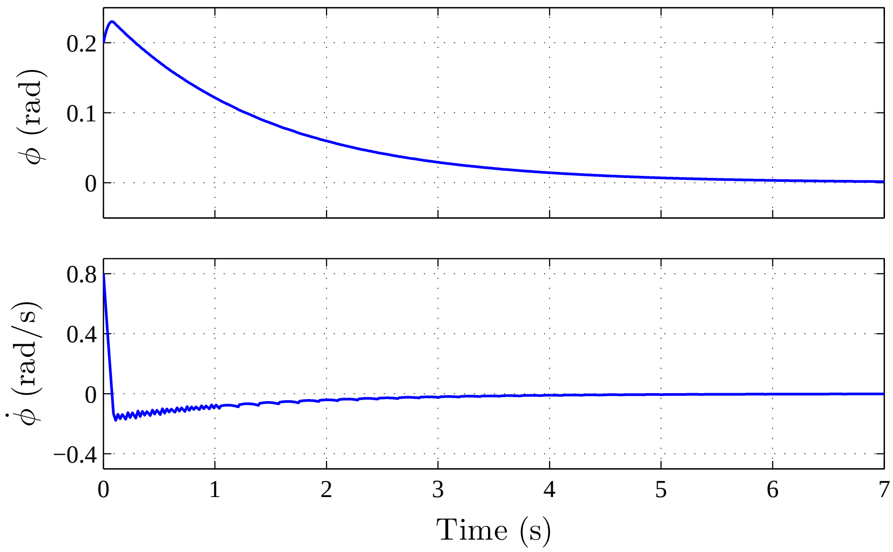

Figure 3.3: Simulation results for $\sigma = 0.1$

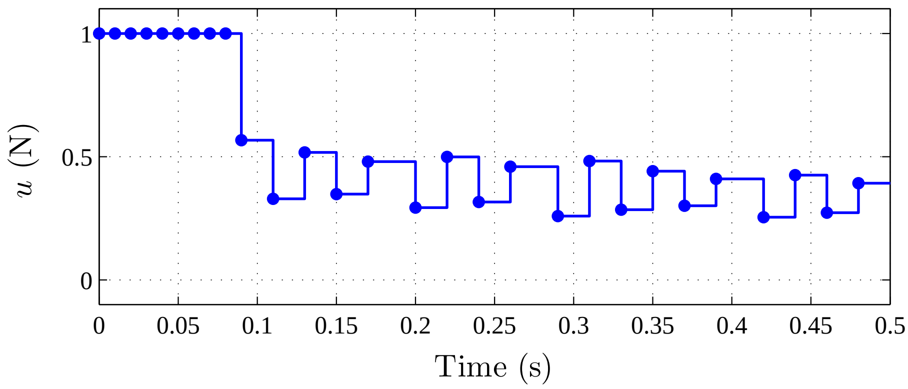

Figure 3.4: Control input for the simulation with $\sigma = 0.1$ where a circles indicate the appearance of an event

3.2.2 Controller Synthesis

In Corollary 3.1 a method to maximize the level of a given contractive invariant set for a controlled linear system with the event-triggered mechanism is presented. However an open problem is how to find the control matrix $\boldsymbol{K}$ and invariant set matrix $\boldsymbol{P}$. Therefore a controller synthesis is to be presented to design the invariant set jointly with the control matrix under the event-triggered control method. Thereby the aim is to maximize the size of the invariant ellipsoid for a given event-triggering parameter σ. One alternative to measure the geometrical size of the invariant ellipsoid is the volume, which is proportional to $(\det(\boldsymbol{P}^{-1}))^{1/2}$. Because of monotonic function $\log(\cdot)$, the maximization of $(\det(\boldsymbol{P}^{-1}))^{1/2}$ is equivalent to the maximization of $\operatorname{logdet}(\boldsymbol{P}^{-1})$. Straightforward considering the inverse of matrix $\boldsymbol{P}$, the maximization of $\operatorname{logdet}(\boldsymbol{P}^{-1})$ is equivalent to the minimization of $\operatorname{logdet}(\boldsymbol{P})$.

The problem can be stated as

Problem 3.1 *For the closed-loop system* (3.16) *find an event-triggered controller* (3.6) *such that for a given* σ *the volume of the invariant ellipsoid* $\mathcal{E}(\boldsymbol{P},1)$ *is maximized subject to condition* (3.15) *i.e.*

$$\begin{aligned}&\min_{\boldsymbol{K},\boldsymbol{P}} \textit{logdet}(\boldsymbol{P}) \;\; \textit{subject to } (3.16), (3.15) \textit{ and} \\ &\boldsymbol{x}(k+1)^T\boldsymbol{P}\boldsymbol{x}(k+1)-\boldsymbol{x}^T(k)\boldsymbol{P}\boldsymbol{x}(k)<0 \;\; \forall \boldsymbol{x}\in\mathcal{E}(\boldsymbol{P},\rho)\backslash\{0\}.\end{aligned} \tag{3.33}$$

Theorem 3.2 *A solution to Problem 3.1 is obtained from the LMI optimization problem*

$$\min -\textit{logdet}(\boldsymbol{S}) \quad \textit{subject to} \tag{3.34a}$$

$$\begin{pmatrix} 1 & * \\ \boldsymbol{w}_j^T & \boldsymbol{G}^T+\boldsymbol{G}-\boldsymbol{S}\end{pmatrix} \geq 0, \tag{3.34b}$$

$$\begin{pmatrix} \boldsymbol{G}^T+\boldsymbol{G}-\boldsymbol{S} & * & * & * \\ \boldsymbol{0} & \boldsymbol{G}^T+\boldsymbol{G}-\alpha\boldsymbol{I} & * & * \\ \boldsymbol{\Phi}\boldsymbol{G}+\boldsymbol{\Gamma}(\boldsymbol{\Theta_i}\boldsymbol{G}) & \boldsymbol{\Gamma}(\boldsymbol{\Theta_i}\boldsymbol{G}) & \boldsymbol{S} & * \\ \boldsymbol{G} & \boldsymbol{0} & \boldsymbol{0} & \frac{\alpha}{\sigma^2}\boldsymbol{I}\end{pmatrix} > 0 \tag{3.34c}$$

for all $(i,j)\in\mathbb{I}\times\mathbb{J}$ *with* $\boldsymbol{\Theta_i}\boldsymbol{G}=(\boldsymbol{D}_i\boldsymbol{K}+\boldsymbol{D}_i^-\boldsymbol{H})\boldsymbol{G}=(\boldsymbol{D}_i\boldsymbol{Y}+\boldsymbol{D}_i^-\boldsymbol{W})$ *and the LMI variables* $\boldsymbol{S}\in\mathbb{R}^{n\times n}$ *symmetric and positive definite,* $\boldsymbol{W}\in\mathbb{R}^{m\times n}$, $\boldsymbol{Y}\in\mathbb{R}^{m\times n}$ *unrestricted,* $\boldsymbol{w}_j$ *being the* j*-th row of* $\boldsymbol{W}$, $\boldsymbol{G}\in\mathbb{R}^{n\times n}$ *invertible and* $\alpha>0$. *The control gain and the Lyapunov matrix result from*

$$\boldsymbol{K}=\boldsymbol{Y}\boldsymbol{G}^{-1}, \quad \boldsymbol{P}=\boldsymbol{S}^{-1}.$$

Proof. Consider a quadratic Lyapunov function

$$V(k)=\boldsymbol{x}(k)^T\boldsymbol{P}\boldsymbol{x}(k). \tag{3.35}$$

Following the same lines as the proof of Theorem 3.1 it can be shown based on the inequality

$$\begin{pmatrix} \boldsymbol{P}-\hat{\boldsymbol{\Phi}}_i^T\boldsymbol{P}\hat{\boldsymbol{\Phi}}_i-\kappa\sigma^2\boldsymbol{I} & * \\ -\boldsymbol{\Theta}_i^T\boldsymbol{\Gamma}^T\boldsymbol{P}\hat{\boldsymbol{\Phi}}_i & \kappa\boldsymbol{I}-\boldsymbol{\Theta}_i^T\boldsymbol{\Gamma}^T\boldsymbol{P}\boldsymbol{\Gamma}\boldsymbol{\Theta}_i\end{pmatrix} > 0 \tag{3.36}$$

that $\Delta V(k) = V(k+1) - V(k) < 0$ along the trajectories of the closed-loop system (3.16) for all $\boldsymbol{x}(k) \in \mathcal{L}(\boldsymbol{H})\backslash\{0\}$. Applying the Schur complement (3.36) is equivalent to

$$\begin{pmatrix} \boldsymbol{P} - \kappa\sigma^2\boldsymbol{I} & * & * \\ \boldsymbol{0} & \kappa\boldsymbol{I} & * \\ \hat{\boldsymbol{\Phi}}_i & \boldsymbol{\Gamma\Theta}_i & \boldsymbol{P}^{-1} \end{pmatrix} > 0. \tag{3.37}$$

Using Schur-Complement again (3.37) is transformed to

$$\begin{pmatrix} \boldsymbol{P} & * & * & * \\ \boldsymbol{0} & \kappa\boldsymbol{I} & * & * \\ \hat{\boldsymbol{\Phi}}_i & \boldsymbol{\Gamma\Theta}_i & \boldsymbol{P}^{-1} & * \\ \boldsymbol{I} & \boldsymbol{0} & \boldsymbol{0} & \frac{1}{\kappa\sigma^2}\boldsymbol{I} \end{pmatrix} > 0. \tag{3.38}$$

Pre-/post-multiplying (3.38) by $\mathrm{diag}\big(\boldsymbol{G}^T, \boldsymbol{G}^T, \boldsymbol{I}, \boldsymbol{I}\big)$ and $\mathrm{diag}\big(\boldsymbol{G}, \boldsymbol{G}, \boldsymbol{I}, \boldsymbol{I}\big)$ respectively yields

$$\begin{pmatrix} \boldsymbol{G}^T\boldsymbol{P}\boldsymbol{G} & * & * & * \\ \boldsymbol{0} & \kappa\boldsymbol{G}^T\boldsymbol{G} & * & * \\ \hat{\boldsymbol{\Phi}}_i\boldsymbol{G} & \boldsymbol{\Gamma\Theta}_i\boldsymbol{G} & \boldsymbol{P}^{-1} & * \\ \boldsymbol{G} & \boldsymbol{0} & \boldsymbol{0} & \frac{1}{\kappa\sigma^2}\boldsymbol{I} \end{pmatrix} > 0. \tag{3.39}$$

Since the identity matrix $\boldsymbol{I}$ and $\boldsymbol{P}$ are symmetric and positive definite and $\kappa \geq 0$, also

$$\big(\kappa^{-1}\boldsymbol{I} - \boldsymbol{G}\big)^T \kappa\boldsymbol{I}\,\big(\kappa^{-1}\boldsymbol{I} - \boldsymbol{G}\big) \geq \boldsymbol{0} \tag{3.40}$$

$$\big(\boldsymbol{P}^{-1} - \boldsymbol{G}\big)^T \boldsymbol{P}\,\big(\boldsymbol{P}^{-1} - \boldsymbol{G}\big) \geq \boldsymbol{0} \tag{3.41}$$

hold as inversion and congruence transformation do not affect definiteness. The inequalities (3.40) and (3.41) are equivalent to

$$\kappa\boldsymbol{G}^T\boldsymbol{G} \geq \boldsymbol{G}^T + \boldsymbol{G} - \kappa^{-1}\boldsymbol{I} \tag{3.42}$$

$$\boldsymbol{G}^T\boldsymbol{P}\boldsymbol{G} \geq \boldsymbol{G}^T + \boldsymbol{G} - \boldsymbol{P}^{-1} \tag{3.43}$$

Therefore, a sufficient condition for (3.39) is

$$\begin{pmatrix} \boldsymbol{G}^T + \boldsymbol{G} - \boldsymbol{P}^{-1} & * & * & * \\ \boldsymbol{0} & \boldsymbol{G}^T + \boldsymbol{G} - \kappa^{-1}\boldsymbol{I} & * & * \\ \hat{\boldsymbol{\Phi}}_i\boldsymbol{G} & \boldsymbol{\Gamma\Theta}_i\boldsymbol{G} & \boldsymbol{P}^{-1} & * \\ \boldsymbol{G} & \boldsymbol{0} & \boldsymbol{0} & \frac{1}{\kappa\sigma^2}\boldsymbol{I} \end{pmatrix} > 0. \tag{3.44}$$

Substituting $\boldsymbol{S} = \boldsymbol{P}^{-1}$, $\boldsymbol{K} = \boldsymbol{Y}\boldsymbol{G}^{-1}$, $\boldsymbol{H} = \boldsymbol{W}\boldsymbol{G}^{-1}$ and $\alpha = 1/\kappa$ the inequalities (3.44) and (3.34c) are equivalent. Furthermore the constraint $\mathcal{E}(\boldsymbol{P}, 1) \subset \mathcal{L}(\boldsymbol{H})$ can be written as

$$\begin{pmatrix} 1 & * \\ \boldsymbol{h}_j^T & \boldsymbol{P} \end{pmatrix} \geq 0, \quad j \in \mathbb{J}. \tag{3.45}$$

Pre-/post-multiplying (3.45) $\mathrm{diag}(\boldsymbol{I}, \boldsymbol{G}^T)$ and $\mathrm{diag}(\boldsymbol{I}, \boldsymbol{G})$ respectively yields

$$\begin{pmatrix} 1 & * \\ \boldsymbol{G}^T \boldsymbol{h}_j^T & \boldsymbol{G}^T \boldsymbol{P} \boldsymbol{G} \end{pmatrix} \geq 0, \quad j \in \mathbb{J}. \tag{3.46}$$

Using (3.43) and substituting $\boldsymbol{w}_j^T = \boldsymbol{G}^T \boldsymbol{h}_j^T$ it is shown that (3.34b) is a sufficient condition for (3.46).

For inspecting the objective function Problem 3.1 we substitute $\boldsymbol{P} = \boldsymbol{S}^{-1}$. Since $-\mathrm{logdet}(\boldsymbol{S})$ is already defined in the MATLAB toolbox YALMIP [Lö04] it can be solved directly using the SeDuMi solver [Stu99]. This completes the proof. □

Remark 3.2. The presented results can be easily generalized to the case with delay in the model. The discretization of the delayed time-continuous can refer to Eq. (2.1). The augmented system (2.1) can be identically analyzed by using the presented approach in this chapter for the actuator saturation case.

Illustrative Example

To illustrate the controller synthesis result an example is presented as follows.

Example 3.2 Consider the second order inverted pendulum system (3.32) in Example 3.1 again. Table 3.2 gives the results from the application of Theorem 3.2 and from the

σ	$\boldsymbol{K}$	$\boldsymbol{H}$	update rate
0.1	$\begin{pmatrix}6.3717 & 2.6619\end{pmatrix}$	$\begin{pmatrix}2.2412 & 0.4264\end{pmatrix}$	21.8 %
0.06	$\begin{pmatrix}8.9800 & 2.3006\end{pmatrix}$	$\begin{pmatrix}2.1490 & 0.3805\end{pmatrix}$	50.6 %
0.02	$\begin{pmatrix}11.2366 & 1.9868\end{pmatrix}$	$\begin{pmatrix}2.1132 & 0.3549\end{pmatrix}$	99.9 %

Table 3.2

simulation with the initial state $\boldsymbol{x}(0) = \begin{pmatrix}0.2 & 0.8\end{pmatrix}^T$ and a simulation time of 10 seconds. Meanwhile Fig. 3.5 shows the corresponding contractive invariant ellipsoids. The obtained ellipsoids are always bigger than the ones from Example 3.1 with the random selected control gain and ellipsoidal estimate.

Fig. 3.6 shows the contractive invariant ellipsoids for $\sigma = 0.06$ from Corollary 3.1 with the ellipsoid and control gain parameters from Example 3.1 and Theorem 3.2 as well as the path under the initial state $\boldsymbol{x}(0) = \begin{pmatrix}-0.6303 & 1.426\end{pmatrix}$ (red). The initial state is chosen inside the estimated ellipsoid derived from Theorem 3.2 but outside the one obtained from Corollary 3.1. The path under the random controller (dashed) is obviously diverging and the controller synthesis allows to realize a larger ellipsoid such that the path (solid) is converging to the origin, which shows the effectiveness of the proposed controller synthesis approach.

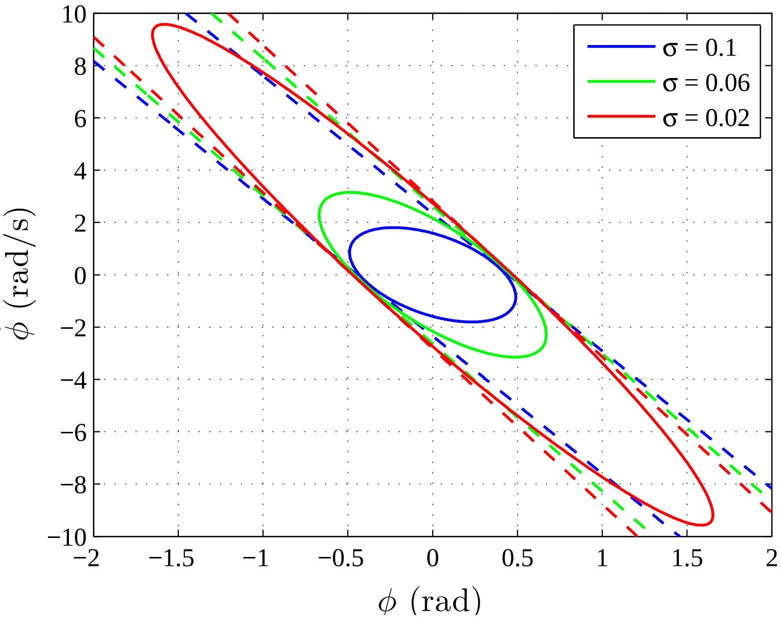

Figure 3.5: Invariant ellipsoids determined by controller synthesis for different σ

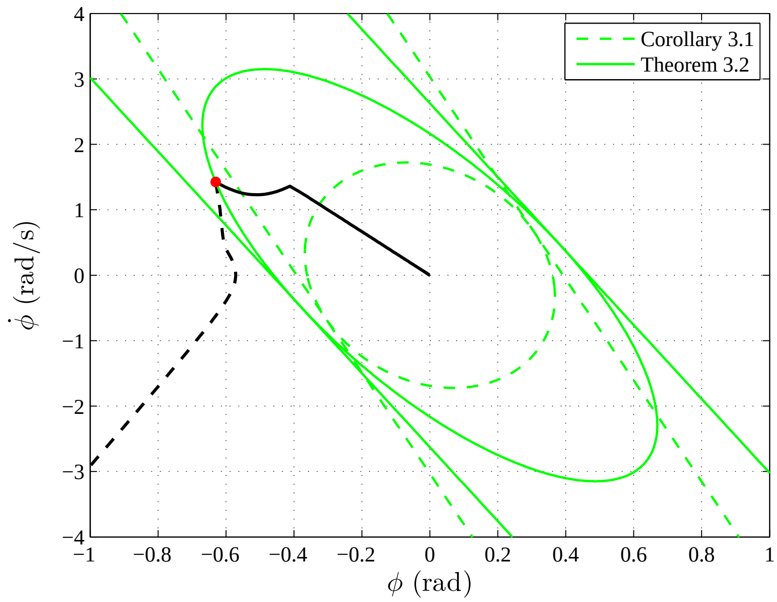

Figure 3.6: Comparison of Corollary 3.1 (dashed) and Theorem 3.2 (solid)

3.3 Conclusion

In this chapter an event-triggering condition and controller synthesis approach is studied for the linear system subject to actuator saturation. By synthesizing the feedback control gain and the event-triggering conditions in LMIs an optimization for obtaining the maximal contractive invariant set is achieved. Compared with the existing results in [LKJ12, KLJ12, SPTZ13] the results presented in this chaper allow the controller design in an optimization problem by the presented criteria, which is a new contribution to the event-triggered control.

4 Event-Triggered Control Subject to Bounded Disturbance

Tackling disturbance in system and control theory has received much attention for a long run. Analyzing the dynamics of control system suffering disturbance with the only knowledge of upper bound and lower bound is an alternative to stochastic techniques that need to know the statistical distribution of model errors and disturbance. This alternative looks to be more acceptable in practice in many situations [PNTN06]. For investigating the robustness of event-triggered control to exogenous disturbance, [HDT13, VGH13] derive a $\mathcal{L}_2$ gain for quantifying the control performance. In [HSB08] ultimate boundedness under the event-triggered control is studied by defining a region around the origin in which the control inputs are not updated. However in [HDT13, VGH13, HSB08] the exogenous disturbance is not explicitly considered in controller design. Additionally the controller design is considered separately from the event-triggering conditions. In this chapter the controller design is investigated jointly with event-triggering conditions aiming to reject the exogenous disturbance by minimizing the positively invariant set.

4.1 Problem Formulation

In this chapter the event-triggered control of a discrete-time linear system subject to time-varying but bounded disturbance is considered

$$\boldsymbol{z}(k+1) = \boldsymbol{\Phi}\boldsymbol{z}(k) + \boldsymbol{\Gamma}\boldsymbol{u}(k) + \boldsymbol{D}\boldsymbol{w}(k), \tag{4.1}$$

where $\boldsymbol{z}(k) \in \mathbb{R}^n$ is the state vector, $\boldsymbol{\Phi} \in \mathbb{R}^{n\times n}$ is the system matrix, $\boldsymbol{\Gamma} \in \mathbb{R}^{n\times m}$ is the input matrix, and $\boldsymbol{u}(k) \in \mathbb{R}^m$ is the control signal. $\boldsymbol{w}(k) \in \mathbb{R}^l$ is the disturbance vector with the disturbance input matrix $\boldsymbol{D} \in \mathbb{R}^{n\times l}$, where a derivation is given in appendix section A.4. Furthermore the boundedness of the disturbance is assumed

$$\boldsymbol{w}(k) \in \mathcal{W} := \{\boldsymbol{w}(k) | \|\boldsymbol{w}(k)\|_2 \leq 1\}. \tag{4.2}$$

Remark 4.1. In order derive the discrete-time system equation (4.1) from a continuous-time model please refer to Section A.4. Further, it is discussed how the system equation (4.1) is transformed to obtain the boundary of 1 in (4.2) for a disturbance signal arbitrarily bounded.

The event-triggered controller is considered by

$$\boldsymbol{u}(k) = \boldsymbol{K}\hat{\boldsymbol{z}}^{+}(k), \tag{4.3}$$

where $\hat{\boldsymbol{z}}^{+}(k)$ is a signal determined at k-th step with

$$\hat{\boldsymbol{z}}^{+}(k) = \begin{cases} \boldsymbol{z}(k) & \text{if } \boldsymbol{u}(k) \text{ is updated} \\ \hat{\boldsymbol{z}}^{+}(k-1) & \text{if } \boldsymbol{u}(k) \text{ is not updated.} \end{cases} \tag{4.4}$$

The decision for control updates is made by the event-triggering condition which is introduced in Section 4.2. With a disturbance of time-varying bounded uncertainty it is interesting to find the "smallest" compact set containing the origin by a synthesized control design (4.3) since it is impossible to achieve an asymptotical stability. First introduce the following definitions and notations.

Definition 4.1 *[Bla94] System* (4.1) *with the control* $\boldsymbol{u}(k) = \boldsymbol{K}\hat{\boldsymbol{z}}^{+}(k)$ *is said to be Uniformly Ultimately Bounded (UUB) in a convex and compact set* $\mathcal{S}$ *containing the origin in its interior iff for every initial condition* $\boldsymbol{z}(0) = \boldsymbol{z}_0$*, there exists* $T(\boldsymbol{z}_0)$ *such that for* $k \geq T(\boldsymbol{z}_0)$ *we have* $\boldsymbol{z}(k) \in \mathcal{S}$*.*

Notation 4.1 *Given a positive definite symmetric matrix* $\boldsymbol{P}$*,* $\mathcal{E}(\boldsymbol{P}, 1)$ *represents the following ellipsoid*

$$\mathcal{E}(\boldsymbol{P}, 1) = \left\{\boldsymbol{z} \in \mathbb{R}^n : \boldsymbol{z}^T\boldsymbol{P}\boldsymbol{z} \leq 1\right\} \tag{4.5}$$

In the following the ellipsoidal technique is used to prove that the system (4.1) under the event-triggered control to be proposed is UUB. The use of the ellipsoidal approximation is motivated by its simple structure and direct relationship with quadratic Lyapunov functions [KPK11, HLC02]. Furthermore LMI techniques can also be easily employed to help find the minimal invariant ellipsoid which represents the performance of disturbance rejection and design a controller by efficient optimization methods.

4.2 Main Result

In this section two different event-triggering conditions are studied based on the state error and the control input error respectively in order to derive corresponding controller.

4.2.1 State Error Based UUB Event-Triggered Control

Consider the event-triggering condition

$$\|\hat{\boldsymbol{z}}^{+}(k-1) - \boldsymbol{z}(k)\|_2 > \sigma\|\boldsymbol{z}(k)\|_2 \tag{4.6}$$

where $\sigma \in \mathbb{R}^+$. Based on this Eq. (4.4) can be rewritten as

$$\hat{\boldsymbol{z}}^+(k) = \begin{cases} \boldsymbol{z}(k) & \text{if } \|\hat{\boldsymbol{z}}^+(k-1) - \boldsymbol{z}(k)\|_2 > \sigma\|\boldsymbol{z}(k)\|_2 \\ \hat{\boldsymbol{z}}^+(k-1) & \text{if } \|\hat{\boldsymbol{z}}^+(k-1) - \boldsymbol{z}(k)\|_2 \leq \sigma\|\boldsymbol{z}(k)\|_2 \end{cases} \tag{4.7}$$

Now the controller synthesis problem proving that system (4.1) under event-triggering condition (4.7) by the ellipsoidal technique is UUB can be formulated as

Problem 4.1 *For the discrete-time system* (4.1) *find an event-triggered controller* (4.3), (4.7) *under the event-triggering condition* (4.6) *for a given σ such that there exist an ellipsoid $\mathcal{E}(\boldsymbol{P}, 1)$, in which the system* (4.1) *is UUB.*

Define the error variable

$$\boldsymbol{e}^+(k) = \hat{\boldsymbol{z}}^+(k) - \boldsymbol{z}(k). \tag{4.8}$$

Based on the definition (4.7) the inequality

$$\|\boldsymbol{e}^+(k)\|_2 \leq \sigma\|\boldsymbol{z}(k)\|_2 \tag{4.9}$$

is always satisfied at the k-th step. With the control input $\boldsymbol{u}(k) = \boldsymbol{K}\hat{\boldsymbol{z}}^+(k)$ and $\hat{\boldsymbol{z}}^+(k) = \boldsymbol{e}^+(k) + \boldsymbol{z}(k)$ the closed-loop system of (4.1) is given by

$$\boldsymbol{z}(k+1) = (\boldsymbol{\Phi} + \boldsymbol{\Gamma}\boldsymbol{K})\boldsymbol{z}(k) + \boldsymbol{\Gamma}\boldsymbol{K}\boldsymbol{e}^+(k) + \boldsymbol{D}\boldsymbol{w}(k). \tag{4.10}$$

This model (4.10) enables a closed-loop system with a state error. Then the solution to Problem 4.1 can be formulated:

Theorem 4.1 *For the discrete-time system* (4.1) *with a given σ in the event generator* (4.6)*, a given constant $\bar{\beta} \in (0, 1]$ and a constant $\alpha_2, 0 \leq \alpha_2 < \bar{\beta}$, if there exist the LMI variables $\boldsymbol{S} \in \mathbb{R}^{n\times n}$ symmetric and positive definite, $\boldsymbol{W} \in \mathbb{R}^{m\times n}$ unrestricted, $\kappa_3 \geq 0$, $\alpha_1 > 0$, $\boldsymbol{G} \in \mathbb{R}^{n\times n}$ invertible satisfying* (4.11)

$$\begin{pmatrix} (\bar{\beta} - \alpha_2)(\boldsymbol{G}^T + \boldsymbol{G} - \boldsymbol{S}) & * & * & * & * & * \\ \boldsymbol{0} & \boldsymbol{G}^T + \boldsymbol{G} - \alpha_1\boldsymbol{I} & * & * & * & * \\ \boldsymbol{0} & \boldsymbol{0} & \kappa_3\boldsymbol{I} & * & * & * \\ \boldsymbol{0} & \boldsymbol{0} & \boldsymbol{0} & \alpha_2 - \kappa_3 & * & * \\ \boldsymbol{\Phi}\boldsymbol{G} + \boldsymbol{\Gamma}\boldsymbol{W} & \boldsymbol{\Gamma}\boldsymbol{W} & \boldsymbol{D} & \boldsymbol{0} & \boldsymbol{S} & * \\ \boldsymbol{G} & \boldsymbol{0} & \boldsymbol{0} & \boldsymbol{0} & \boldsymbol{0} & \frac{\alpha_1}{\sigma^2}\boldsymbol{I} \end{pmatrix} > 0 \tag{4.11}$$

the system (4.1) *is UUB in $\mathcal{E}(\boldsymbol{P}, 1)$. The control gain and the Lyapunov matrix result from*

$$\boldsymbol{K} = \boldsymbol{W}\boldsymbol{G}^{-1}, \quad \boldsymbol{P} = \boldsymbol{S}^{-1}.$$

Proof. For designing the controller introduce the quadratic Lyapunov function

$$V(k) = \boldsymbol{z}(k)^T\boldsymbol{P}\boldsymbol{z}(k) \tag{4.12}$$

with $\boldsymbol{P} \in \mathbb{R}^{n\times n}$ symmetric and positive definite. Meanwhile the matrix $\boldsymbol{P}$ defines an ellipsoid $\mathcal{E}(\boldsymbol{P},1)$. Now a controller is to be searched for such that the difference of the Lyapunov function $\Delta V = V(k+1) - V(k)$ along the trajectories of the closed-loop system (4.10) for every $\boldsymbol{z}(k) \notin \mathcal{E}(\boldsymbol{P},1)$ satisfies

$$\Delta V < -\beta V(k), \tag{4.13}$$

where $\beta \in [0,1)$. By substituting (4.10) into (4.13) with the denotation $\boldsymbol{\Phi}_c = \boldsymbol{\Phi} + \boldsymbol{\Gamma}\boldsymbol{K}$ it requires to show

$$\begin{aligned}\Delta V = &(\boldsymbol{\Phi}_c\boldsymbol{z}(k) + \boldsymbol{\Gamma}\boldsymbol{K}\boldsymbol{e}^+(k) + \boldsymbol{D}\boldsymbol{w}(k))^T\boldsymbol{P}\\ &(\boldsymbol{\Phi}_c\boldsymbol{z}(k) + \boldsymbol{\Gamma}\boldsymbol{K}\boldsymbol{e}^+(k) + \boldsymbol{D}\boldsymbol{w}(k))\\ &- \boldsymbol{z}(k)^T\boldsymbol{P}\boldsymbol{z}(k) < -\beta\boldsymbol{z}(k)^T\boldsymbol{P}\boldsymbol{z}(k),\end{aligned} \tag{4.14}$$

Reorganizing (4.14) yields

$$\begin{pmatrix}\boldsymbol{z}(k)\\ \boldsymbol{e}^+(k)\\ \boldsymbol{w}(k)\\ 1\end{pmatrix}^T \hat{\boldsymbol{P}}_1 \begin{pmatrix}\boldsymbol{z}(k)\\ \boldsymbol{e}^+(k)\\ \boldsymbol{w}(k)\\ 1\end{pmatrix} > 0 \tag{4.15}$$

with

$$\hat{\boldsymbol{P}}_1 = \begin{pmatrix}\bar{\beta}\boldsymbol{P} - \boldsymbol{\Phi}_c^T\boldsymbol{P}\boldsymbol{\Phi}_c & * & * & *\\ -\boldsymbol{K}^T\boldsymbol{\Gamma}^T\boldsymbol{P}\boldsymbol{\Phi}_c & -\boldsymbol{K}^T\boldsymbol{\Gamma}^T\boldsymbol{P}\boldsymbol{\Gamma}\boldsymbol{K} & * & *\\ -\boldsymbol{D}^T\boldsymbol{P}\boldsymbol{\Phi}_c & -\boldsymbol{D}^T\boldsymbol{P}\boldsymbol{\Gamma}\boldsymbol{K} & -\boldsymbol{D}^T\boldsymbol{P}\boldsymbol{D} & *\\ \boldsymbol{0} & \boldsymbol{0} & \boldsymbol{0} & \boldsymbol{0}\end{pmatrix} \tag{4.16}$$

and $\bar{\beta} = 1 - \beta$. The constraint (4.9) can be rewritten as

$$\begin{pmatrix}\boldsymbol{z}(k)\\ \boldsymbol{e}^+(k)\\ \boldsymbol{w}(k)\\ 1\end{pmatrix}^T \begin{pmatrix}\sigma^2\boldsymbol{I} & \boldsymbol{0} & \boldsymbol{0} & \boldsymbol{0}\\ \boldsymbol{0} & -\boldsymbol{I} & \boldsymbol{0} & \boldsymbol{0}\\ \boldsymbol{0} & \boldsymbol{0} & \boldsymbol{0} & \boldsymbol{0}\\ \boldsymbol{0} & \boldsymbol{0} & \boldsymbol{0} & 0\end{pmatrix} \begin{pmatrix}\boldsymbol{z}(k)\\ \boldsymbol{e}^+(k)\\ \boldsymbol{w}(k)\\ 1\end{pmatrix} \geq 0. \tag{4.17}$$

$\boldsymbol{z}(k) \notin \mathcal{E}(\boldsymbol{P},1)$ can be rewritten as

$$\begin{pmatrix}\boldsymbol{z}(k)\\ \boldsymbol{e}^+(k)\\ \boldsymbol{w}(k)\\ 1\end{pmatrix}^T \begin{pmatrix}\boldsymbol{P} & \boldsymbol{0} & \boldsymbol{0} & \boldsymbol{0}\\ \boldsymbol{0} & \boldsymbol{0} & \boldsymbol{0} & \boldsymbol{0}\\ \boldsymbol{0} & \boldsymbol{0} & \boldsymbol{0} & \boldsymbol{0}\\ \boldsymbol{0} & \boldsymbol{0} & \boldsymbol{0} & -1\end{pmatrix} \begin{pmatrix}\boldsymbol{z}(k)\\ \boldsymbol{e}^+(k)\\ \boldsymbol{w}(k)\\ 1\end{pmatrix} > 0. \tag{4.18}$$

And Eq. (4.2) can be equivalently rewritten as

$$\begin{pmatrix}\boldsymbol{z}(k)\\ \boldsymbol{e}^+(k)\\ \boldsymbol{w}(k)\\ 1\end{pmatrix}^T \begin{pmatrix}\boldsymbol{0} & \boldsymbol{0} & \boldsymbol{0} & \boldsymbol{0}\\ \boldsymbol{0} & \boldsymbol{0} & \boldsymbol{0} & \boldsymbol{0}\\ \boldsymbol{0} & \boldsymbol{0} & -\boldsymbol{I} & \boldsymbol{0}\\ \boldsymbol{0} & \boldsymbol{0} & \boldsymbol{0} & 1\end{pmatrix} \begin{pmatrix}\boldsymbol{z}(k)\\ \boldsymbol{e}^+(k)\\ \boldsymbol{w}(k)\\ 1\end{pmatrix} \geq 0. \tag{4.19}$$

By S-procedure combine (4.15) with (4.17), (4.18) and (4.19) to (4.20) with variables $\kappa_i \geq 0, i = 1, 2, 3$

$$\begin{pmatrix} \bar{\beta}\boldsymbol{P} - \boldsymbol{\Phi}_c^T \boldsymbol{P} \boldsymbol{\Phi}_c - \kappa_1 \sigma^2 \boldsymbol{I} - \kappa_2 \boldsymbol{P} & * & * & * \\ -\boldsymbol{K}^T \boldsymbol{\Gamma}^T \boldsymbol{P} \boldsymbol{\Phi}_c & \kappa_1 \boldsymbol{I} - \boldsymbol{K}^T \boldsymbol{\Gamma}^T \boldsymbol{P} \boldsymbol{\Gamma} \boldsymbol{K} & * & * \\ -\boldsymbol{D}^T \boldsymbol{P} \boldsymbol{\Phi}_c & -\boldsymbol{D}^T \boldsymbol{P} \boldsymbol{\Gamma} \boldsymbol{K} & \kappa_3 \boldsymbol{I} - \boldsymbol{D}^T \boldsymbol{P} \boldsymbol{D} & * \\ \boldsymbol{0} & \boldsymbol{0} & \boldsymbol{0} & \kappa_2 - \kappa_3 \end{pmatrix} > 0 \tag{4.20}$$

By Schur-Complement (4.20) yields

$$\begin{pmatrix} (\bar{\beta} - \kappa_2)\boldsymbol{P} - \kappa_1 \sigma^2 \boldsymbol{I} & * & * & * & * \\ \boldsymbol{0} & \kappa_1 \boldsymbol{I} & * & * & * \\ \boldsymbol{0} & \boldsymbol{0} & \kappa_3 \boldsymbol{I} & * & * \\ \boldsymbol{0} & \boldsymbol{0} & \boldsymbol{0} & \kappa_2 - \kappa_3 & * \\ \boldsymbol{\Phi}_c & \boldsymbol{\Gamma} \boldsymbol{K} & \boldsymbol{D} & 0 & \boldsymbol{P}^{-1} \end{pmatrix} > 0 \tag{4.21}$$

Using Schur-Complement again (4.21) is equivalent to

$$\begin{pmatrix} (\bar{\beta} - \kappa_2)\boldsymbol{P} & * & * & * & * & * \\ \boldsymbol{0} & \kappa_1 \boldsymbol{I} & * & * & * & * \\ \boldsymbol{0} & \boldsymbol{0} & \kappa_3 \boldsymbol{I} & * & * & * \\ \boldsymbol{0} & \boldsymbol{0} & \boldsymbol{0} & \kappa_2 - \kappa_3 & * & * \\ \boldsymbol{\Phi}_c & \boldsymbol{\Gamma} \boldsymbol{K} & \boldsymbol{D} & 0 & \boldsymbol{P}^{-1} & * \\ \boldsymbol{I} & \boldsymbol{0} & \boldsymbol{0} & 0 & 0 & \frac{1}{\kappa_1 \sigma^2} \boldsymbol{I} \end{pmatrix} > 0 \tag{4.22}$$

Pre-/post-multiplying (4.22) by diag $\left(\boldsymbol{G}^T, \boldsymbol{G}^T, \boldsymbol{I}, \boldsymbol{I}, \boldsymbol{I}, \boldsymbol{I}\right)$ and its transposed one results in (4.23).

$$\begin{pmatrix} (1 - \kappa_2)\boldsymbol{G}^T \boldsymbol{P} \boldsymbol{G} & * & * & * & * & * \\ \boldsymbol{0} & \kappa_1 \boldsymbol{G}^T \boldsymbol{G} & * & * & * & * \\ \boldsymbol{0} & \boldsymbol{0} & \kappa_3 \boldsymbol{I} & * & * & * \\ \boldsymbol{0} & \boldsymbol{0} & \boldsymbol{0} & \kappa_2 - \kappa_3 & * & * \\ \boldsymbol{\Phi}_c \boldsymbol{G} & \boldsymbol{\Gamma} \boldsymbol{K} \boldsymbol{G} & \boldsymbol{D} & 0 & \boldsymbol{P}^{-1} & * \\ \boldsymbol{G} & \boldsymbol{0} & \boldsymbol{0} & 0 & 0 & \frac{1}{\kappa_1 \sigma^2} \boldsymbol{I} \end{pmatrix} > 0 \tag{4.23}$$

Since the identity matrix $\boldsymbol{I}$ and $\boldsymbol{P}$ are symmetric and positive definite, also

$$\left(\kappa_1^{-1} \boldsymbol{I} - \boldsymbol{G}\right)^T \kappa_1 \boldsymbol{I} \left(\kappa_1^{-1} \boldsymbol{I} - \boldsymbol{G}\right) \geq \boldsymbol{0} \tag{4.24}$$
$$\left(\boldsymbol{P}^{-1} - \boldsymbol{G}\right)^T \boldsymbol{P} \left(\boldsymbol{P}^{-1} - \boldsymbol{G}\right) \geq \boldsymbol{0} \tag{4.25}$$

hold as inversion and congruence transformation do not affect definiteness. The inequalities (4.24) and (4.25) are equivalent to

$$\kappa_1 \boldsymbol{G}^T \boldsymbol{G} \geq \boldsymbol{G}^T + \boldsymbol{G} - \kappa_1^{-1} \boldsymbol{I} \tag{4.26}$$
$$\boldsymbol{G}^T \boldsymbol{P} \boldsymbol{G} \geq \boldsymbol{G}^T + \boldsymbol{G} - \boldsymbol{P}^{-1} \tag{4.27}$$

Therefore, a sufficient condition for (4.23) is obtained by substituting $\boldsymbol{S} = \boldsymbol{P}^{-1}$, $\boldsymbol{W} = \boldsymbol{KG}$ and $\alpha_1 = 1/\kappa_1$

$$\begin{pmatrix} (\bar{\beta}-\kappa_2)(\boldsymbol{G}^T+\boldsymbol{G}-\boldsymbol{S}) & * & * & * & * & * \\ \boldsymbol{0} & \boldsymbol{G}^T+\boldsymbol{G}-\alpha_1\boldsymbol{I} & * & * & * & * \\ \boldsymbol{0} & \boldsymbol{0} & \kappa_3\boldsymbol{I} & * & * & * \\ \boldsymbol{0} & \boldsymbol{0} & \boldsymbol{0} & \kappa_2-\kappa_3 & * & * \\ \boldsymbol{\Phi G}+\boldsymbol{\Gamma W} & \boldsymbol{\Gamma W} & \boldsymbol{D} & \boldsymbol{0} & \boldsymbol{S} & * \\ \boldsymbol{G} & \boldsymbol{0} & \boldsymbol{0} & \boldsymbol{0} & \boldsymbol{0} & \frac{\alpha_1}{\sigma^2}\boldsymbol{I} \end{pmatrix} > 0. \tag{4.28}$$

The condition (4.28) is bilinear because of the term $(\bar{\beta}-\kappa_2)(\boldsymbol{G}^T+\boldsymbol{G}-\boldsymbol{S})$. However κ_2 need satisfy $0 \le \kappa_2 \le \bar{\beta} \le 1$ for holding the positive definiteness of (4.28). Using a gridding approach over the range $[0, \bar{\beta})$ the variable κ_2 can be found, i.e. κ_2 is increased from 0 to $\bar{\beta}$ with a given step size until condition (4.11) is satisfied. The found constant is set $\alpha_2 = \kappa_2 \in [0, \bar{\beta})$. It completes the proof here. □

Remark 4.2. An ellipsoid $\mathcal{E}(\boldsymbol{P}, 1)$ found in Theorem 4.1 is also a positively invariant set. This can be proved by showing $\boldsymbol{z}(k+1) \in \mathcal{E}(\boldsymbol{P}, 1)$ when $\boldsymbol{z}(k) \in \mathcal{E}(\boldsymbol{P}, 1)$, which can be guaranteed by the sufficient conditions in Theorem 4.1. A brief proof is given in the following Corollary.

Corollary 4.1 *For the discrete-time system* (4.1) *with a given* σ *in event generator* (4.6)*, a given constant* $\bar{\beta} \in (0, 1]$ *and a constant* $\alpha_2, 0 \le \alpha_2 < \bar{\beta}$*, if there exist the LMI variables* $\boldsymbol{S} \in \mathbb{R}^{n\times n}$ *symmetric and positive definite,* $\boldsymbol{W} \in \mathbb{R}^{m\times n}$ *unrestricted,* $\kappa_3 \ge 0$*,* $\alpha_1 > 0$*,* $\boldsymbol{G} \in \mathbb{R}^{n\times n}$ *invertible satisfying* (4.11)*, the* $\mathcal{E}(\boldsymbol{P}, 1)$ *is a positively invariant set.*

Proof. For each $\boldsymbol{z}(k) \in \mathcal{E}(\boldsymbol{P}, 1)$ the proof can be achieved if $\boldsymbol{z}(k+1) \in \mathcal{E}(\boldsymbol{P}, 1)$ is true. $\boldsymbol{z}(k+1) \in \mathcal{E}(\boldsymbol{P}, 1)$ can be written

$$\begin{pmatrix} \boldsymbol{z}(k) \\ \boldsymbol{e}^+(k) \\ \boldsymbol{w}(k) \\ 1 \end{pmatrix}^T \hat{\boldsymbol{P}}_3 \begin{pmatrix} \boldsymbol{z}(k) \\ \boldsymbol{e}^+(k) \\ \boldsymbol{w}(k) \\ 1 \end{pmatrix} \ge 0 \tag{4.29}$$

with

$$\hat{\boldsymbol{P}}_3 = \begin{pmatrix} -\boldsymbol{\Phi}_c^T\boldsymbol{P}\boldsymbol{\Phi}_c & * & * & * \\ -\boldsymbol{\Gamma}^T\boldsymbol{P}\boldsymbol{\Phi}_c & -\boldsymbol{\Gamma}^T\boldsymbol{P}\boldsymbol{\Gamma} & * & * \\ -\boldsymbol{D}^T\boldsymbol{P}\boldsymbol{\Phi}_c & -\boldsymbol{D}^T\boldsymbol{P}\boldsymbol{\Gamma} & -\boldsymbol{D}^T\boldsymbol{P}\boldsymbol{D} & * \\ \boldsymbol{0} & \boldsymbol{0} & \boldsymbol{0} & 1 \end{pmatrix} \tag{4.30}$$

$\boldsymbol{z}(k) \in \mathcal{E}(\boldsymbol{P}, 1)$ can be equivalently rewritten

$$\begin{pmatrix} \boldsymbol{z}(k) \\ \boldsymbol{e}^+(k) \\ \boldsymbol{w}(k) \\ 1 \end{pmatrix}^T \begin{pmatrix} -\boldsymbol{P} & \boldsymbol{0} & \boldsymbol{0} & \boldsymbol{0} \\ \boldsymbol{0} & \boldsymbol{0} & \boldsymbol{0} & \boldsymbol{0} \\ \boldsymbol{0} & \boldsymbol{0} & \boldsymbol{0} & \boldsymbol{0} \\ \boldsymbol{0} & \boldsymbol{0} & \boldsymbol{0} & 1 \end{pmatrix} \begin{pmatrix} \boldsymbol{z}(k) \\ \boldsymbol{e}^+(k) \\ \boldsymbol{w}(k) \\ 1 \end{pmatrix} \ge 0. \tag{4.31}$$

By S-procedure we combine (4.29) with (4.17), (4.31) and (4.19)

$$\begin{pmatrix} \kappa_2\boldsymbol{P} - \boldsymbol{\Phi}_c^T\boldsymbol{P}\boldsymbol{\Phi}_c - \kappa_1\sigma^2\boldsymbol{I} & * & * & * \\ -\boldsymbol{K}^T\boldsymbol{\Gamma}^T\boldsymbol{P}\boldsymbol{\Phi}_c & \kappa_1\boldsymbol{I} - \boldsymbol{K}^T\boldsymbol{\Gamma}^T\boldsymbol{P}\boldsymbol{\Gamma}\boldsymbol{K} & * & * \\ -\boldsymbol{D}^T\boldsymbol{P}\boldsymbol{\Phi}_c & -\boldsymbol{D}^T\boldsymbol{P}\boldsymbol{\Gamma}\boldsymbol{K} & \kappa_3\boldsymbol{I} - \boldsymbol{D}^T\boldsymbol{P}\boldsymbol{D} & * \\ \mathbf{0} & \mathbf{0} & \mathbf{0} & 1-\kappa_2-\kappa_3 \end{pmatrix} \geq 0 \tag{4.32}$$

By setting $1 - \kappa_2 = \bar{\kappa}_2$ (4.32) is a special case of (4.20) when $\bar{\beta} = 1$. It completes the proof here. □

This proof is valid also for the input error based event-triggered control approach to be presented in the next section.

With all the ellipsoids $\mathcal{E}(\boldsymbol{P}, 1)$ satisfying the UUB conditions in Theorem 4.1, it is interesting to derive from among them the "smallest" one to get the least conservative estimate of the invariant set under disturbance. Meanwhile the unique synthesized controller that corresponds to the best performance rejecting the exogenous disturbance. The "smallest" ellipsoidal approximation should be achieved from the minimization of a measure that reflects its geometrical size. Generally the usually considered measures for this minimization are: the volume (that can be equivalently interpreted as the minimization of the function logdet($\boldsymbol{S}$) [BGFB94, p. 11] that corresponds to the maximization of the ellipsoid matrix determinant) and the sum of squares of the semiaxes (that corresponds to the minimization of the trace of the ellipsoid matrix inverse tr($\boldsymbol{S}$)). It should be pointed out that the volume optimization can lead to ellipsoids that are "flat" in some directions. In this case despite the volume is minimized, in some directions the ellipsoidal region may be a bad estimate of the invariant set. In contrast the trace minimization leads to ellipsoids that tend to be homogeneous in all directions. Furthermore the function logdet($\cdot$) is concave on $\boldsymbol{S}$ and tr($\cdot$) is linear. Since the function tr($\cdot$) is already well defined in the MATLAB toolbox YALMIP [Lö4] and hence can be solved directly using the SeDuMi solver [Stu99] we formulate the optimization problem as such that by minimizing the level set ρ the ellipsoid can also be minimized. The extended optimization problem can be formulated

$$\min \ \mathrm{tr}(\boldsymbol{S}) \quad \text{subject to (4.11)} \tag{4.33}$$

Remark 4.3. The minimal tr($\boldsymbol{S}$) in extended optimization problem is also obtained through the gridding $\alpha_2 = \kappa_2 \in [0, \bar{\beta})$. The accuracy can be achieved as precisely as expected by giving a certain step size during the gridding procedure, where the smaller step size renders more computing time, meanwhile closer to the optimum.

Remark 4.4. With the found ellipsoid $\mathcal{E}(\boldsymbol{P}, 1)$ in Theorem 4.1 for any initial state $\boldsymbol{z}_0 \notin \mathcal{E}(\boldsymbol{P}, 1)$ of the system (4.1) a lower bound $T(\boldsymbol{z}_0)$ in Definition 4.1 can be estimated based on the exponential convergence rate $\bar{\beta}$

$$T(\boldsymbol{z}_0) \geq -\frac{\log \boldsymbol{z}_0^T\boldsymbol{P}\boldsymbol{z}_0}{\log \bar{\beta}}. \tag{4.34}$$

4.2.2 Control Input Error based UUB Event-Triggered Control

In this subsection sufficient conditions for the controller synthesis based on the control input error are given. Consider the event-triggering condition

$$\|\boldsymbol{K}(\hat{\boldsymbol{z}}^+(k-1)-\boldsymbol{z}(k))\|_2 > \sigma\|\boldsymbol{K}\boldsymbol{z}(k)\|_2 \tag{4.35}$$

where the control gain $\boldsymbol{K}$ is obtained after the controller synthesis and $\sigma \in \mathbb{R}^+$ is given. For a single input system, the physical meaning is more straightforward than the state error based event generator (4.6). For example for a electrical motor controlled system, the control input can be the input voltage on the motor. When the previous input voltage value is close to the recalculated one, the update of the recalculated input can be skipped.

Correspondingly, Eq. (4.4) can be rewritten as

$$\hat{\boldsymbol{z}}^+(k) = \begin{cases} \boldsymbol{z}(k) & \text{if } \|\boldsymbol{K}(\hat{\boldsymbol{z}}^+(k-1)-\boldsymbol{z}(k))\|_2 > \sigma\|\boldsymbol{K}\boldsymbol{z}(k)\|_2 \\ \hat{\boldsymbol{z}}^+(k-1) & \text{if } \|\boldsymbol{K}(\hat{\boldsymbol{z}}^+(k-1)-\boldsymbol{z}(k))\|_2 \leq \sigma\|\boldsymbol{K}\boldsymbol{z}(k)\|_2 \end{cases} \tag{4.36}$$

Based on (4.36) define the error variable

$$\boldsymbol{e}^+(k) = \boldsymbol{K}\hat{\boldsymbol{z}}^+(k) - \boldsymbol{K}\boldsymbol{z}(k) \tag{4.37}$$

at the k-th step. Equivalently

$$\|\boldsymbol{e}^+(k)\|_2 \leq \sigma\|\boldsymbol{K}\boldsymbol{z}(k)\|_2 \tag{4.38}$$

is always satisfied at the k-th step. The equivalent expression for (4.38) is

$$\begin{pmatrix} \boldsymbol{z}(k) \\ \boldsymbol{e}^+(k) \\ \boldsymbol{w}(k) \\ 1 \end{pmatrix}^T \begin{pmatrix} \sigma^2\boldsymbol{K}^T\boldsymbol{K} & \boldsymbol{0} & \boldsymbol{0} & \boldsymbol{0} \\ \boldsymbol{0} & -\boldsymbol{I} & \boldsymbol{0} & \boldsymbol{0} \\ \boldsymbol{0} & \boldsymbol{0} & \boldsymbol{0} & \boldsymbol{0} \\ \boldsymbol{0} & \boldsymbol{0} & \boldsymbol{0} & 0 \end{pmatrix} \begin{pmatrix} \boldsymbol{z}(k) \\ \boldsymbol{e}^+(k) \\ \boldsymbol{w}(k) \\ 1 \end{pmatrix} \geq 0. \tag{4.39}$$

The closed-loop system (4.1) can be rewritten as

$$\boldsymbol{z}(k+1) = (\boldsymbol{\Phi} + \boldsymbol{\Gamma}\boldsymbol{K})\boldsymbol{z}(k) + \boldsymbol{\Gamma}\boldsymbol{e}^+(k) + \boldsymbol{D}\boldsymbol{w}(k). \tag{4.40}$$

Similarly the control design problem for designing the event-triggering law and the control law can be formulated as

Problem 4.2 *For the closed-loop system* (4.40) *find an event-triggered controller* (4.3), (4.36) *for a given* σ *such that there exist an ellipsoid* $\mathcal{E}(\boldsymbol{P}, 1)$, *in which the system* (4.1) *is UUB.*

The following theorem gives a solution to Problem 4.2.

Theorem 4.2 *For the discrete-time system* (4.40) *with a given* σ *in event generator* (4.35)*, a constant* $\bar{\beta} \in (0,1]$ *and a constant* $\alpha_2, 0 \leq \alpha_2 \leq \bar{\beta}$*, if there exist the LMI variables* $\boldsymbol{S} \in \mathbb{R}^{n\times n}$ *symmetric and positive definite,* $\boldsymbol{W} \in \mathbb{R}^{m\times n}$ *unrestricted,* $\kappa_3 \geq 0$*,* $\alpha_1 > 0$*,* $\boldsymbol{G} \in \mathbb{R}^{n\times n}$ *invertible satisfying* (4.41)

$$\begin{pmatrix} (\bar{\beta}-\alpha_2)(\boldsymbol{G}^T+\boldsymbol{G}-\boldsymbol{S}) & * & * & * & * & * \\ \boldsymbol{0} & 2\boldsymbol{I}-\alpha_1\boldsymbol{I} & * & * & * & * \\ \boldsymbol{0} & \boldsymbol{0} & \kappa_3\boldsymbol{I} & * & * & * \\ \boldsymbol{0} & \boldsymbol{0} & \boldsymbol{0} & \alpha_2-\kappa_3 & * & * \\ \boldsymbol{\Phi G}+\boldsymbol{\Gamma W} & \boldsymbol{\Gamma} & \boldsymbol{D} & 0 & \boldsymbol{S} & * \\ \boldsymbol{W} & \boldsymbol{0} & \boldsymbol{0} & 0 & \boldsymbol{0} & \frac{\alpha_1}{\sigma^2}\boldsymbol{I} \end{pmatrix} > 0 \tag{4.41}$$

the system (4.1) *is UUB in* $\mathcal{E}(\boldsymbol{P},1)$*. The control gain and the Lyapunov matrix result from*

$$\boldsymbol{K}=\boldsymbol{W}\boldsymbol{G}^{-1}, \quad \boldsymbol{P}=\boldsymbol{S}^{-1}.$$

Proof. The proof of Theorem 4.2 follows the same lines as the one of Theorem 4.1. Similarly we search for a Lyapunov function $V(k)$ of same form as (4.12). The difference of the Lyapunov function $\Delta V = V(k+1)-V(k)$ along the trajectories of the closed-loop system (4.40) for every $\boldsymbol{z}(k) \notin \mathcal{E}(\boldsymbol{P},1)$ satisfies

$$\Delta V < -\beta V(k), \tag{4.42}$$

where $\beta \in [0,1)$. By substituting (4.40) into (4.42) we obtain

$$\begin{aligned} \Delta V = {} & (\boldsymbol{\Phi}_c\boldsymbol{z}(k)+\boldsymbol{\Gamma}\boldsymbol{e}^+(k)+\boldsymbol{D}\boldsymbol{w}(k))^T\boldsymbol{P} \\ & (\boldsymbol{\Phi}_c\boldsymbol{z}(k)+\boldsymbol{\Gamma}\boldsymbol{e}^+(k)+\boldsymbol{D}\boldsymbol{w}(k)) \\ & -\boldsymbol{z}(k)^T\boldsymbol{P}\boldsymbol{z}(k) < -\beta\boldsymbol{z}(k)^T\boldsymbol{P}\boldsymbol{z}(k), \end{aligned} \tag{4.43}$$

Reorganizing (4.43) yields

$$\begin{pmatrix} \boldsymbol{z}(k) \\ \boldsymbol{e}^+(k) \\ \boldsymbol{w}(k) \\ 1 \end{pmatrix}^T \hat{\boldsymbol{P}}_2 \begin{pmatrix} \boldsymbol{z}(k) \\ \boldsymbol{e}^+(k) \\ \boldsymbol{w}(k) \\ 1 \end{pmatrix} > 0 \tag{4.44}$$

with

$$\hat{\boldsymbol{P}}_2 = \begin{pmatrix} \bar{\beta}\boldsymbol{P}-\boldsymbol{\Phi}_c^T\boldsymbol{P}\boldsymbol{\Phi}_c & * & * & * \\ -\boldsymbol{\Gamma}^T\boldsymbol{P}\boldsymbol{\Phi}_c & -\boldsymbol{\Gamma}^T\boldsymbol{P}\boldsymbol{\Gamma} & * & * \\ -\boldsymbol{D}^T\boldsymbol{P}\boldsymbol{\Phi}_c & -\boldsymbol{D}^T\boldsymbol{P}\boldsymbol{\Gamma} & -\boldsymbol{D}^T\boldsymbol{P}\boldsymbol{D} & * \\ \boldsymbol{0} & \boldsymbol{0} & \boldsymbol{0} & 0 \end{pmatrix} \tag{4.45}$$

and $\bar{\beta} = 1-\beta$. By S-procedure we combine (4.44) with (4.39), (4.18) and (4.19) to (4.46).

$$\begin{pmatrix} \bar{\beta}\boldsymbol{P} - \boldsymbol{\Phi}_c^T\boldsymbol{P}\boldsymbol{\Phi}_c - \kappa_1\sigma^2\boldsymbol{K}^T\boldsymbol{K} - \kappa_2\boldsymbol{P} & * & * & * \\ -\boldsymbol{\Gamma}^T\boldsymbol{P}\boldsymbol{\Phi}_c & \kappa_1\boldsymbol{I} - \boldsymbol{\Gamma}^T\boldsymbol{P}\boldsymbol{\Gamma} & * & * \\ -\boldsymbol{D}^T\boldsymbol{P}\boldsymbol{\Phi}_c & -\boldsymbol{D}^T\boldsymbol{P}\boldsymbol{\Gamma} & \kappa_3\boldsymbol{I} - \boldsymbol{D}^T\boldsymbol{P}\boldsymbol{D} & * \\ \boldsymbol{0} & \boldsymbol{0} & \boldsymbol{0} & \kappa_2 - \kappa_3 \end{pmatrix} > 0 \tag{4.46}$$

By Schur-Complement (4.46) yields

$$\begin{pmatrix} (\bar{\beta} - \kappa_2)\boldsymbol{P} - \kappa_1\sigma^2\boldsymbol{K}^T\boldsymbol{K} & * & * & * & * \\ \boldsymbol{0} & \kappa_1\boldsymbol{I} & * & * & * \\ \boldsymbol{0} & \boldsymbol{0} & \kappa_3\boldsymbol{I} & * & * \\ \boldsymbol{0} & \boldsymbol{0} & \boldsymbol{0} & \kappa_2 - \kappa_3 & * \\ \boldsymbol{\Phi}_c & \boldsymbol{\Gamma} & \boldsymbol{D} & 0 & \boldsymbol{P}^{-1} \end{pmatrix} > 0 \tag{4.47}$$

Using Schur-Complement again (4.47) is equivalent to

$$\begin{pmatrix} (\bar{\beta} - \kappa_2)\boldsymbol{P} & * & * & * & * & * \\ \boldsymbol{0} & \kappa_1\boldsymbol{I} & * & * & * & * \\ \boldsymbol{0} & \boldsymbol{0} & \kappa_3\boldsymbol{I} & * & * & * \\ \boldsymbol{0} & \boldsymbol{0} & \boldsymbol{0} & \kappa_2 - \kappa_3 & * & * \\ \boldsymbol{\Phi}_c & \boldsymbol{\Gamma} & \boldsymbol{D} & 0 & \boldsymbol{P}^{-1} & * \\ \boldsymbol{K} & \boldsymbol{0} & \boldsymbol{0} & 0 & \boldsymbol{0} & \frac{1}{\kappa_1\sigma^2}\boldsymbol{I} \end{pmatrix} > 0 \tag{4.48}$$

Pre-/post-multiplying (4.48) by diag $\left(\boldsymbol{G}^T, \boldsymbol{I}, \boldsymbol{I}, \boldsymbol{I}, \boldsymbol{I}, \boldsymbol{I}\right)$ and its transposed one results in (4.49).

$$\begin{pmatrix} (1 - \kappa_2)\boldsymbol{G}^T\boldsymbol{P}\boldsymbol{G} & * & * & * & * & * \\ \boldsymbol{0} & \kappa_1\boldsymbol{I} & * & * & * & * \\ \boldsymbol{0} & \boldsymbol{0} & \kappa_3\boldsymbol{I} & * & * & * \\ \boldsymbol{0} & \boldsymbol{0} & \boldsymbol{0} & \kappa_2 - \kappa_3 & * & * \\ \boldsymbol{\Phi}_c\boldsymbol{G} & \boldsymbol{\Gamma} & \boldsymbol{D} & 0 & \boldsymbol{P}^{-1} & * \\ \boldsymbol{K}\boldsymbol{G} & \boldsymbol{0} & \boldsymbol{0} & 0 & \boldsymbol{0} & \frac{1}{\kappa_1\sigma^2}\boldsymbol{I} \end{pmatrix} > 0 \tag{4.49}$$

Same by employing the inequality relaxation (4.26) and

$$\kappa_1\boldsymbol{I}^T\boldsymbol{I} \geq \boldsymbol{I}^T + \boldsymbol{I} - \kappa_1^{-1}\boldsymbol{I} \tag{4.50}$$

a sufficient condition for (4.49) is given by (4.41) by using the same substitution as in Theorem 4.1. This completes the proof here. □

For considering the minimization of the invariant set $\mathcal{E}(\boldsymbol{P}, 1)$ the same optimization problem as in previous subsection can be formulated:

$$\min \ \mathrm{tr}(\boldsymbol{S}) \quad \text{subject to (4.41)} \tag{4.51}$$

4.3 Simulations and Comparisons

In this section examples and comparisons are presented to illustrate the effectiveness of the approaches presented in this chapter. The size of the region of admitted invariant set and the transmission reduction by the designed controllers as the two performance indices are focused on. The transmission reduction is measured for a given runtime by the following ratio

$$R_{\text{event}} = \frac{\text{the number of control input updates}}{\text{the number of steps}}. \tag{4.52}$$

Example 4.1 Consider the inverted pendulum as shown in Fig. 3.1. The relationship between σ in the event-triggering condition (4.6) and the ellipsoidal invariant set is to be investigated. The linearized dynamic model of the inverted pendulum is given by

$$\begin{pmatrix} \dot{\phi}(t) \\ \ddot{\phi}(t) \end{pmatrix} = \begin{pmatrix} 0 & 1 \\ \frac{(m+M)g}{M\ell} & 0 \end{pmatrix} \begin{pmatrix} \phi(t) \\ \dot{\phi}(t) \end{pmatrix} + \begin{pmatrix} 0 \\ \frac{-1}{M\ell} \end{pmatrix} (F(t) + w(t))$$

where ϕ is the pendulum angle, F is the force acting on the cart that for the control system is the control input u. The inverted pendulum has the pendulum mass $m = 0.1\,\text{kg}$ and the cart mass $M = 0.1\,\text{kg}$, the pendulum length $\ell = 0.545\,\text{m}$. Gravitational acceleration is considered here equal to $g = 9.81\,\text{m/s}^2$. Disturbance signal is assumed piecewise constant and changes only at the beginning of each measurement interval h with $\|w(t)\|_2 \leq 1$. The discretization is executed with respect to $h = 10\,\text{ms}$ such that the sampled-data system subject to control input disturbance is

$$\boldsymbol{z}(k+1) = \boldsymbol{\Phi}\boldsymbol{z}(k) + \boldsymbol{\Gamma}(\boldsymbol{u}(k) + \boldsymbol{w}(k)), \tag{4.53}$$

with $\boldsymbol{\Phi} = \begin{pmatrix} 1.0018 & 0.01 \\ 0.36 & 1.0018 \end{pmatrix}$, $\boldsymbol{\Gamma} = \begin{pmatrix} -0.001 \\ -0.184 \end{pmatrix}$, z_1 and z_2 indicating the pendulum angle and the pendulum angular velocity. A more detailed discussion about the derivation of the sampled-data system, especially about the disturbance term is presented in appendix section A.4. By solving the optimization problems formulated in (4.33) and (4.51) respectively for a set of given $\sigma = 0.05$, 0.09 and 0.11 one can obtain the corresponding estimate of the minimal ellipsoidal invariant sets, which are drawn in Fig. 4.1 and 4.2. The results show that generally the size of the ellipsoidal invariant set decreases with the decreasing of σ in the event generators (4.6) and (4.35). And in this case the control input error based event-triggered control supplies smaller ellipsoid invariant sets, which are reflected also by the dynamic transients in the following simulations. Consider the disturbance $\boldsymbol{w}(k) = \sin(0.1k)$ and initial state $\boldsymbol{z}(0) = \begin{pmatrix} 0.15 & 0 \end{pmatrix}^T$. It leads the following results with a whole runtime 10 s in simulation (see Tables 4.1 and 4.2). The update rate R_{event} increases when parameter σ in the event generators correspondingly decreases.

For demonstrating the effectiveness of the synthesized controller, the comparisons between the obtained controllers from the methods presented in this chapter and the selected LQR controller $\boldsymbol{K} = \begin{pmatrix} 9.48 & 2.53 \end{pmatrix}$ and $\sigma = 0.11$, whose stability is verified through

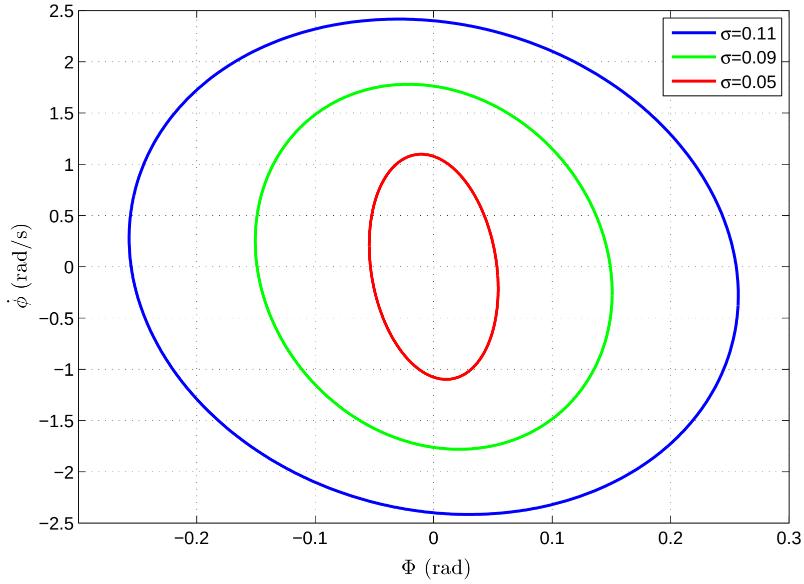

Figure 4.1: Ellipsoidal estimate based on state error based event-triggered control

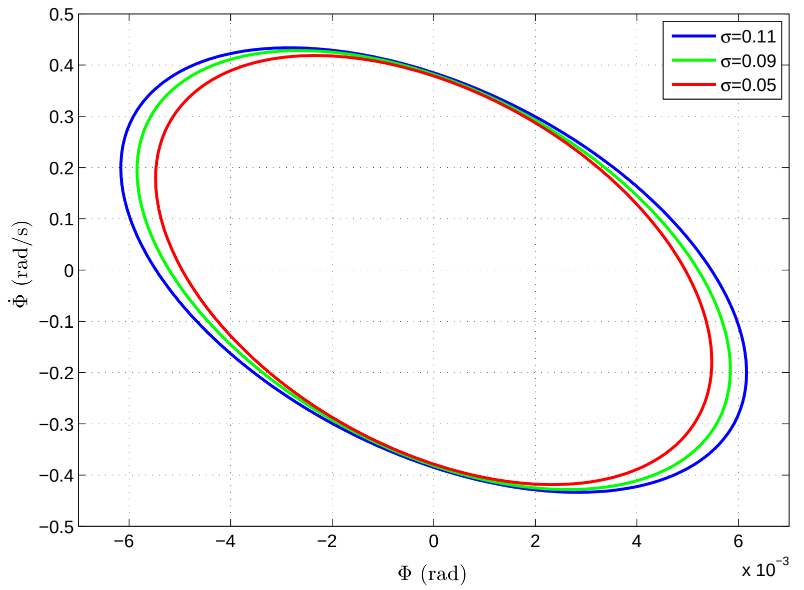

Figure 4.2: Ellipsoidal estimate based on control input error based event-triggered control

σ	$\boldsymbol{K}$	$\mathrm{tr}(\boldsymbol{S})$	update rate R_{event}
0.11	$\begin{pmatrix}10.176 & 5.5\end{pmatrix}$	5.907	62.24 %
0.09	$\begin{pmatrix}14.647 & 5.52\end{pmatrix}$	3.193	67.03 %
0.05	$\begin{pmatrix}32.87 & 5.61\end{pmatrix}$	1.209	84.72 %

Table 4.1: Simulation results based on state error based event-triggered control for different σ

σ	$\boldsymbol{K}$	$\mathrm{tr}(\boldsymbol{S})$	update rate R_{event}
0.11	$\begin{pmatrix}217.121 & 6.532\end{pmatrix}$	0.188	58.74 %
0.09	$\begin{pmatrix}225.136 & 6.572\end{pmatrix}$	0.184	63.54 %
0.05	$\begin{pmatrix}230.686 & 6.6\end{pmatrix}$	0.175	78.72 %

Table 4.2: Simulation results based on control input error based event-triggered control for different σ

the result [HDT13, Theorem III] considering event-triggered control, are made. The disturbance and initial states are set same as aforementioned. The trajectories in Fig. 4.3 derived from the methods presented in this chapter show the smaller oscillation in amplitude than the ones generated from the LQR controller for both event-generators. And as the estimated ellipsoid for the invariant set in Fig. 4.2 control input error based results give the smaller oscillation in amplitude compared with state error based ones. However a claim can not be made that in general cases control input error based event-triggered control can always obtain smaller invariant sets compared with the state error based one. In addition the update rates for LQR controller are 66.033 % and 62.54 % with respect to state error based event-triggered control and control input error based event-triggered control, which are both bigger than the results from our methods respectively.

4.4 Experimental Implementation

For further investigating the applicability of the methods presented in this chapter in real world, the methods are applied in an electronic double integrator circuit (DIC) system. The physical construction of the DIC is shown in Fig. 4.4. By substituting the parameters of resistors and capacitors the mathematical model can be described by

$$\begin{aligned}\dot{\boldsymbol{z}}(t) &= \begin{pmatrix}0 & -21.28\\ 0 & 0\end{pmatrix}\boldsymbol{z}(t) + \begin{pmatrix}0\\ -21.28\end{pmatrix}\boldsymbol{u}(t)\\ \boldsymbol{y}(t) &= \begin{pmatrix}1 & 0\end{pmatrix}\boldsymbol{z}(t),\end{aligned} \tag{4.54}$$

where z_1 and z_2 represent the voltages as marked in Fig. 4.4. The control aims to make the circuit output voltage $\boldsymbol{y}$ track a reference signal that is set constant 2.5 V in this experiment by inputting appropriate voltage (control signal $\boldsymbol{u}$). For tracking a reference

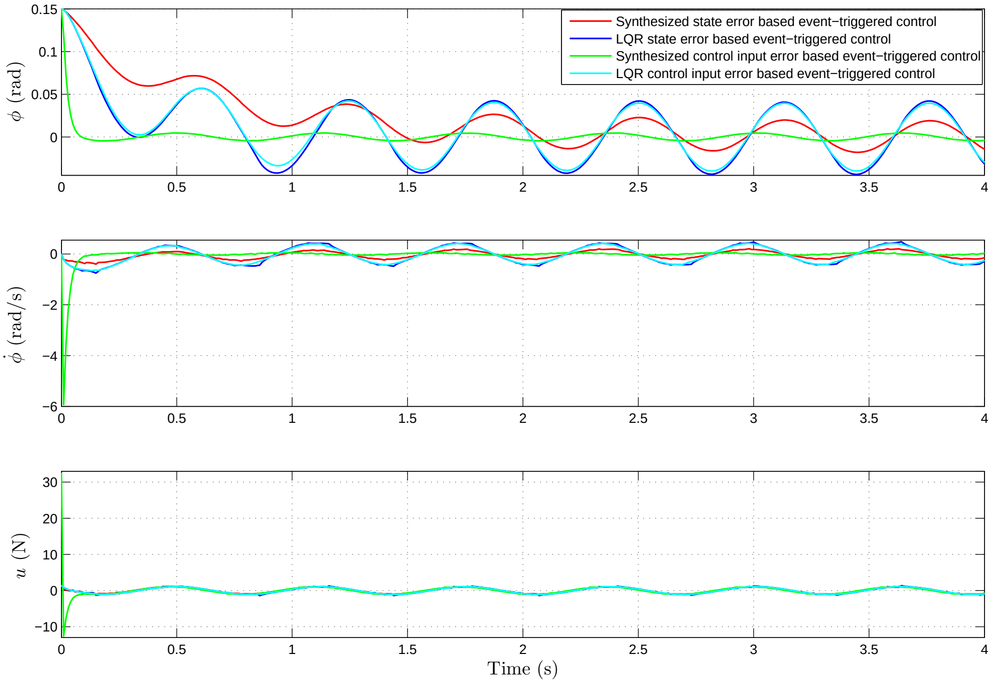

Figure 4.3: Transient dynamics of the inverted pendulum system

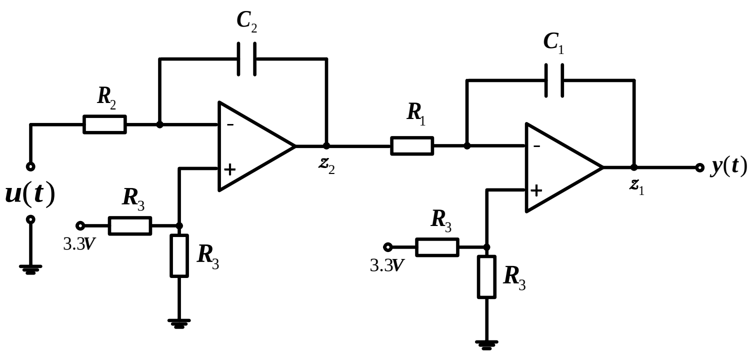

Figure 4.4: Electronic double integrator circuit

signal it can be realized by introducing the reference input with full-state feedback (see Section A.5).

The experiment uses a microcontroller NXP LPC2294 as the computing unit. The measurement interval is $h = 10\,\mathrm{ms}$ such that a sampled-data system can be derived after discretization

$$\boldsymbol{z}(k+1) = \begin{pmatrix} 1 & -0.2128 \\ 0 & 1 \end{pmatrix} \boldsymbol{z}(k) + \begin{pmatrix} 0.0226 \\ -0.2128 \end{pmatrix} \boldsymbol{u}(k). \tag{4.55}$$

In order to conspicuously test the performance of disturbance rejection a piecewise constant disturbance $\boldsymbol{w}(k) = \sin(\frac{2\pi}{1000}k)$ on the control input at the beginning of each measurement interval is artificially injected. The model yields

$$\boldsymbol{z}(k+1) = \begin{pmatrix} 1 & -0.2128 \\ 0 & 1 \end{pmatrix} \boldsymbol{z}(k) + \begin{pmatrix} 0.0226 \\ -0.2128 \end{pmatrix} (\boldsymbol{u}(k) + \boldsymbol{w}(k)). \tag{4.56}$$

After solving the optimization problems presented in (4.33) and (4.51) by setting the $\sigma = 0.05$ in the both event generator, one can have the control gain $\boldsymbol{K} = \begin{pmatrix} -6.5373 & 5.3955 \end{pmatrix}$ for state error based approach and $\boldsymbol{K} = \begin{pmatrix} -10.4951 & 5.8165 \end{pmatrix}$ for control input error based approach. The corresponding obtained ellipsoidal estimates are shown in Fig. 4.5 with $\mathrm{tr}(\boldsymbol{S}) = 0.491$ for state error based event-triggered control and $\mathrm{tr}(\boldsymbol{S}) = 0.251$ for control input error based event-triggered control. It is expected that the control input

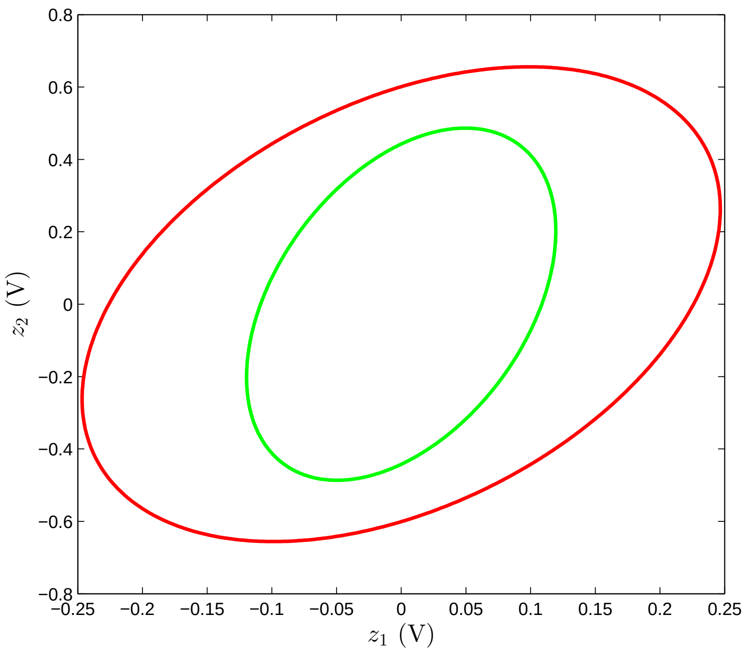

Figure 4.5: Ellipsoidal estimate from state error based event-triggered control (Red one) and control input error based event-triggered control (Green one) under $\sigma = 0.05$

error based approach should achieve better performance of disturbance rejection.

The experimental results after a runtime of 50 s are shown in Fig. 4.6. Based on observation for this specific experiment a smaller oscillation of the states in amplitude is achieved by the control input error based one (the green one). It shows that the ellipsoid estimate in Fig. 4.5 is not very conservative. Additionally the update rate R_{event}=36.82 % for input error based control is also smaller than the update rate R_{event}=55.34 % for the state error based control. One reason can be that the less aggressive oscillation of states can render a lower possibility of satisfying the event-triggering condition such that less updates are required.

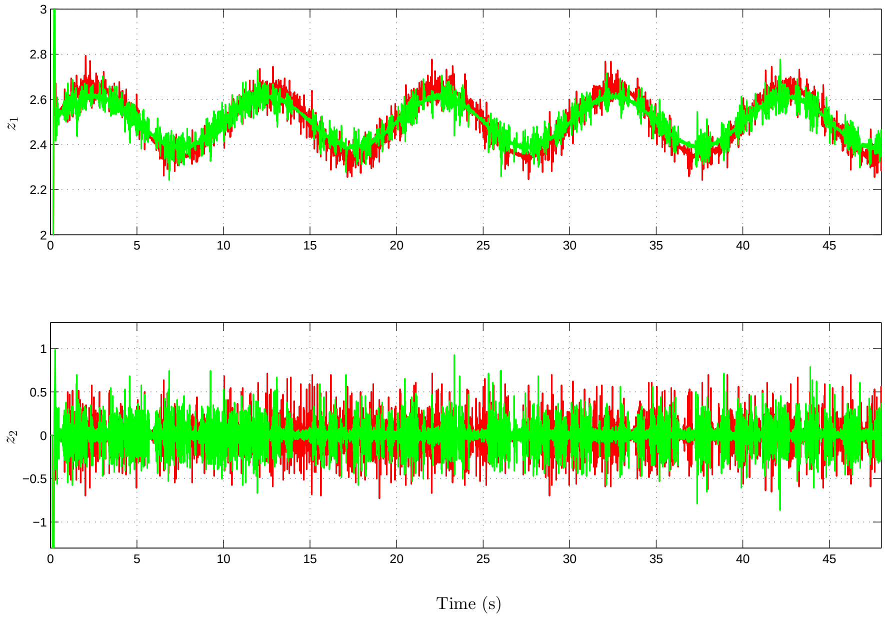

Figure 4.6: Transient dynamics of DIC with state error based event-triggered control (Red one) and control input error based event-triggered control (Green one) under $\sigma = 0.05$

4.5 Conclusion

In this chapter event-triggered synthesis approaches are studied for rejecting bounded exogenous disturbance. By synthesizing the feedback control gain and the event-triggering conditions in LMIs the uniform ultimate boundedness of the discrete-time linear system is guaranteed. Furthermore an optimization approach is given to minimize the ellipsoidal invariant set. Simulation results and experimental implementation are made for demonstrating the effectiveness and advantages of the approaches.

5 Event-Triggered Control for Multiple Embedded Control Systems

In multiple embedded control systems computation and communication resources are often limited. When several control tasks are implemented on one processor platform competing for the limited resource an efficient distribution of the resource and an application of proper controller are essential. For a control loop based on periodic sampling control many control theories such as Least Quadratic Regulator (LQR) are successfully applied in digital control [ÅW90]. However the periodic sampling may lead to an unnecessary usage of some computational resources. For example, a control system that is already close to the equilibrium points need less computing resources than another that is severely disturbed [GcH09, MFFR02]. In a very limited computational resources scenario many tasks compete for the same CPU such that it is impossible to allocate the desired periodic sampling rate to each controller. Thus a more efficient usage of the limited computing resource in the applications is proposed to offer a satisfactory performance. Some typical applications with limited resource are automotive systems and mobile phones subject to the constraints on physical size and power consumption so that the computing speed, memory size and communication bandwidth are limited.

The problems of efficient scheduling and control on embedded control systems have attracted many researchers for the last ten years. The related work can be roughly classified into offline scheduling and online scheduling.

In a seminal work [SLSS96] an offline optimization problem of determining the optimal sampling periods for different feedback controllers in an embedded system is formulated. The optimized cost function for each controller is described by an exponential function of the sampling rate. The paper offers an optimal solution considering the CPU utilization constraint. Taking the stability radius as a performance criterion [PPBSV05] develops a sampling period assignment policy for a multiple of state feedback controllers in offline. In the work [RS00, LB02, GIL07] an optimal state feedback controller is designed jointly with a control task sequence in an offline optimization problem. The control tasks are implemented according to the determined non-preemptive cyclic sequence perpetually. However by using exhaustive search method [RS00,GIL07], the resolution of this problem suffers combinatoric explosion. A pruning algorithm that can inhibit the exponential growth is proposed in [LB02]. The benefit of this co-design approach is that the controller and scheduler are harmonized with each other. The jitter due to the scheduling is incorporated in the model and thus taken into account in the control design.

In the other category the online scheduling is granted more attentions, in which the basic common idea is to introduce a feedback from the controlled systems to the scheduling of CPU resource. [BLCA02] proposes the elastic scheduling that changes the utilization rate in order to handle overload conditions, when for example a new task is admitted to the computing system. The elastic scheduling idea is applied to the case of control tasks with variable execution times in [LSCB00]. Based on LQ cost function [EHÅ00, CEBÅ02] present online optimization method for adjusting the sampling period online based on the current processor load.

In the approaches [MLB+09, HC05, CMV+06, CVMC11, GcH05, GcH09, CA06] the current plant states are incorporated in online scheduling. A heuristic cost function for quantifying the control performance is online optimized by considering the current plant states in [MLB+09]. [HC05, CMV+06] take use of a LQ cost function related to the sampling period and the current state for adjusting the sampling period online. Thereby also the expected future plant noise is taken into account. This approach is complemented and implemented by considering the computational delay and designing a noise estimator as the evaluation of the cost function depends on the noise intensity in [CVMC11]. However as mentioned in [CVMC11], the noise estimation and scheduler execution can not be very often carried out because of the computational overhead. Therefore it is assumed that the noise intensity is varied less frequent than the scheduler execution.

In a parallel line of research with non-preemptive control strategy [CA06, GcH05, GcH09] investigate the design of scheduler and controller jointly. In [CA06] the controller and scheduler is determined by solving an infinite-horizon optimization problem using relaxed dynamic programming. However this approach involves a large scheduling overhead. [GcH09] decomposes the control and scheduling problem into two subproblems. In the first subproblem a periodic control task sequence is determined by using the branch and bound method for a H_2 performance criterion. Based on derived control task sequence the optimal control gains are derived in the second subproblem applying the lifting technique. Further a state feedback scheduler is proposed to improve the control performance with respect to the off-line scheduling sequence.

Another promising methodology handling the integrated control and scheduling embedded system is event-triggered control [Årz99, ÅCES00, Lem10], under which the control task is only executed when a defined application's error signal exceeds a specified threshold. In other words, the event-triggering condition indirectly provides a measure of how valuable the current state is to maintain the expected control performance. In this way a sporadic sequence of control tasks is excited in a reaction to the variation of current states. The aim usually is that the average rate of this sporadic task set can be much reduced compared with the rate of a periodic task set. So far most of the studies on event-triggered control consider only one control loop [Årz99, ÅB99, Cog09, HDT13, HSB08, HJC08, Tab07]. However the event-triggering conditions indeed can function as a resource distributor for a multiple control loops, for example when one control loop decides the skipping of the control tasks the attention of CPU can be directed to another control loop instead. By suitably designing the event generators dependent on the current plant states and the concerted controllers the overall performance of all control loops is expected to be improved.

In this chapter, tendentiously started from the control engineer point of view a scheduling and control synthesized design approach for a multiple of control loops is presented. The approach takes advantage of the basic idea from event-triggered control in order to improve the overall control performance compared with the traditional periodic sampling control. The controllers are executed in a non-preemptive way and the scheduler can be efficiently computed. The effectiveness of the approaches is demonstrated by an experiment.

5.1 Problem Formulation

5.1.1 Real-Time Scheduling Model

Consider the control system shown in Fig. 5.1 consisting of a set of plants $\mathbb{P} = \{\mathrm{P}_i, i = 1, 2, ..., M\}$ controlled by a set of control tasks $\mathbb{T} = \{\mathrm{T}_i, i = 1, 2, ..., M\}$ using a single embedded processor. For distributing the limited computational resources a scheduler

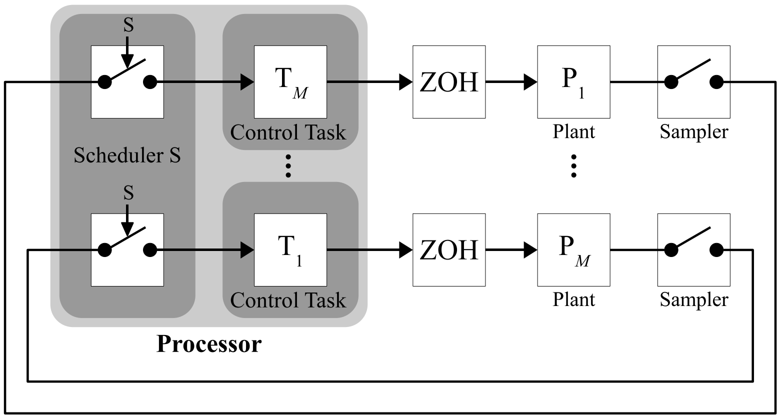

Figure 5.1: Problem description

(S) that determines the task sequence and execution manners is implemented on the processor. The approach to be presented is developed on the basis of periodic sampling with the purpose of improving the traditionally most used control strategy. It is well-known that based on the non-preemptive scheduling aggressive controllers can be designed such as LQR control since the minimal constant input-output delays can be given. The use of this property can be taken if a proper scheduling strategy can be found. However combining this with the scheduling for a multiple of control loops is not a trivial work.

Consider the general periodic sequence

$$\delta(l) = \delta(l + p), \quad p \geq M, \quad \forall l \in \mathbb{N}_0,\ p \in \mathbb{N}_0, \tag{5.1}$$

where p denotes the period length. Note that the sampling interval is not necessary to be equidistant. For illustrating the approach to be presented in a convenient way, consider the M-periodic scheduling law as a special case of (5.1) with respect to the problem setup

$$\delta(l) = \mod(M, l) + 1, \quad \forall l \in \mathbb{N}_0, \tag{5.2}$$

where mod denotes the modulo operation. A periodic sampling control based on the scheduling law (5.2) can be demonstrated in Fig. 5.2. At time instants $t_l, l \in \mathbb{N}_0$ a

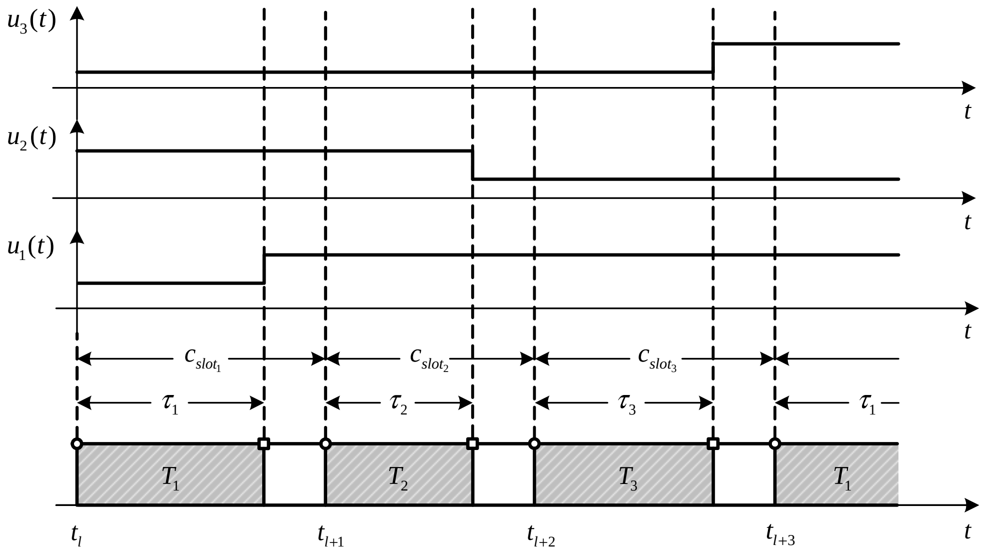

Figure 5.2: Timing diagram for periodic sampling control where a new measurement is indicated by a circle, a control update by a square, and the execution of the control task T_i by the hatching

control task is started. During the time interval τ_i in a slot $c_{slot_i}, i = 1, 2, ..., M$, CPU is occupied by the task T_i. The control input u_i for plant P_i is updated after the time delay τ_i induced by the control task. Note that between the control update and the next measurement there may be an idle time to account for non-control tasks.

In the approach the concrete operations in a complete control task that amount to the input-output time delay τ_i are schematically described in Fig. 5.3. The measurement of plant's states requires the time τ_{sc_i}. After a scheduling algorithm, which consists of an event-generator, with an execution time τ_{d_i} and the computation of the control signal with an execution time τ_{c_i}, the control signal is updated (τ_{ca_i}) at the time instant $t_l + \tau_i$, with $\tau_i = \tau_{sc_i} + \tau_{d_i} + \tau_{c_i} + \tau_{ca_i}$. The slot size $c_{slot_i} = t_{l+1} - t_l \geq \tau_i$ is constant based on the worst case assumption. Under the M-periodic scheduling for the traditional periodic sampling control, denote

$$h_s = t_{l+M} - t_l = \sum_{i=1}^{M} c_{slot_i}, \tag{5.3}$$

which is constant for each plant P_i.

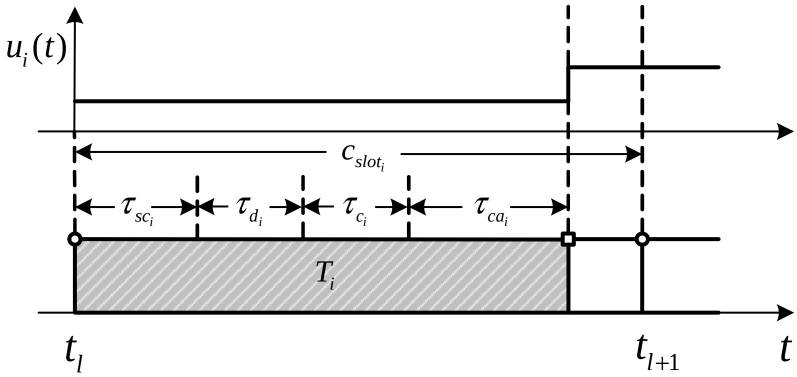

Figure 5.3: Concrete procedures in c_{slot_i}

Now the event-triggered control theme is to be introduced. When event-generator in the scheduling time τ_{d_i} decides that a new control input can be spared the operations in a control task T_i can be reduced to only measurement and scheduling as shown in Fig. 5.4. Now the control task T_i counts to the time $\tau_{sc_i} + \tau_{d_i}$. The slot size is denoted by c_{ss_i} and $c_{ss_i} \geq \tau_{sc_i} + \tau_{d_i}$ due to the inclusion of non-control tasks. Under the

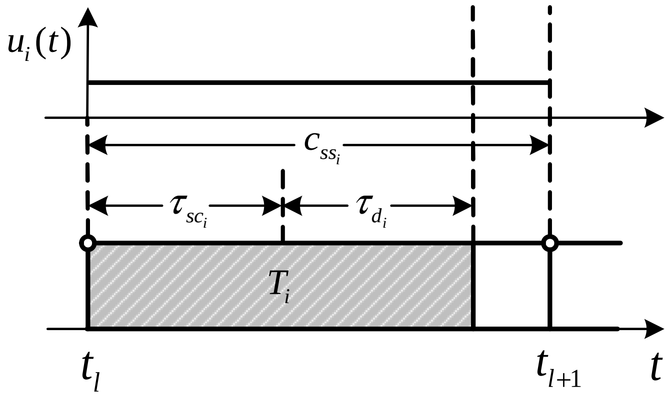

Figure 5.4: Concrete operations in c_{ss_i}

proposed strategy an example for the multiple control tasks scheduling is described in Fig. 5.5. Before the time instant t_{l+5} the control input $u_i(t), i = 1, 2, 3$ for each process is sequentially updated. After time instant t_{l+5} the control inputs for plant 3 and plant 1 are not updated because of the scheduler's decisions. By using zero order hold (ZOH) the previous control inputs are held for the plant 3 and plant 1. By skipping the control inputs updates the measurement intervals from the samplers in fact are shortened for all plants, which do not introduce any risk of a slower reaction to some unexpected disturbance than the periodic sequence. From another side the plant 2 can be expected to get more CPU time for the disturbance rejection and performance improvements compared with the periodic sampling control.

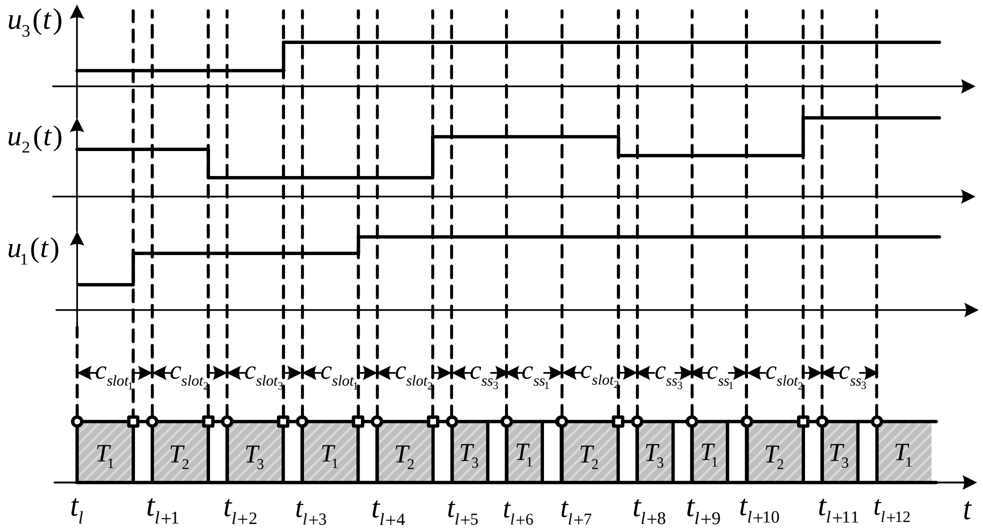

Figure 5.5: An example of the implementation

The rescheduling strategy implies an assumption

$$\tau_{d_i} < \tau_{c_i} + \tau_{ca_i}, \tag{5.4}$$

where the scheduling algorithm costs time τ_{d_i} that is not longer than the sum of control signal execution time and the transmission time. Otherwise it is not beneficial to introduce the scheduling algorithm to skip control input updates. It could be easily fitting for the scenarios that the communication between micro-controller and the actuator costs a relatively long time. For examples, the digital-to-analog (D/A) convertors have a slow conversion speed such as high accuracy R-2R ladder; the transmission takes a long time due to wireless transmission; multiple control inputs need to be updated one by one that costs a long time; networked control systems with limited communication band width. From another side, the scheduling approaches of low complexity are necessary for the satisfaction of the assumption (5.4). In section 5.2, a low complexity of scheduling algorithm will be presented and investigated in order to offer a wide applicability of the proposed approaches.

5.1.2 Plant Models and Control Performance

In this chapter the considered plant $\mathrm{P}_i \in \mathbb{P}$ is described by the time-delayed continuous linear differential equation

$$\dot{\boldsymbol{x}}_i(t) = \boldsymbol{A}_i \boldsymbol{x}_i(t) + \boldsymbol{B}_i \boldsymbol{u}_i(t - \tau_i) \tag{5.5}$$

where $\boldsymbol{x}_i(t) \in \mathbb{R}^{n_i}$ is the state vector, $\boldsymbol{A}_i \in \mathbb{R}^{n_i \times n_i}$ is the system matrix, $\boldsymbol{B}_i \in \mathbb{R}^{n_i \times m_i}$ is the input matrix, and $\boldsymbol{u}_i(t - \tau_i) \in \mathbb{R}^{m_i}$ is the control signal with the input delay τ_i.

The measurement intervals for a plant by the sampler based on aforementioned theme are combinations of c_{slot_i} and c_{ss_i}, $i = 1, ..., M$. The general case is $c_{slot_i} \neq c_{slot_j}$ and $c_{ss_i} \neq c_{ss_j}, i \neq j$, $i, j = 1, ..., M$. Denote the set of possible measurement intervals

$$\mathbb{MI} = \left\{ \sum_{i=1}^{M} \mu_i c_{slot_i} + (1 - \mu_i) c_{ss_i} \mid \mu_i = \{0, 1\} \right\}. \tag{5.6}$$

First discretize the model (5.5) using ZOH to an augmented sampled-data system model with respect to the measurement interval $h_i \in \mathbb{MI}$

$$\boldsymbol{z}_i(k_i + 1) = \boldsymbol{\Phi}_i(h_i)\boldsymbol{z}_i(k_i) + \boldsymbol{\Gamma}_i(h_i)\boldsymbol{u}_i(k_i) \tag{5.7}$$

with

$$\begin{aligned}
\boldsymbol{z}_i(k_i) &= \begin{pmatrix} \boldsymbol{x}_i(k_i)^T & \boldsymbol{u}_i(k_i - 1)^T \end{pmatrix}^T \\
\boldsymbol{\Phi}_i(h_i) &= \begin{pmatrix} e^{\boldsymbol{A}_i h_i} & \int_{h_i - \tau_i}^{h_i} e^{\boldsymbol{A}_i s} ds \boldsymbol{B}_i \\ \boldsymbol{0} & \boldsymbol{0} \end{pmatrix} \\
\boldsymbol{\Gamma}_i(h_i) &= \begin{pmatrix} \int_0^{h_i - \tau_i} e^{\boldsymbol{A}_i s} ds \boldsymbol{B}_i \\ \boldsymbol{I} \end{pmatrix},
\end{aligned}$$

where $\boldsymbol{x}_i(k_i)$ is the measured states for plant P_i at time instant $t_{k_i}, k_i \in \mathbb{N}_0$. In the M-periodic scheduling law $t_{k_i} = t_{i+Mk}$. Note that the step number k_i for a plant P_i corresponds the time instant which is different from k_j for a different plant P_j.

In this chapter the concerned control performance is the infinite horizon linear quadratic cost function for the continuous-time system (5.5)

$$J_i = \int_0^{\infty} \begin{pmatrix} \boldsymbol{x}_i(s) \\ \boldsymbol{u}_i(s - \tau_i) \end{pmatrix}^T \begin{pmatrix} \boldsymbol{Q}_{c_i} & \boldsymbol{0} \\ \boldsymbol{0} & \boldsymbol{R}_{c_i} \end{pmatrix} \begin{pmatrix} \boldsymbol{x}_i(s) \\ \boldsymbol{u}_i(s - \tau_i) \end{pmatrix} ds. \tag{5.8}$$

where $\boldsymbol{Q}_{c_i} \in \mathbb{R}^{n \times n}$ is symmetric and positive semi-definite and $\boldsymbol{R}_{c_i} \in \mathbb{R}^{m \times m}$ is symmetric and positive definite. This cost function can equivalently be written as

$$J_i = \sum_{k=0}^{\infty} \underbrace{\int_{t_{k_i}}^{t_{k_i}+h} \begin{pmatrix} \boldsymbol{x}_i(s) \\ \boldsymbol{u}_i(s - \tau_i) \end{pmatrix}^T \begin{pmatrix} \boldsymbol{Q}_{c_i} & \boldsymbol{0} \\ \boldsymbol{0} & \boldsymbol{R}_{c_i} \end{pmatrix} \begin{pmatrix} \boldsymbol{x}_i(s) \\ \boldsymbol{u}_i(s - \tau_i) \end{pmatrix} ds}_{\Delta J_i(k_i)}. \tag{5.9}$$

Considering the continuous-time state equation (5.5) over one measurement interval $h_i \in \mathbb{MI}$ one can obtain

$$\Delta J_i(k_i) = \begin{pmatrix} \boldsymbol{x}_i(k_i) \\ \boldsymbol{u}_i(k_i - 1) \\ \boldsymbol{u}_i(k_i) \end{pmatrix}^T \boldsymbol{Q}_{d_i} \begin{pmatrix} \boldsymbol{x}_i(k_i) \\ \boldsymbol{u}_i(k_i - 1) \\ \boldsymbol{u}_i(k_i) \end{pmatrix} = \begin{pmatrix} \boldsymbol{z}_i(k_i) \\ \boldsymbol{u}_i(k_i) \end{pmatrix}^T \boldsymbol{Q}_{d_i} \begin{pmatrix} \boldsymbol{z}_i(k_i) \\ \boldsymbol{u}_i(k_i) \end{pmatrix}, \tag{5.10}$$

where the cost matrix $\boldsymbol{Q}_{d_i}$ consists of two parts integrated over time interval $[0, \tau_i]$ and $[\tau_i, h_i]$

$$\boldsymbol{Q}_{d_i} = (\boldsymbol{Q}_{d0_i} + \boldsymbol{Q}_{d1_i}) = \left[\begin{array}{c|c} \boldsymbol{Q}_{d_i,11} & \boldsymbol{Q}_{d_i,12} \\ \hline \boldsymbol{Q}_{d_i,12}^T & \boldsymbol{Q}_{d_i,22} \end{array}\right] \tag{5.11a}$$

$$\boldsymbol{Q}_{d0_i} = \int_0^{\tau_i} \left[\begin{array}{cc|c} \hat{\boldsymbol{A}}_{\boldsymbol{i}}^T \boldsymbol{Q}_{c_i} \hat{\boldsymbol{A}}_{\boldsymbol{i}} & \hat{\boldsymbol{A}}_{\boldsymbol{i}}^T \boldsymbol{Q}_{c_i} \hat{\boldsymbol{B}}_{\boldsymbol{1}i} & \boldsymbol{0} \\ \hat{\boldsymbol{B}}_{\boldsymbol{1}i}^T \boldsymbol{Q}_{c_i} \hat{\boldsymbol{A}}_{\boldsymbol{i}} & \hat{\boldsymbol{B}}_{\boldsymbol{1}i}^T \boldsymbol{Q}_{c_i} \hat{\boldsymbol{B}}_{\boldsymbol{1}i} + \boldsymbol{R}_{c_i} & \boldsymbol{0} \\ \hline \boldsymbol{0} & \boldsymbol{0} & \boldsymbol{0} \end{array}\right] dt \tag{5.11b}$$

$$\boldsymbol{Q}_{d1_i} = \int_{\tau_i}^{h_i} \left[\begin{array}{cc|c} \hat{\boldsymbol{A}}_{\boldsymbol{i}}^T \boldsymbol{Q}_{c_i} \hat{\boldsymbol{A}}_{\boldsymbol{i}} & \boldsymbol{0} & \hat{\boldsymbol{A}}_{\boldsymbol{i}}^T \boldsymbol{Q}_{c_i} \hat{\boldsymbol{B}}_{\boldsymbol{0}i} \\ \boldsymbol{0} & \boldsymbol{0} & \boldsymbol{0} \\ \hline \hat{\boldsymbol{B}}_{\boldsymbol{0}i}^T \boldsymbol{Q}_{c_i} \hat{\boldsymbol{A}}_{\boldsymbol{i}} & \boldsymbol{0} & \hat{\boldsymbol{B}}_{\boldsymbol{0}i}^T \boldsymbol{Q}_{c_i} \hat{\boldsymbol{B}}_{\boldsymbol{0}i} + \boldsymbol{R}_{c_i} \end{array}\right] dt, \tag{5.11c}$$

where

$$\hat{\boldsymbol{A}}_{\boldsymbol{i}} = e^{\boldsymbol{A}_i h_i}, \quad \hat{\boldsymbol{B}}_{\boldsymbol{0}i} = e^{\boldsymbol{A}_i (h_i - \tau_i)} \int_0^{h_i - \tau_i} e^{\boldsymbol{A}_i s} ds \boldsymbol{B}_i,$$
$$\hat{\boldsymbol{B}}_{\boldsymbol{1}i} = e^{\boldsymbol{A}_i (h_i - \tau_i)} \int_0^{\tau_i} e^{\boldsymbol{A}_i s} ds \boldsymbol{B}_i.$$

Thus the discretized cost function of (5.10) is given by

$$J_i = \sum_{k_i=0}^{\infty} \begin{pmatrix} \boldsymbol{z}_i(k_i) \\ \boldsymbol{u}_i(k_i) \end{pmatrix}^T \boldsymbol{Q}_{d_i} \begin{pmatrix} \boldsymbol{z}_i(k_i) \\ \boldsymbol{u}_i(k_i) \end{pmatrix}. \tag{5.12}$$

Remark 5.1. The discretization of the cost function can refer to Section A.4 with respect to different h_i.

In the following section first the scheduling algorithm will be presented with the motivations: 1) When the status of a plant is considered the worst one among all, the control input must be updated in its control task in order to improve its control performance. 2) When a plant is not the worst one, in its control task an event triggering generator decides whether the actual control input is necessary to be updated. With this strategy the worst one always tends to be allocated more resource while the others would not lose its sensitivity to unexpected disturbance. And the performance is strictly guaranteed by the corresponding controller and event-triggering condition synthesis.

5.2 Scheduling Algorithms and Controller Designs

5.2.1 Evaluating Control Performance

The measurement of control performance in this chapter sticks to the LQ cost function (5.12). The continuous-time quadratic cost function for the infinite prediction horizon can be described as

$$J_i(t_{i+Mk}) = \int_{t_{i+Mk}}^{\infty} \begin{pmatrix} \boldsymbol{x}_i(s) \\ \boldsymbol{u}_i(s-\tau_i) \end{pmatrix}^T \begin{pmatrix} \boldsymbol{Q}_{c_i} & \boldsymbol{0} \\ \boldsymbol{0} & \boldsymbol{R}_{c_i} \end{pmatrix} \begin{pmatrix} \boldsymbol{x}_i(s) \\ \boldsymbol{u}_i(s-\tau_i) \end{pmatrix} ds. \tag{5.13}$$

The equivalent discrete time quadratic cost function at time instant t_{i+Mk} for the infinite prediction horizon can be described as

$$J_i(t_{i+Mk}) = J_i(k_i) = \sum_{j=0}^{\infty} \begin{pmatrix} \boldsymbol{z}_i(k_i+j) \\ \boldsymbol{u}_i(k_i+j) \end{pmatrix}^T \boldsymbol{Q}_{d_i} \begin{pmatrix} \boldsymbol{z}_i(k_i+j) \\ \boldsymbol{u}_i(k_i+j) \end{pmatrix}. \tag{5.14}$$

In order to determine the worst performance assume that all the plants are implemented in the periodic sampling control way with respect to h_s defined in (5.3). The infinite horizon optimal control [Nai03, pp. 222] proves that the cost for a control system can be expressed by

$$J_i(k_i) = \boldsymbol{z}_i(k_i)^T \boldsymbol{P}_{\infty_i} \boldsymbol{z}_i(k_i) \tag{5.15}$$

in each control task, where $\boldsymbol{P}_{\infty_i}$ is the solution of the Ricatti equation

$$\begin{aligned} &\boldsymbol{\Phi}_i^T(h_s)\boldsymbol{P}_{\infty_i}\boldsymbol{\Phi}_i(h_s) - \boldsymbol{P}_{\infty_i} + \boldsymbol{Q}_{d_i,11} - \left(\boldsymbol{\Phi}_i^T(h_s)\boldsymbol{P}_{\infty_i}\boldsymbol{\Gamma}_i(h_s) + \boldsymbol{Q}_{d_i,12}\right) \\ &\left(\boldsymbol{Q}_{d_i,22} + \boldsymbol{\Gamma}_i^T(h_s)\boldsymbol{P}_{\infty_i}\boldsymbol{\Gamma}_i(h_s)\right)\left(\boldsymbol{\Gamma}_i^T(h_s)\boldsymbol{P}_{\infty_i}\boldsymbol{\Phi}_i(h_s) + \boldsymbol{Q}_{d_i,12}^T\right) = 0, \end{aligned} \tag{5.16}$$

where $\boldsymbol{Q}_{d_i,11}$, $\boldsymbol{Q}_{d_i,12}$ and $\boldsymbol{Q}_{d_i,22}$ are derived from Eq. (5.11).

With the cost function of (5.15) a comparison among all control systems is possible to determine the worst one that has the biggest cost. Then the plant with the worst performance is expected to be updated more often such that the performance can be improved. However within a control task measuring all plants and calculating $J_i(k_i),\ i = 1, ..., M$ could demand a long scheduling time τ_{d_i}, which results in a big overhead. Therefore instead of measuring all plants and processing all the states' information a compromised way by measuring and calculating only a $J_i(k_i)$ within the i-th system control task T_i is considered. Then compare with the previous calculated $J_{\delta(j+Mk)}(t_{j+Mk}),\ j \neq i$ in preceding control tasks T_j. The comparison can be described as follows

$$\begin{aligned} J_{max}(k_i) = \max \{ & J_i(t_{i+Mk}), J_{\delta(i+Mk-1)}(t_{i+Mk-1}), \\ & ..., J_{\delta(i+(k-1)M+1)}(t_{i+(k-1)M+1}) \} . \end{aligned} \tag{5.17}$$

Here the equivalent expressions of continuous-time cost function $J_i(t_{i+Mk})$ and discrete-time cost function $J_i(k_i)$ in Eq. (5.17) is abused. In this compromised way the matrix calculations of $J_i(k_i),\ i = 1, ..., M$ in fact are distributed in each individual control task. In Eq. (5.17) only scalar comparisons among them are required to determine the maximal one i.e. the worst control performance. Note that the asynchronous evaluation of the worst control performance may induce a maximal h_s time slow reaction to a disturbed plant, which is still not worse than the periodic sampling.

Now a pseudo algorithm that will be implemented in a control task is shown in Algorithm 5.1. When sampler measures the i-th plant at time instant t_{i+Mk}, the control task is described.

Algorithm 5.1 Real-time scheduling

Input: $\boldsymbol{z}_i(k_i)$ // *Measure the i-th plant*
Output: Update Decision
if $J_{max}(k_i) == J_i(k_i)$ **then**
  Execute Controller_1();
  Update the actuator;
else if An event is triggered **then**
  Execute Controller_2();
  Update the actuator;
else
  No update and go to next control task;
end if

In the pseudo Algorithm 5.1, the Controller_1(), Controller_2() and the event generator will be presented in the following section. Physically the algorithm can be interpreted as two procedures 1) If the plant is the worst one, who needs more resource? 2) Can the plant spare the resource since it is not the worst one? The designs of them will be elaborated in the following sections. The control design aims to optimize the control performance i.e. minimizing the cost function (5.12).

5.2.2 Controller Design for The Plant with The Worst Performance

In this subsection the controller design i.e. (Controller_1()) the case that the plant is detected with the worst performance is investigated. According to the strategy the plant is expected to be controlled more often. Thus the control input value is always updated in the control task. The controller design targets at minimizing the cost (5.8) under the uncertain measurement interval $h_i \in \mathbb{MI}$. As long as no ambiguity arises for notational convenience the plant index i is ignored since only one single plant is considered in the following analysis. Define a new set

$$\mathbb{MI}^- = \mathbb{MI} \setminus \{\sum_{i=1}^{M} c_{ss_i}\}, \tag{5.18}$$

which is used to describe all the possibilities of measurement intervals in this case. Then the system model is

$$\boldsymbol{z}(k+1) = \boldsymbol{\Phi}(h)\boldsymbol{z}(k) + \boldsymbol{\Gamma}(h)\boldsymbol{u}(k), \quad h \in \mathbb{MI}^-. \tag{5.19}$$

Denote the closed-loop system matrix $\boldsymbol{\Phi}_{wc}(h) = \boldsymbol{\Phi}(h) + \boldsymbol{\Gamma}(h)\boldsymbol{K}_w$. And consider the state feedback controller

$$\boldsymbol{u}(k) = \boldsymbol{K}_w \boldsymbol{z}(k), \tag{5.20}$$

where matrix $\boldsymbol{K}_w$ is constant to be determined in following.

Problem 5.1 *For the discrete-time system* (5.19) *find a controller* (5.20) *such that the cost function* (5.12) *is minimized.*

For designing the controller introduce the quadratic Lyapunov function

$$V_w(k) = \boldsymbol{z}(k)^T \boldsymbol{P}_w \boldsymbol{z}(k) \tag{5.21}$$

with $\boldsymbol{P}_w \in \mathbb{R}^{(n+m)\times(n+m)}$ symmetric positive definite. Now search for a controller such that the difference of the Lyapunov function $\Delta V_w = V_w(k+1) - V_w(k)$ along the trajectories of the closed-loop system (5.19) satisfies

$$\boldsymbol{z}(k+1)^T \boldsymbol{P}_w \boldsymbol{z}(k+1) - \boldsymbol{z}(k)^T \boldsymbol{P}_w \boldsymbol{z}(k) \leq -\Delta J(k). \tag{5.22}$$

With the satisfaction of (5.22) the asymptotic stability of system (5.19) can be guaranteed, which implies $\lim\limits_{k\to\infty} \boldsymbol{z}(k) = \boldsymbol{0}$. Therefore $\lim\limits_{k\to\infty} V_w(k) = 0$ holds. By summing (5.22) up from $k = 0$ to $k = \infty$ it yields

$$J \leq \boldsymbol{z}(0)^T \boldsymbol{P}_w \boldsymbol{z}(0) \leq \operatorname{tr}(\boldsymbol{P}_w) \left\| \boldsymbol{z}(0) \right\|^2. \tag{5.23}$$

It implies the cost J is upper-bounded by $\boldsymbol{z}(0)^T \boldsymbol{P}_w \boldsymbol{z}(0)$. Since the inevitable uncertainty of measurement intervals in the control system (5.19) a suboptimal solution of Problem (5.1) is sought in order to allow an LMI formulation. Consequently, the control gain can be determined offline. Problem (5.1) can be reformulated as

Problem 5.2 *For the discrete-time system* (5.19) *find a controller* (5.20) *such that the upper bound of the cost function* (5.12) *is minimized i.e.*

$$\min_{\boldsymbol{K}_w} tr(\boldsymbol{P}_w). \tag{5.24}$$

Theorem 5.1 *A solution to Problem* (5.2) *is obtained from the LMI optimization problem*

$$\min tr(\boldsymbol{S}_w^{-1}) \quad \textit{subject to} \tag{5.25a}$$

$$\begin{pmatrix} \boldsymbol{G}_w^T + \boldsymbol{G}_w - \boldsymbol{S}_w & * & * \\ \boldsymbol{\Phi}(h)\boldsymbol{G}_w + \boldsymbol{\Gamma}(h)\boldsymbol{Y}_w & \boldsymbol{S}_w & * \\ \begin{pmatrix} \boldsymbol{G}_w \\ \boldsymbol{Y}_w \end{pmatrix} & \boldsymbol{0} & \boldsymbol{Q}_d^{-1} \end{pmatrix} \geq 0, \tag{5.25b}$$

with the LMI variables $\boldsymbol{S}_w \in \mathbb{R}^{(n+m)\times(n+m)}$ *symmetric and positive definite,* $\boldsymbol{G}_w \in \mathbb{R}^{(n+m)\times(n+m)}$ *invertible,* $\boldsymbol{Y}_w \in \mathbb{R}^{m\times(n+m)}$ *unrestricted and* $h \in \mathbb{MI}^-$. *The control gain and the Lyapunov matrix result from*

$$\boldsymbol{K}_w = \boldsymbol{Y}_w \boldsymbol{G}_w^{-1}, \quad \boldsymbol{P}_w = \boldsymbol{S}_w^{-1}.$$

Proof. Substituting (5.19) into (5.22) results in

$$\boldsymbol{z}(k)^T \boldsymbol{P}_w \boldsymbol{z}(k) - \boldsymbol{z}(k)^T \boldsymbol{\Phi}_{wc}^T(h) \boldsymbol{P}_w \boldsymbol{\Phi}_{wc}(h) \boldsymbol{z}(k) \geq \Delta J(k) \tag{5.26}$$

And

$$\begin{aligned}\Delta J(h) &= \begin{pmatrix}\boldsymbol{z}(k)\\ \boldsymbol{u}(k)\end{pmatrix}^T \boldsymbol{Q}_d \begin{pmatrix}\boldsymbol{z}(k)\\ \boldsymbol{u}(k)\end{pmatrix}\\ &= \boldsymbol{z}^T(k)\begin{pmatrix}\boldsymbol{I} & \boldsymbol{K}_w^T\end{pmatrix}\boldsymbol{Q}_d\begin{pmatrix}\boldsymbol{I} & \boldsymbol{K}_w^T\end{pmatrix}^T\boldsymbol{z}(k),\end{aligned} \tag{5.27}$$

Combining (5.26) and (5.27) leads to

$$\boldsymbol{P}_w - \boldsymbol{\Phi}_{wc}^T(h)\boldsymbol{P}_w\boldsymbol{\Phi}_{wc}(h) - \begin{pmatrix}\boldsymbol{I} & \boldsymbol{K}_w^T\end{pmatrix}\boldsymbol{Q}_d\begin{pmatrix}\boldsymbol{I} & \boldsymbol{K}_w^T\end{pmatrix}^T \geq 0, \tag{5.28}$$

which by Schur complement can be written as

$$\begin{pmatrix}\boldsymbol{P}_w & * & *\\ (\boldsymbol{\Phi}(h)+\boldsymbol{\Gamma}(h)\boldsymbol{K}_w) & \boldsymbol{P}_w^{-1} & *\\ \begin{pmatrix}\boldsymbol{I}\\ \boldsymbol{K}_w\end{pmatrix} & \boldsymbol{0} & \boldsymbol{Q}_d^{-1}\end{pmatrix} \geq 0. \tag{5.29}$$

Pre-/post-multiplying diag $\left(\boldsymbol{G}_w^T, \boldsymbol{I}, \boldsymbol{I}\right)$ and its transposed one results in

$$\begin{pmatrix}\boldsymbol{G}_w^T\boldsymbol{P}_w\boldsymbol{G}_w & * & *\\ \boldsymbol{\Phi}(h)\boldsymbol{G}_r+\boldsymbol{\Gamma}(h)\boldsymbol{K}_w\boldsymbol{G}_w & \boldsymbol{P}_w^{-1} & *\\ \begin{pmatrix}\boldsymbol{G}_w\\ \boldsymbol{K}_w\boldsymbol{G}_w\end{pmatrix} & \boldsymbol{0} & \boldsymbol{Q}_d^{-1}\end{pmatrix} \geq 0. \tag{5.30}$$

Since $\boldsymbol{P}_w$ is symmetric and positive definite, also

$$\left(\boldsymbol{P}_w^{-1} - \boldsymbol{G}_w\right)^T \boldsymbol{P}_w \left(\boldsymbol{P}_w^{-1} - \boldsymbol{G}_w\right) \geq \boldsymbol{0} \tag{5.31}$$

holds as inversion and congruence transformation do not affect definiteness. The inequality (5.31) is equivalent to

$$\boldsymbol{G}_w^T\boldsymbol{P}_w\boldsymbol{G}_w \geq \boldsymbol{G}_w^T + \boldsymbol{G}_w - \boldsymbol{P}_w^{-1}. \tag{5.32}$$

Therefore, a sufficient condition is given by (5.25b) by substituting $\boldsymbol{S}_w = \boldsymbol{P}_w^{-1}$ and $\boldsymbol{K}_w = \boldsymbol{Y}_w\boldsymbol{G}_w$. For solving the minimization problem (5.24) the matrix substitution $\boldsymbol{S}_w = \boldsymbol{P}_w^{-1}$ in the stability constraint (5.25b) needs to be considered. Thus, $\mathrm{tr}(\boldsymbol{S}^{-1})$ represents an equivalent objective function to (5.24). This completes the proof. □

5.2.3 Event-Triggered Controller Design

In this subsection, the Controller_2() and the event generator in the pseudo algorithm are investigated. Two synthesis approaches of the event-generator and the controller are presented in order to minimize the cost function (5.12).

Controller Synthesis Based on State Error

The system model is modeled as

$$\boldsymbol{z}(k+1) = \boldsymbol{\Phi}(h)\boldsymbol{z}(k) + \boldsymbol{\Gamma}(h)\boldsymbol{u}(k), \quad h \in \mathbb{MI}. \tag{5.33}$$

For the event-triggered control a full state-feedback control law is considered

$$\boldsymbol{u}(k) = \boldsymbol{K}_e \hat{\boldsymbol{z}}^+(k), \tag{5.34}$$

where $\hat{\boldsymbol{z}}^+(k)$ is a signal with

$$\hat{\boldsymbol{z}}^+(k) = \begin{cases} \boldsymbol{z}(k) & \text{if } \boldsymbol{u}(k) \text{ is updated} \\ \hat{\boldsymbol{z}}^+(k-1) & \text{if } \boldsymbol{u}(k) \text{ is not updated.} \end{cases} \tag{5.35}$$

The decision for control updates is made by the event-triggering condition.

Consider the event-triggering condition

$$\|\hat{\boldsymbol{z}}^+(k-1) - \boldsymbol{z}(k)\|_2 > \sigma \|\boldsymbol{z}(k)\|_2, \tag{5.36}$$

where $\sigma \in \mathbb{R}^+$. Therefore the Eq. (5.35) can be rewritten as

$$\hat{\boldsymbol{z}}^+(k) = \begin{cases} \boldsymbol{z}(k), & \text{if } \|\hat{\boldsymbol{z}}^+(k-1) - \boldsymbol{z}(k)\|_2 > \sigma \|\boldsymbol{z}(k)\|_2 \\ \hat{\boldsymbol{z}}^+(k-1), & \text{if } \|\hat{\boldsymbol{z}}^+(k-1) - \boldsymbol{z}(k)\|_2 \leq \sigma \|\boldsymbol{z}(k)\|_2 \end{cases} \tag{5.37}$$

Now the synthesis problem can be formulated as

Problem 5.3 *For the discrete-time system* (5.33) *find an event-triggered controller* (5.34) *under the event-triggering condition* (5.37) *for a given* σ *such that cost function* (5.12) *is minimized, i.e.*

$$\min_{\boldsymbol{K}} J \text{ subject to } (5.33), (5.34) \text{ and } (5.37). \tag{5.38}$$

Define the error variable

$$\boldsymbol{e}^+(k) = \hat{\boldsymbol{z}}^+(k) - \boldsymbol{z}(k). \tag{5.39}$$

Based on the definition (5.37) the inequality

$$\|\boldsymbol{e}^+(k)\|_2 \leq \sigma \|\boldsymbol{z}(k)\|_2 \tag{5.40}$$

is always satisfied in the time interval $(t_k, t_{k+1}]$. With the control input $\boldsymbol{u}(k) = \boldsymbol{K}_e \hat{\boldsymbol{z}}^+(k)$ and $\hat{\boldsymbol{z}}^+(k) = \boldsymbol{e}^+(k) + \boldsymbol{z}(k)$ the closed-loop system of (5.33) is given by

$$\boldsymbol{z}(k+1) = (\boldsymbol{\Phi}(h) + \boldsymbol{\Gamma}(h)\boldsymbol{K}_e)\boldsymbol{z}(k) + \boldsymbol{\Gamma}(h)\boldsymbol{K}_e\boldsymbol{e}^+(k) \tag{5.41}$$

with the denotation $\boldsymbol{\Phi}_{ec}(h) = \boldsymbol{\Phi}(h) + \boldsymbol{\Gamma}(h)\boldsymbol{K}_e$. This model (5.41) enables a closed-loop system with a control input error. For designing the controller analogously introduce the quadratic Lyapunov function

$$V_e(k) = \boldsymbol{z}(k)^T \boldsymbol{P}_e \boldsymbol{z}(k), \tag{5.42}$$

with $\boldsymbol{P}_e \in \mathbb{R}^{(n+m)\times(n+m)}$ symmetric positive definite. The suitable matrix $\boldsymbol{P}_e$ and control gain $\boldsymbol{K}_e$ are sought to fulfill the difference of the Lyapunov function $\triangle V_e(k) = V_e(k+1) - V_e(k)$

$$\boldsymbol{z}(k+1)^T \boldsymbol{P}_e \boldsymbol{z}(k+1) - \boldsymbol{z}(k)^T \boldsymbol{P}_e \boldsymbol{z}(k) \leq -\triangle J(k), \tag{5.43}$$

where the decreasing of the Lyapunov function is penalized by the cost $\triangle J(k)$ stepwise. Same as (5.23) it yields

$$J < \boldsymbol{z}(0)^T \boldsymbol{P}_e \boldsymbol{z}(0) < \operatorname{tr}(\boldsymbol{P}_e) \left\| \boldsymbol{z}(0) \right\|^2. \tag{5.44}$$

This implies that that the cost function J is upper-bounded by $\boldsymbol{z}(0)^T \boldsymbol{P}_e \boldsymbol{z}(0)$. The closed-loop system (5.41) with the event-triggering condition (5.35) and state error (5.40) lead to a hybrid system with uncertainty of measurement intervals, where the event-triggering condition (5.35) indicates the switching law of the hybrid system. As the switching is state dependent and thus not known before runtime, similarly a suboptimal solution of Problem (5.3) is to be derived. Problem (5.3) can be reformulated as

Problem 5.4 *For the closed-loop system* (5.41) *find an event-triggered controller* (5.34) *such that for a given σ the upper bound $tr(\boldsymbol{P}_e)$ of the cost function* (5.12) *is minimized subject to condition* (5.40)*, i.e.*

$$\min_{\boldsymbol{K}_e} tr(\boldsymbol{P}_e) \text{ subject to } (5.41) \text{ and } (5.40). \tag{5.45}$$

Theorem 5.2 *A solution to Problem 5.4 is obtained from the LMI optimization problem*

$$\min tr(\boldsymbol{S}_e^{-1}) \quad \text{subject to} \tag{5.46a}$$

$$\begin{pmatrix} \boldsymbol{G}_e^T + \boldsymbol{G}_e - \boldsymbol{S}_e & * & * & * & * \\ \boldsymbol{0} & \boldsymbol{G}_e^T + \boldsymbol{G}_e - \alpha \boldsymbol{I} & * & * & * \\ \boldsymbol{\Phi}(h)\boldsymbol{G}_e + \boldsymbol{\Gamma}(h)\boldsymbol{W}_e & \boldsymbol{\Gamma}(h)\boldsymbol{W}_e & \boldsymbol{S}_e & * & * \\ \boldsymbol{G}_e & \boldsymbol{0} & \boldsymbol{0} & \frac{\alpha}{\sigma^2}\boldsymbol{I} & * \\ \begin{pmatrix} \boldsymbol{G}_e \\ \boldsymbol{W}_e \end{pmatrix} & \begin{pmatrix} \boldsymbol{0} \\ \boldsymbol{W}_e \end{pmatrix} & \boldsymbol{0} & \boldsymbol{0} & \boldsymbol{Q}_d^{-1} \end{pmatrix} > \boldsymbol{0} \tag{5.46b}$$

with the LMI variables $\alpha > 0$, $\boldsymbol{S}_e \in \mathbb{R}^{(n+m)\times(n+m)}$ symmetric and positive definite, $\boldsymbol{G}_e \in \mathbb{R}^{(n+m)\times(n+m)}$ invertible, $\boldsymbol{W}_e \in \mathbb{R}^{m\times(n+m)}$ unrestricted and $h \in \mathbb{MI}$. The control gain and the Lyapunov matrix result from

$$\boldsymbol{K}_e = \boldsymbol{W}_e \boldsymbol{G}_e^{-1}, \quad \boldsymbol{P}_e = \boldsymbol{S}_e^{-1}.$$

Proof. The proof can refer to the proof of Theorem 2.1 with the consideration $h \in \mathbb{MI}$. □

Controller Synthesis Based on Control Input Error

Sufficient conditions for the controller synthesis based on the control input error that is often used as event-triggering conditions [DH12, HDT13] are given in this section. As an alternative for the control system design, the results are presented in the following. Because of the same proving technique, the proof procedures are omitted. One can refer to the proof of Theorem 2.2.

Consider the event-triggering condition

$$\|\boldsymbol{K}_e(\hat{\boldsymbol{z}}^+(k-1) - \boldsymbol{z}(k))\|_2 > \sigma\|\boldsymbol{K}_e\boldsymbol{z}(k)\|_2 \tag{5.47}$$

where the $\boldsymbol{K}_e$ is obtained after the controller synthesis and $\sigma \in \mathbb{R}^+$. This event generator is similarly motivated by the fact that the control input update can be skipped when the actual control input value changes little compared with the previous one. Correspondingly, (5.35) can be rewritten as

$$\hat{\boldsymbol{z}}^+(k) = \begin{cases} \boldsymbol{z}(k) & \text{if } \|\boldsymbol{K}_e(\hat{\boldsymbol{z}}^+(k-1)-\boldsymbol{z}(k))\|_2 > \sigma\|\boldsymbol{K}_e\boldsymbol{z}(k)\|_2 \\ \hat{\boldsymbol{z}}^+(k-1) & \text{if } \|\boldsymbol{K}_e(\hat{\boldsymbol{z}}^+(k-1)-\boldsymbol{z}(k))\|_2 \leq \sigma\|\boldsymbol{K}_e\boldsymbol{z}(k)\|_2 \end{cases} \tag{5.48}$$

Based on (5.48) define the error variable

$$\boldsymbol{e}^+(k) = \boldsymbol{K}_e\hat{\boldsymbol{z}}^+(k) - \boldsymbol{K}_e\boldsymbol{z}(k). \tag{5.49}$$

Equivalently

$$\|\boldsymbol{e}^+(k)\|_2 \leq \sigma\|\boldsymbol{K}_e\boldsymbol{z}(k)\|_2 \tag{5.50}$$

is always satisfied in the time interval $(t_k, t_{k+1}]$. The equivalent expression for (5.50) is

$$\begin{pmatrix} \boldsymbol{z}(k) \\ \boldsymbol{e}^+(k) \end{pmatrix}^T \begin{pmatrix} \sigma^2\boldsymbol{K}_e^T\boldsymbol{K}_e & \boldsymbol{0} \\ \boldsymbol{0} & -\boldsymbol{I} \end{pmatrix} \begin{pmatrix} \boldsymbol{z}(k) \\ \boldsymbol{e}^+(k) \end{pmatrix} \geq 0. \tag{5.51}$$

The closed-loop system can be rewritten as

$$\boldsymbol{z}(k+1) = (\boldsymbol{\Phi}(h) + \boldsymbol{\Gamma}(h)\boldsymbol{K}_e)\boldsymbol{z}(k) + \boldsymbol{\Gamma}(h)\boldsymbol{e}^+(k). \tag{5.52}$$

Based on the same Lyapunov function (5.42), stability constraint (5.43), and the resulting upper bound of the cost function (5.44) as in the previous subsection the synthesis problem for designing the event-triggering law and the control law can be formulated as

Problem 5.5 *For the closed-loop system* (5.52) *find an event-triggered controller* (5.34) *such that for a given* σ*, the upper bound of the cost function* (5.12) *is minimized subject to condition* (5.50)*, i.e.*

$$\min_{\boldsymbol{K}_e} tr(\boldsymbol{P}_e) \;\; \textit{subject to } (5.52) \textit{ and } (5.50). \tag{5.53}$$

Theorem 5.3 *A solution to Problem 5.5 is obtained from the LMI optimization problem*

$$\min tr(\boldsymbol{S}_e^{-1}) \quad \textit{subject to} \tag{5.54a}$$

$$\begin{pmatrix} \boldsymbol{G}_e^T + \boldsymbol{G}_e - \boldsymbol{S}_e & * & * & * & * \\ \boldsymbol{0} & (2-\alpha)\boldsymbol{I} & * & * & * \\ \boldsymbol{\Phi}(h)\boldsymbol{G}_e + \boldsymbol{\Gamma}(h)\boldsymbol{W}_e & \boldsymbol{\Gamma}(h) & \boldsymbol{S}_e & * & * \\ \boldsymbol{W}_e & \boldsymbol{0} & \boldsymbol{0} & \frac{\alpha}{\sigma^2}\boldsymbol{I} & * \\ \begin{pmatrix} \boldsymbol{G}_e \\ \boldsymbol{W}_e \end{pmatrix} & \begin{pmatrix} \boldsymbol{0} \\ \boldsymbol{I} \end{pmatrix} & \boldsymbol{0} & \boldsymbol{0} & \boldsymbol{Q}_d^{-1} \end{pmatrix} > \boldsymbol{0} \tag{5.54b}$$

with the LMI variables $\alpha > 0$, $\boldsymbol{S}_e \in \mathbb{R}^{(n+m)\times(n+m)}$ *symmetric and positive definite,* $\boldsymbol{G}_e \in \mathbb{R}^{(n+m)\times(n+m)}$ *invertible,* $\boldsymbol{W}_e \in \mathbb{R}^{m\times(n+m)}$ *unrestricted and* $h \in \mathbb{MI}$. *The control gain and the Lyapunov matrix result from*

$$\boldsymbol{K}_e = \boldsymbol{W}_e\boldsymbol{G}_e^{-1}, \quad \boldsymbol{P}_e = \boldsymbol{S}_e^{-1}.$$

5.2.4 Stability and Controller Synthesis

The two subsections 5.2.2 and 5.2.3 derive the controller designs for the two cases in the scheduling strategy. However the stability of the switches between the two controllers are not encompassed. For excluding the instabilities aroused the successive switches between the controllers (5.20) and (5.34) the following constraints upon Lyapunov functions $\boldsymbol{z}(k)^T\boldsymbol{P}_w\boldsymbol{z}(k)$ and $\boldsymbol{z}(k)^T\boldsymbol{P}_e\boldsymbol{z}(k)$, $\forall\boldsymbol{z}(k)$ can be included

$$\boldsymbol{z}(k)^T\boldsymbol{P}_w\boldsymbol{z}(k) - \boldsymbol{z}(k+1)^T\boldsymbol{P}_e\boldsymbol{z}(k+1) < 0 \tag{5.55}$$

$$\boldsymbol{z}(k)^T\boldsymbol{P}_e\boldsymbol{z}(k) - \boldsymbol{z}(k+1)^T\boldsymbol{P}_w\boldsymbol{z}(k+1) < 0, \tag{5.56}$$

By using the same matrix transformation techniques the sufficient conditions can be formulated:

$$\begin{pmatrix} \boldsymbol{G}_w^T + \boldsymbol{G}_w - \boldsymbol{S}_w & * \\ \boldsymbol{\Phi}(h)\boldsymbol{G}_w + \boldsymbol{\Gamma}(h)\boldsymbol{Y}_w & \boldsymbol{S}_e \end{pmatrix} \geq 0, \quad h \in \mathbb{MI}^- \tag{5.57}$$

and

$$\begin{pmatrix} \boldsymbol{G}_e^T + \boldsymbol{G}_e - \boldsymbol{S}_e & * \\ \boldsymbol{\Phi}(h)\boldsymbol{G}_e + \boldsymbol{\Gamma}(h)\boldsymbol{W}_e & \boldsymbol{S}_w \end{pmatrix} \geq 0, \quad h \in \mathbb{MI} \tag{5.58}$$

So far a complete synthesis controller design can be formulated

Theorem 5.4 *The complete controllers design in the control pseudo Algorithm 5.1 is obtained from solving the LMI optimization problem*

$$\min tr(\boldsymbol{S}_w^{-1}),\ tr(\boldsymbol{S}_e^{-1}) \tag{5.59a}$$

$$\begin{cases} \textit{subject to } (5.25b), (5.46b), (5.57), (5.58), \textit{ if with event generator } (5.36) \\ \textit{subject to } (5.25b), (5.54b), (5.57), (5.58), \textit{ if with event generator } (5.47) \end{cases} \tag{5.59b}$$

with the LMI variables $\boldsymbol{S}_e \in \mathbb{R}^{(n+m)\times(n+m)}$, $\boldsymbol{S}_w \in \mathbb{R}^{(n+m)\times(n+m)}$ *symmetric and positive definite,* $\boldsymbol{G}_e \in \mathbb{R}^{(n+m)\times(n+m)}$, $\boldsymbol{G}_w \in \mathbb{R}^{(n+m)\times(n+m)}$ *invertible,* $\boldsymbol{W}_e \in \mathbb{R}^{m\times(n+m)}$, $\boldsymbol{Y}_w \in \mathbb{R}^{m\times(n+m)}$ *unrestricted and* $\alpha > 0$*. The control gains and the Lyapunov matrices result from*

$$\boldsymbol{K}_e = \boldsymbol{W}_e \boldsymbol{G}_e^{-1}, \quad \boldsymbol{P}_e = \boldsymbol{S}_e^{-1}, \quad \boldsymbol{K}_w = \boldsymbol{Y}_w \boldsymbol{G}_w^{-1}, \quad \boldsymbol{P}_w = \boldsymbol{S}_w^{-1}.$$

Remark 5.2. Theorem 5.4 offers the complete controller designs covering the strict stability issues. The optimization has two objective functions that is not supported by the toolbox CVX. However the two functions can be combined into one. The Eq. (5.59a) can be reformulated as

$$\min \operatorname{tr} \begin{pmatrix} \boldsymbol{S}_w^{-1} & \boldsymbol{0} \\ \boldsymbol{0} & \boldsymbol{S}_e^{-1} \end{pmatrix}. \tag{5.60}$$

Then the optimization in Theorem 5.4 can be efficiently solved in Matlab by toolbox CVX.

Remark 5.3. Two event-triggered control design approaches are proposed. The physical motivations behind the two event generators are different. Through massive numerical simulations, one can not outperform the other generally. However one observation is that σ usually can be allowed bigger after solving the optimization problems in control input error based method for SIMO systems. The reason could be that $\boldsymbol{K}_e\boldsymbol{z}$ for SIMO systems is a scaler, the simpler structure of which can bring more robustness in the non-fulfillment of the event generator. And basically increasing σ in the event generators means increasing the tolerance with respect to the errors, which enables the possibility of sparing the control input updates. It can be expected that the spared resource is allocated to the plant with worst performance by the former part in the pseudo algorithm. This point is clearly demonstrated by the following experiment.

5.3 Experimental Implementation

For demonstrating the applicability and effectiveness of the proposed approach in real world, an experimental implementation by simultaneously controlling two double integrator circuits (DICs) and an inverted pendulum is presented. Control of DIC or inverted pendulum systems is often considered as benchmark experiment in control field because of their naturally instable property without control.

5.3.1 Hardware and Modelling

DIC System

The physical construction of the DIC is schematically shown in Fig. 5.6. By substituting

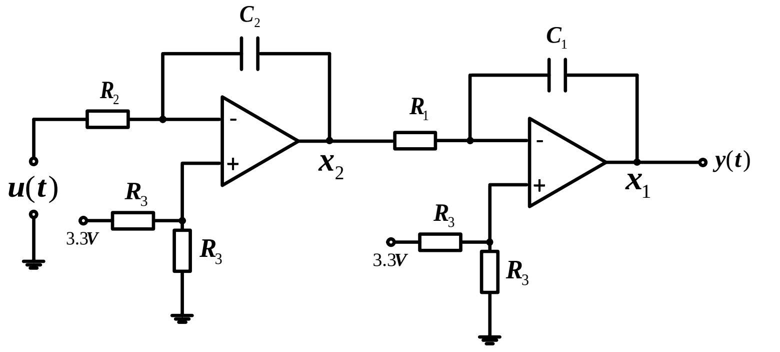

Figure 5.6: Electronic double integrator circuit

the parameters of resistors and capacitors the mathematical model can be described

$$\begin{aligned}\dot{\boldsymbol{x}}(t) &= \begin{pmatrix} 0 & -21.28 \\ 0 & 0 \end{pmatrix} \boldsymbol{x}(t) + \begin{pmatrix} 0 \\ -21.28 \end{pmatrix} \boldsymbol{u}(t-\tau) \\ \boldsymbol{y}(t) &= \begin{pmatrix} 1 & 0 \end{pmatrix} \boldsymbol{x}(t), \end{aligned} \tag{5.61}$$

where x_1 and x_2 represent the voltages as marked in Fig. 5.6. The control aims to make the circuit output voltage $\boldsymbol{y}$ track a reference signal by inputting appropriate voltage (control signal $\boldsymbol{u}$). In the following experiment the reference signal is set constant 1.6 v for both DICs. The control input is powered directly by pulse width modulator such that no negative voltage is available. Therefore the voltage on the non-inverting input of operational amplifier is shifted to 1.67 V by using a voltage divider R_3. This offset will be added to the calculated control input $\boldsymbol{u}$.

Inverted Pendulum System

The inverted pendulum system to be used as test bed is already shown in Fig. 2.4. The goal of control is to stabilize the pendulum to the upright position. And the cart can stop at the initially released position in the end, which is set as the equilibrium point. Naturally the inverted pendulum system is nonlinear. However a linearization around the equilibrium point the system can be accomplished such that the system can be described as the following linear model

$$\dot{\boldsymbol{x}}(t) = \begin{pmatrix} 0 & 1 & 0 & 0 \\ 0 & -1.001 & -0.5117 & 0 \\ 0 & 0 & 0 & 1 \\ 0 & 2.916 & 30.05 & 0 \end{pmatrix} \boldsymbol{x}(t) + \begin{pmatrix} 0 \\ 0.8455 \\ 0 \\ -2.461 \end{pmatrix} \boldsymbol{u}(t-\tau) \tag{5.62}$$

where the state vector $\boldsymbol{x} = \begin{pmatrix} x_1 & x_2 & x_3 & x_4 \end{pmatrix}^T$ consists of the cart position x_1, cart velocity x_2, angle of the pendulum x_3, and angular velocity of the pendulum x_4. Finally the microcontroller NXP LPC2294 is employed as the computing unit.

5.3.2 Scheduling and Control

As the demonstration the following setups are applied in the experiment. A periodic sequence is chosen for the implementation as shown in Fig. 5.7. For the periodic sampling control the control frequency of the inverted pendulum is twice as much as one DIC. The scheduling and control strategy is developed based on this periodic sequence. Note that the presented approach can be adapted to the general periodic sequence (5.1). The controller design part follows the same procedures by considering all the possible measurement intervals. Calculating $\boldsymbol{P}_{\infty_i}$ by solving the general periodic Riccati equation for evaluating control performance in Section 5.2.1 can refer to [GIL07, BCN91, BC09]. It is expected that the presented strategy can exhibit benefits in sense of the overall control performance in a given setup. For an implementation of the event-triggered

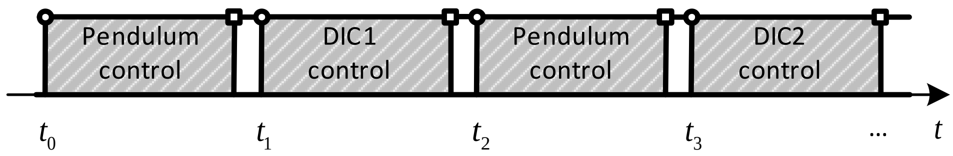

Figure 5.7: Periodic sequence for two DICs and the inverted pendulum system

control tasks, the time-sliced architectures same as [GcH09] is employed (see Fig. 5.8), where $c_{slot_i} = 2c_{ss_i}$. The architecture can be easily realized by the time interrupts routines, which consumes ignorable CPU resource. Subsequently the following setups are

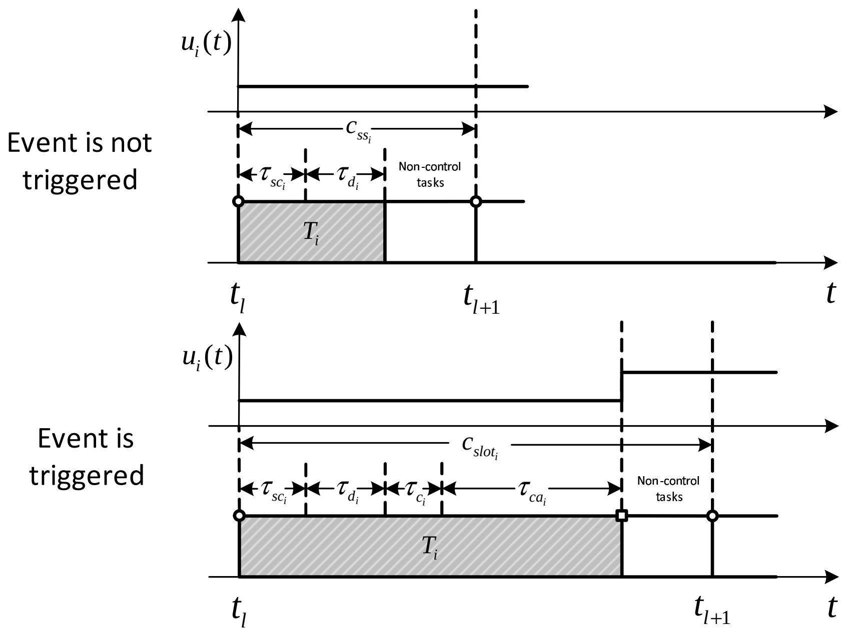

Figure 5.8: Implementation of the event-triggered control tasks

obtained as shown in Table 5.1. Among them the delay τ_{ca} (from controller to actuator) is

Implementation Setups	DIC	Pendulum
τ_{sc}	0.113 ms	0.769 ms
τ_d	0.475 ms	0.85 ms
τ_c	0.031 ms	0.065 ms
τ_{ca}	3.1 ms	3.1 ms

Table 5.1: Time delays for the control inputs

artificially enlarged in order to simulate the long transmission time case such as wireless transmission (see Section 5.1.1) and the others are from the practical measurements for the worst case. And the two time interval $c_{ss_i} = 3.125\,\text{ms}$ and $c_{slot_i} = 6.25\,\text{ms}$ are set same for DICs and inverted pendulum systems. With the given setups the control input delay for DIC counts to 3.744 ms and that for inverted pendulum counts to 4.809 ms. The measurement intervals for DIC have the possibilities $h_{DIC} \in \mathbb{MI}_{DIC} =: \{12.5\,\text{ms}, 15.625\,\text{ms}, 18.75\,\text{ms}, 21.875\,\text{ms}, 25\,\text{ms}\}$ and those for inverted pendulum have the possibilities $h_{Pen} \in \mathbb{MI}_{Pen} =: \{6.25\,\text{ms}, 9.375\,\text{ms}, 12.5\,\text{ms}\}$.

By considering all the given setups in the Theorem (5.4) the control parameters that are listed in Table 5.2 are obtained. The input error based event generator (5.47) is applied for this experiment. The weighting matrices $\boldsymbol{Q}_c$ and $\boldsymbol{R}_c$ are picked in this way in order to obtain physically applicable control parameters. For evaluating the control

Implementation Setups	DIC	Pendulum
weighting matrix $\boldsymbol{Q}_c$	$\begin{pmatrix}100 & 0\\ 0 & 1\end{pmatrix}$	$\begin{pmatrix}35000 & 0 & 0 & 0\\ 0 & 1 & 0 & 0\\ 0 & 0 & 30000 & 0\\ 0 & 0 & 0 & 200\end{pmatrix}$
weighting matrix $\boldsymbol{R}_c$	1	1
σ	0.01	0.05
$\boldsymbol{K}_w$	$\begin{pmatrix}-3.14 & 2.84 & -0.22\end{pmatrix}$	$\begin{pmatrix}145.1 & 93.25 & 295.15 & 50.58 & -0.23\end{pmatrix}$
$\boldsymbol{K}_e$	$\begin{pmatrix}-3.32 & 2.93 & -0.22\end{pmatrix}$	$\begin{pmatrix}141.97 & 91.32 & 292.95 & 50.01 & -0.22\end{pmatrix}$
$\boldsymbol{K}_{LQR}$	$\begin{pmatrix}-3.14 & 2.78 & -0.21\end{pmatrix}$	$\begin{pmatrix}138.29 & 88.12 & 281.32 & 47.88 & -0.2\end{pmatrix}$

Table 5.2: Control parameters

performance (5.17) in control tasks the matrix $\boldsymbol{P}_{\infty_i}$ in (5.15) needs to be calculated. However for different control systems the value of the cost (5.15) can differ a lot because of different physical meanings. Therefore a normalization of the matrix $\boldsymbol{P}_{\infty_i}$ is done by computing $\frac{\boldsymbol{P}_{\infty_i}}{\|\boldsymbol{P}_{\infty_i}\|}$, which is used in Eq. (5.17).

5.3.3 Analysis of Experimental Results

The experiments are carried out for both the approach presented in this chapter and the periodic sampling approach with a runtime 75 s. The dynamics of the control systems are recorded. Note that the experiment can be repeated always with the similar results. One example can be seen in Fig. 5.9. Based on the observations, one can see the dynamics of the both DICs systems are improved in the amplitudes from the presented approach (red ones). One of the reasons indeed can be explained by reading the updating ratios that are calculated by

$$Ratio = \frac{\text{the number of control input updates}}{\text{the number of measurements}} \tag{5.63}$$

as shown in the Table. 5.3. The DICs systems under the control setups update almost all

	DIC1	DIC2	Inverted pendulum
Ratio	99.97 %	99.93 %	90.86 %

Table 5.3: Updating ratios for the experiment

the times. However a part of resource from the inverted pendulum system is spared and reallocated to the DICs systems according to the scheduler. This can also be reflected in the cost as shown in Fig. 5.10, which is calculated for each plant based on the Eq. (5.12) with normalization. Consistently the cost from the presented approach (the red ones) is improved for the DICs systems, while the cost compared with periodic sampling control (the green one) degrades because of the spare of the resource from the inverted pendulum systems. For DIC1 system the cost from the presented approach is 61.93 % of that from periodic sampling control and for DIC2 system the ratio is 56.58 %. For the inverted pendulum systems the ratio is 110.66 % with 10.66 % degradation. Physically it can also be understandable that the inverted pendulum system that is a mechanic system has a relatively bigger inertia compared with the electrical circuit systems. This enables the more possibilities to satisfy the event triggering conditions, namely spare control inputs updates from the inverted pendulum system. One can also observe that the degradation in the cost from the inverted pendulum system is limited by the event-triggered control which considers the cost function in the controller design. It is not difficult to verify that the overall performance according to the percentages from the presented approach is better than the periodic sampling approach, which demonstrates the effectiveness and advantages of the approach.

5.4 Conclusion

The problem that a multiple of control systems are controlled by one single CPU platform is investigated in this chapter. Based on the event-triggered control strategy, the synthesized design of the scheduling and the controller is accomplished. In experiments the effectiveness and advantages from the approach are demonstrated. The contributions can be summarized as follows: 1) The event-triggered control strategy is extended to handle a multiple of control loops for the first time. 2) The presented controllers

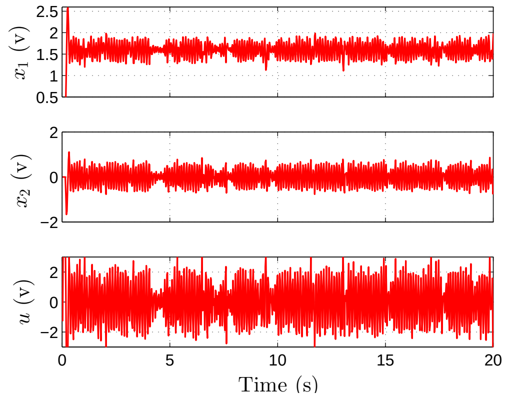

(a) Transient dynamic of DIC1

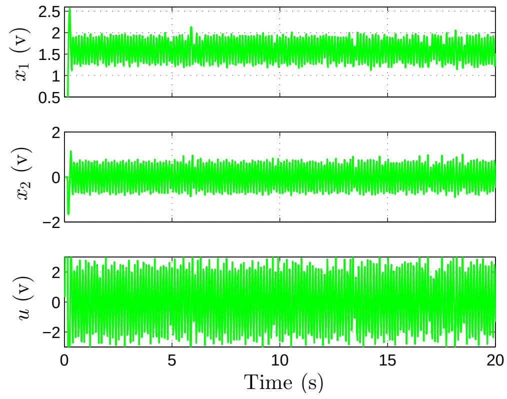

(b) Transient dynamic of DIC1

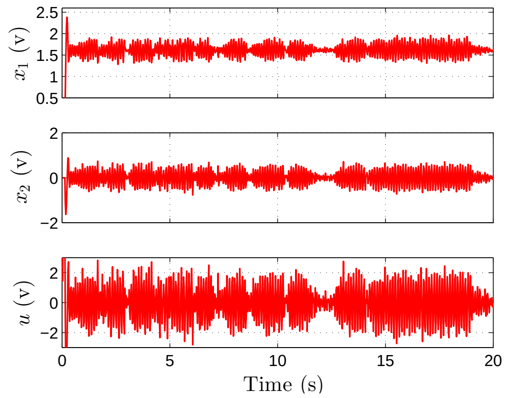

(c) Transient dynamic of DIC2

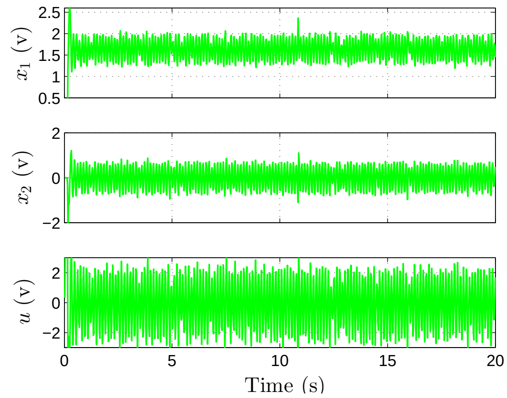

(d) Transient dynamic of DIC2

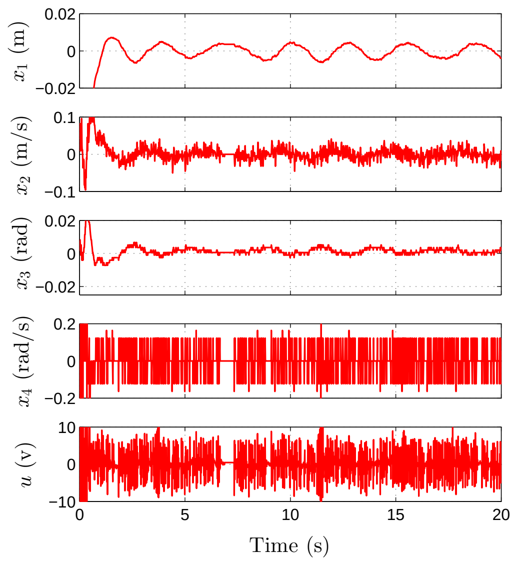

(e) Transient dynamic of inverted pendulum

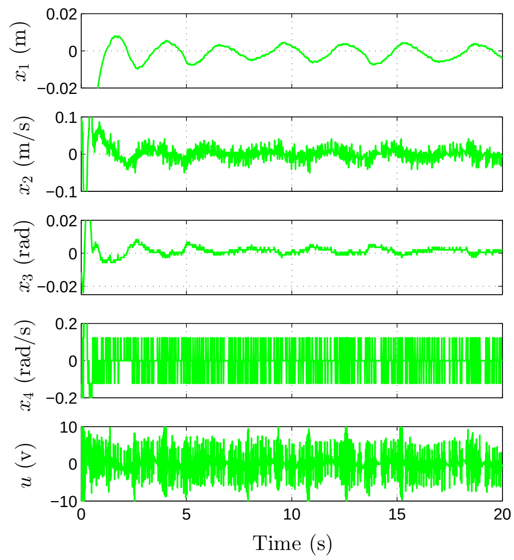

(f) Transient dynamic of inverted pendulum

Figure 5.9: The transient dynamics of control system under the presented approach is listed on the left side (red); the transient dynamics of control system under periodic sampling control is listed on the right side (green)

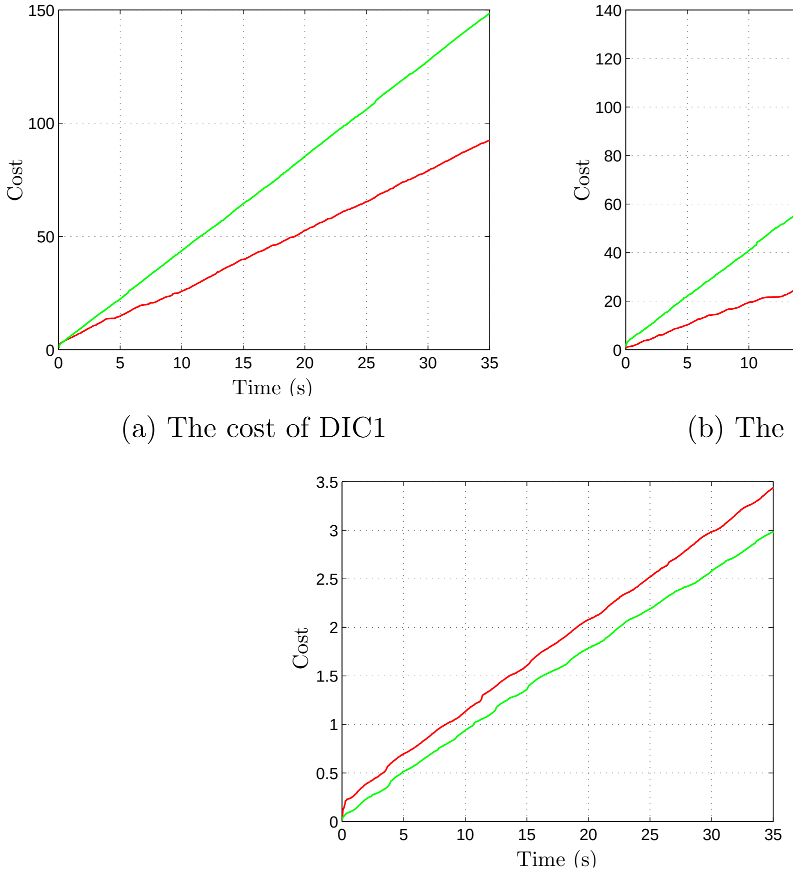

(a) The cost of DIC1

(b) The cost of DIC2

(c) The cost of inverted pendulum

Figure 5.10: The cost for the two approaches: our approach (red) and periodic sampling approach (green)

consider both the stability and the control performance within the design procedures. 3) The proposed scheduling algorithm can be easily implemented non-preemptively with a little consumption of computing resource.

6 Polytopic Representation of Time-Varying Uncertain Systems

Time-varying uncertainty can arise in embedded or networked control applications where limited computation or communication resources have to be scheduled for example uncertain and time-varying sampling period and time-delay [Nil98, DB01, NR07, NHT08, IGL08, vdWNCH10]. Other cases such as time-varying physical parameters or control laws will directly lead to a time-varying system description as well. Usually a robust stability analysis is required when dealing with these control problems. Polytopic representation is recognized as one of the efficient ways to describe the time-varying uncertain system with adjustable accuracy. Based on the polytopic representation effective approaches for controller design and system dynamics analysis can be obtained [Sch99,BM03,CTN07,NR07,Fuj08,CvdWHN09,GOL09,GSL+10]. In this chapter concerning the problem how to construct the polytopic representation of time-varying system an approach is presented based on the Taylor Series expansion. The computation complexity of the approach only increases polynomially with the increasing of required accuracy. The derived results can be applied to stability analysis and controller design.

6.1 Problem formulation

Consider an autonomous time-varying discrete system described by

$$\boldsymbol{z}(k+1) = \boldsymbol{\Phi}(k)\boldsymbol{z}(k), \tag{6.1}$$

where $\boldsymbol{z}(k) \in \mathbb{R}^n$ is the state, k is the sampling instant, $\boldsymbol{\Phi}(k) \in \mathbb{R}^{n\times n}$ is the system matrix. In this formulation, a state feedback controller can be assumed to be already included. The system matrix $\boldsymbol{\Phi}(k)$ changes along with the time going. This can occur, for example, when a continuous-time system is considered

$$\dot{\boldsymbol{x}}(t) = \boldsymbol{A}\boldsymbol{x}(t) + \boldsymbol{B}\boldsymbol{u}(t-\tau(t)), \tag{6.2}$$

where $\boldsymbol{x}(t) \in \mathbb{R}^{n_x}$ is the state vector, $\boldsymbol{u}(t-\tau(t)) \in \mathbb{R}^{m_u}$ is the input vector with time-varying delay $\tau(t)$ and $\boldsymbol{A} \in \mathbb{R}^{n_x\times n_x}$ and $\boldsymbol{B} \in \mathbb{R}^{n_x\times m_u}$ are the system and input matrix respectively. In embedded control systems and networked control systems the time-varying delay can be caused by jitter in the controller execution and network transmission. Time-varying sampling occurs very often with the event-triggered control. Therefore the discretization of the system (6.2) with time-varying sampling period $h_k, \tau_k \leq h_k$

using ZOH yields

$$\boldsymbol{z}(k+1) = \boldsymbol{\Psi}(k)\boldsymbol{z}(k) + \boldsymbol{\Gamma}(k)\boldsymbol{u}(k), \tag{6.3}$$

where

$$\boldsymbol{z}(k) = \begin{pmatrix} \boldsymbol{x}(k) \\ \boldsymbol{u}(k-1) \end{pmatrix}, \qquad \boldsymbol{\Psi}(k) = \begin{pmatrix} e^{\boldsymbol{A}h_k} & \int_{h_k-\tau_k}^{h_k} e^{\boldsymbol{A}s} ds \boldsymbol{B} \\ \boldsymbol{0} & \boldsymbol{0} \end{pmatrix},$$
$$\boldsymbol{\Gamma}(k) = \begin{pmatrix} \int_0^{h_k-\tau_k} e^{\boldsymbol{A}s} ds \boldsymbol{B} \\ \boldsymbol{I} \end{pmatrix}.$$

Then denote the closed loop system $\boldsymbol{\Phi}(k) = \boldsymbol{\Psi}(k) + \boldsymbol{\Gamma}(k)\boldsymbol{K}$, where $\boldsymbol{K}$ is any state-feedback control gain from controller $\boldsymbol{u}(k) = \boldsymbol{K}\boldsymbol{z}(k)$. System (6.3) can be generalized by the model (6.1). Generally speaking, the system matrix $\boldsymbol{\Phi}(k)$ is a function of different physical or control parameters. That is, the system matrix can be represented as

$$\boldsymbol{\Phi}(k) := \boldsymbol{f}(\xi_1(k), \xi_2(k), ..., \xi_l(k)) \tag{6.4}$$

where $\xi_i(k), i = 1, ..., l$ are the time-varying parameters. In many practical situations these parameters are even uncertain and only some upper and lower bounds are known for the parameter values. For example in (6.3), $\xi_1(k) = h_k$ and $\xi_2(k) = \tau_k$ are both bounded and positive. The bounds could be estimated according to the transmission protocol. Without loss of generality, we assume that $\xi_i(k) \in [\underline{\xi}_i, \overline{\xi}_i]$ with $\overline{\xi}_i \geq \underline{\xi}_i \geq 0$, $i = 1, ..., l$.

To study the stability of such systems with time-varying parametric uncertainties, parameter dependent Lyapunov functions (PDLF) have been proved to be a very useful tool [HAPL04, GAC96]. The notion of PDLF is introduced in [BD86], which is

$$V(\boldsymbol{z}) = \boldsymbol{z}^T \boldsymbol{P}(\boldsymbol{\xi})\boldsymbol{z}, \tag{6.5}$$

where $\boldsymbol{P}(\boldsymbol{\xi})$ is an affine function of $\boldsymbol{\xi} = \begin{pmatrix} \xi_1(k) & \xi_2(k) & ... & \xi_l(k) \end{pmatrix}^T$. However, construction of PDLF is not an easy task. In [DB01, GAC96], it has been shown that polytopic representation of such time-varying uncertainties is often an efficient way to derive LMI based formulations of sufficient and necessary conditions for time-varying PDLF. These conditions are especially useful for design of robust controllers. In this case, the structure of the dynamical matrix $\boldsymbol{\Phi}$ is assumed to be of the form

$$\boldsymbol{\Phi}(k) = \sum_{i=1}^{N} \mu_i(k)\boldsymbol{\Phi}_i + \boldsymbol{\Theta}^h, \quad \mu_i(k) \geq 0, \quad \sum_{i=1}^{N} \mu_i(k) = 1. \tag{6.6}$$

where matrix $\boldsymbol{\Phi}_i$, μ_i and $\boldsymbol{\Theta}^h$ represent the vertices of a convex polytope, uncertain parameters and a remainder with a bounded norm, respectively and N is the number of vertices determined by the approach to be presented. With such a polytopic representation results are obtained for the stabilization of uncertain systems with time-varying delays and sampling period in [HDI06, IGL08].

While most works concerning polytopic uncertainties deal with rigorous stability theorems, only a few consider the question how such a polytopic representation can be constructed to keep the number of LMI used for stability conditions as low as possible. In [HDI06], the authors derive the polytopic description of (6.6) via the expansion of Taylor Series, which is an effective and numerically tractable approach [HWG+10].

The link from Taylor expansion series to the polytopic description of system is derived by handling the variables in the Taylor expansion series. For the one-parameter case in [HDI06],

$$\mathbf{\Phi}(k) := \boldsymbol{f}(\xi_1(k)). \tag{6.7}$$

The Taylor expansion series on ξ_1 is

$$\begin{aligned} \boldsymbol{f}(\xi_1) = \boldsymbol{f}(0) + \boldsymbol{f}'(0)\xi_1 + \frac{\boldsymbol{f}''(0)}{2!}\xi_1^2 \\ + \cdots + \frac{\boldsymbol{f}^p(0)}{p!}\xi_1^p + \boldsymbol{o}(p+1). \end{aligned} \tag{6.8}$$

Then by transforming $\boldsymbol{f}(0) + \boldsymbol{f}'(0)\xi_1 + \frac{\boldsymbol{f}''(0)}{2!}\xi_1^2 + \cdots + \frac{\boldsymbol{f}^p(0)}{p!}\xi_1^p$ into a polytopic representation in a form $\sum_{i=1}^{N} \mu_i(k)\mathbf{\Phi}_i, \mu_i(k) \geq 0, \sum_{i=1}^{N} \mu_i(k) = 1$, the matrix function $\boldsymbol{f}(\xi_1)$ can be described in a polytopic way with the remainder of Taylor expansion series $\boldsymbol{o}(p+1)$. However, the procedure is developed only for one single uncertain parameter (the unknown delay time). In case of any number of uncertain parameters the relevant results are still missing. Consider the system matrix $\mathbf{\Phi}(k)$ with multiple uncertain parameters $\xi_1(k), \xi_2(k), ..., \xi_l(k)$

$$\mathbf{\Phi}(k) := \boldsymbol{f}(\xi_1(k), \xi_2(k), ..., \xi_l(k)), \tag{6.9}$$

$$\xi_1(k) \in [\underline{\xi}_1, \overline{\xi}_1],\ \xi_2(k) \in [\underline{\xi}_2, \overline{\xi}_2],\ \dots,\ \xi_l(k) \in [\underline{\xi}_l, \overline{\xi}_l] \tag{6.10}$$

$$\text{where} \quad \overline{\xi}_1 \geq \underline{\xi}_1 \geq 0,\ \overline{\xi}_2 \geq \underline{\xi}_2 \geq 0 \text{ and } \overline{\xi}_l \geq \underline{\xi}_l \geq 0. \tag{6.11}$$

Via the Taylor expansion of matrix function (6.9) at point 0, it yields the matrix polynomial:

$$\begin{aligned} \boldsymbol{f}(\xi_1, \xi_2, ..., \xi_l) = \boldsymbol{f}(0) + \sum_{i=1}^{l} \frac{\partial \boldsymbol{f}}{\partial \xi_i}\xi_i + \sum_{i=1}^{l} \frac{\partial f}{2!\partial \xi_i^2}\xi_i^2 \\ + \sum_{i=1}^{l-1}\sum_{j=i}^{l} \frac{\partial^2 \boldsymbol{f}}{2!\partial \xi_i \partial \xi_j}\xi_i\xi_j + \cdots + \boldsymbol{o}(p+1). \end{aligned} \tag{6.12}$$

In the next section, an approach is presented to transform the general model (6.12) into the polytopic representative form (6.6). Similar work is done also in [GCG93] for a multi-parameter robust stability analysis. In the following an approach to find an appropriate construction rule for the matrix polytopic representation of the uncertain system (6.12) is to be presented.

6.2 Construction of Convex Polytopes

6.2.1 Two-variable Case

For the sake of simplicity of mathematical description, the illustration of the method begins with a system having two uncertain variables only. Recall system Eq. (6.1), and let the system matrix in two-variable case be represented by

$$\boldsymbol{\Phi}(k) := \boldsymbol{f}(\xi_1(k), \xi_2(k)) \tag{6.13}$$

where

$$\begin{array}{l} \xi_1(k) \in [\underline{\xi}_1, \overline{\xi}_1],\ \xi_2(k) \in [\underline{\xi}_2, \overline{\xi}_2] \\ \text{and} \quad \overline{\xi}_1 \geq \underline{\xi}_1 \geq 0,\ \overline{\xi}_2 \geq \underline{\xi}_2 \geq 0. \end{array}$$

Via Taylor Series expansion until order p the matrix polynomial can be obtained

$$\begin{aligned} \boldsymbol{f}(\xi_1, \xi_2) &= f(0) + \frac{\partial \boldsymbol{f}}{\partial \xi_1}\xi_1 + \frac{\partial \boldsymbol{f}}{\partial \xi_2}\xi_2 + \frac{\partial^2 \boldsymbol{f}}{2!\partial \xi_1^2}\xi_1^2 \\ &+ \frac{\partial^2 \boldsymbol{f}}{\partial \xi_1 \partial \xi_2}\xi_1\xi_2 + \frac{\partial^2 \boldsymbol{f}}{2!\partial \xi_2^2}\xi_2^2 \\ &+ \cdots + \boldsymbol{o}(p+1). \end{aligned} \tag{6.14}$$

Note that the assumption of positive uncertain parameters ξ_1 and ξ_2 is not restrictive in practice. In fact, even the exact values of the physical parameters may be unknown, their signs are mostly constant and known. If the sign of some variable $\xi_i, i = 1, ..., l$ is negative in reality, one can still assume ξ_i to be positive by taking a minus sign before ξ_i. An important application of the two-variable case can be the stability analysis of systems with time-varying sampling rate and uncertain delay for system (6.3) [IGL08], which arises often in networked embedded control systems or scheduling problems for multiple control loops.

Arrange the variables $\xi_1^{p_m}\xi_2^{p_n}$, where $0 \leq p_n \leq p, 0 \leq p_m \leq p$ and $p_m + p_n = p$, and order them in an array given below:

$$\begin{array}{llllllll}
1 & \xi_1 & \xi_1^2 & \xi_1^3 & \xi_1^4 & \xi_1^5 & \cdots & \xi_1^p \\
\xi_2 & \xi_1\xi_2 & \xi_1^2\xi_2 & \xi_1^3\xi_2 & \xi_1^4\xi_2 & \cdots & \xi_1^{p-1}\xi_2 & \\
\xi_2^2 & \xi_1\xi_2^2 & \xi_1^2\xi_2^2 & \xi_1^3\xi_2^2 & \cdots & \xi_1^{p-2}\xi_2^2 & & \\
\xi_2^3 & \xi_1\xi_2^3 & \xi_1^2\xi_2^3 & \cdots & \xi_1^{p-3}\xi_2^3 & & & \\
\xi_2^4 & \xi_1\xi_2^4 & \cdots & \xi_1^{p-4}\xi_2^4 & & & & \\
\xi_2^5 & \cdots & \xi_1^{p-5}\xi_2^5 & & & & & \\
\vdots & & & & & & & \\
\xi_2^p & & & & & & &
\end{array}$$

Then collect and group the terms in row. It yields

Group 0: $1,\ \xi_1,\ \xi_1^2,\ \cdots,\ \xi_1^p$.

Group 1: $\xi_2,\ \xi_1\xi_2,\ \xi_1^2\xi_2,\ \cdots,\ \xi_1^{p-1}\xi_2$.

Group 2: $\xi_2^2,\ \xi_1\xi_2^2,\ \xi_1^2\xi_2^2,\ \cdots,\ \xi_1^{p-2}\xi_2^2$.

$\vdots$

Group p: ξ_2^p.

First consider the group 1: $\xi_2,\ \xi_1\xi_2,\ \xi_1^2\xi_2,\ \cdots,\ \xi_1^{p-1}\xi_2$. After sorting out the common factor ξ_2, it gives $1,\ \xi_1\ \xi_1^2\ \cdots,\ \xi_1^{p-1}$. The classical Gauss method shows that there exist some uncertain parameters $\mu_i^{(1)}(k)$ satisfying the linear equation:

$$\begin{pmatrix} 1 & \cdots & \cdots & \cdots & 1 \\ \underline{\xi}_1 & \overline{\xi}_1 & \cdots & \cdots & \overline{\xi}_1 \\ \underline{\xi}_1^2 & \underline{\xi}_1^2 & \overline{\xi}_1^2 & \cdots & \overline{\xi}_1^2 \\ \vdots & & & \ddots & \vdots \\ \underline{\xi}_1^{p-1} & \cdots & \cdots & \underline{\xi}_1^{p-1} & \overline{\xi}_1^{p-1} \end{pmatrix} \begin{pmatrix} \mu_1^{(1)}(k) \\ \mu_2^{(1)}(k) \\ \vdots \\ \mu_p^{(1)}(k) \end{pmatrix} = \begin{pmatrix} 1 \\ \xi_1(k) \\ \xi_1^2(k) \\ \vdots \\ \xi_1^{p-1}(k) \end{pmatrix}. \tag{6.15}$$

The uncertain parameters $\mu_i^{(1)}, i = 1, ..., p$ (superscript (1) indicates the group 1) can be computed by the recursive formula

$$\mu_1^{(1)} = 1 - \frac{\xi_1 - \underline{\xi}_1}{\overline{\xi}_1 - \underline{\xi}_1},\ \mu_p^{(1)} = \frac{\xi_1^{p-1} - \underline{\xi}_1^{p-1}}{\overline{\xi}_1^{p-1} - \underline{\xi}_1^{p-1}}$$

$$\mu_l^{(1)} = \frac{\xi_1^{l-1} - \underline{\xi}_1^{l-1}}{\overline{\xi}_1^{l-1} - \underline{\xi}_1^{l-1}} - \frac{\xi_1^l - \underline{\xi}_1^l}{\overline{\xi}_1^l - \underline{\xi}_1^l}, \quad l = 2, ..., p-1.$$

It is easy to verify that

$$\mu_i^{(1)} \geq 0, i = 1, ..., p$$

and

$$\sum_{i=1}^{p} \mu_i^{(1)} = 1.$$

Define the matrix

$$\boldsymbol{\Lambda}_1 := \begin{pmatrix} 1 & \cdots & \cdots & \cdots & 1 \\ \underline{\xi}_1 & \overline{\xi}_1 & \cdots & \cdots & \overline{\xi}_1 \\ \underline{\xi}_1^2 & \underline{\xi}_1^2 & \overline{\xi}_1^2 & \cdots & \overline{\xi}_1^2 \\ \vdots & & & \ddots & \vdots \\ \underline{\xi}_1^{p-1} & \cdots & \cdots & \underline{\xi}_1^{p-1} & \overline{\xi}_1^{p-1} \end{pmatrix}$$

Consider the polynomials in the Taylor Series expansion with variables about ξ_2, $\xi_1\xi_2$, $\xi_1^2\xi_2$, $\cdots$, $\xi_1^{p-1}\xi_2$ such that a matrix form can be rewritten as

$$\begin{aligned} &\frac{\partial \boldsymbol{f}}{\partial \xi_2}\xi_2 + \frac{\partial^2 \boldsymbol{f}}{\partial \xi_1 \partial \xi_2}\xi_1\xi_2 + \frac{\partial^3 \boldsymbol{f}}{2!\partial \xi_1^2 \partial \xi_2}\xi_1^2\xi_2 + \cdots + \frac{\partial^p \boldsymbol{f}}{(p-1)!\partial \xi_1^{p-1}\partial \xi_2}\xi_1^{p-1}\xi_2 \\ &= \underbrace{\left(\frac{\partial \boldsymbol{f}}{\partial \xi_2}, \frac{\partial^2 \boldsymbol{f}}{\partial \xi_1 \partial \xi_2}, \frac{\partial^3 \boldsymbol{f}}{2!\partial \xi_1^2 \partial \xi_2}, \cdots, \frac{\partial^p \boldsymbol{f}}{(p-1)!\partial \xi_1^{p-1}\partial \xi_2}\right)}_{\boldsymbol{M}_1} \xi_2 \begin{pmatrix} \boldsymbol{I} \\ \xi_1 \boldsymbol{I} \\ \xi_1^2 \boldsymbol{I} \\ \vdots \\ \xi_1^{p-1}\boldsymbol{I} \end{pmatrix} \end{aligned} \tag{6.16}$$

Eq. (6.16) with substitution of Eq. (6.15) can be rewritten as

$$\begin{aligned} \xi_2 \cdot \boldsymbol{\Xi}_1 : &= \xi_2 \cdot \boldsymbol{M}_1(\boldsymbol{\Lambda}_1 \otimes \boldsymbol{I}) \begin{pmatrix} \mu_1^{(1)}(k)\boldsymbol{I} \\ \mu_2^{(1)}(k)\boldsymbol{I} \\ \vdots \\ \mu_p^{(1)}(k)\boldsymbol{I} \end{pmatrix} \\ &= \xi_2 \cdot \sum_{i=1}^{p} \mu_i \cdot \boldsymbol{M}_1 \left(\mathrm{col}_i(\boldsymbol{\Lambda}_1) \otimes \boldsymbol{I}\right), \end{aligned} \tag{6.17}$$

Note that $\boldsymbol{\Xi}_1$ is a convex polytope, where $\boldsymbol{M}_1 \left(\mathrm{col}_i(\boldsymbol{\Lambda}_1) \otimes \boldsymbol{I}\right), i = 1, ...p$ are the vertices. Define $\boldsymbol{\Xi}_1(i) = \boldsymbol{M}_1 \left(\mathrm{col}_i(\boldsymbol{\Lambda}_1) \otimes \boldsymbol{I}\right)$, $i = 1, 2, ..., p$.

Consider the same processing rule on other groups. From group 2 to group p, after sorting out the common factors ξ_2^2, ξ_2^3, $\cdots$, ξ_2^p, the corresponding convex polytopes with the Gaussian method can be obtained. These polytopes are denoted $\boldsymbol{\Xi}_2$, $\cdots$, $\boldsymbol{\Xi}_p$. For the group 0, the Gaussian method can be used directly without sorting out any common factor. The corresponding convex polytope is denoted as Ξ_0. Analogously, define $\Xi_j(i)$ the vertices of polytope Ξ_j and define $\mu_i^{(j)}$ the uncertain parameter of polytope Ξ_j, $j \in \{0\} \bigcup \{2, 3..., p\}$.

The polynomial in Taylor expansion series to order p except the remainder can be represented in the following

$$
\begin{aligned}
&\underbrace{\begin{pmatrix}\Xi_0 & \Xi_1 & \cdots & \Xi_p\end{pmatrix}}_{\Xi} \left(\begin{pmatrix} 1 \\ \xi_2 \\ \vdots \\ \xi_2^p \end{pmatrix} \otimes \boldsymbol{I} \right) \\
&= \Xi \left(\left(\boldsymbol{N} \begin{pmatrix} \nu_1 \\ \nu_2 \\ \vdots \\ \nu_{p+1} \end{pmatrix} \right) \otimes \boldsymbol{I} \right) \\
&= \Xi \left(\boldsymbol{N} \otimes \boldsymbol{I} \right) \left(\boldsymbol{\nu} \otimes \boldsymbol{I} \right)
\end{aligned}
\tag{6.18}
$$

where the matrix $\boldsymbol{N}$ and the uncertain parameters $\boldsymbol{\nu} = \left(\nu_1, \nu_2, ..., \nu_p\right)^T$ come from the utilization of Gaussian method on the variable vector $(1, \xi_2, ..., \xi_2^p)^T$:

$$
\underbrace{\begin{pmatrix}
1 & \cdots & \cdots & \cdots & 1 \\
\underline{\xi}_2 & \overline{\xi}_2 & \cdots & \cdots & \overline{\xi}_2 \\
\underline{\xi}_2^2 & \underline{\xi}_2^2 & \overline{\xi}_2^2 & \cdots & \overline{\xi}_2^2 \\
\vdots & & & \ddots & \vdots \\
\underline{\xi}_2^p & \cdots & \cdots & \underline{\xi}_2^p & \overline{\xi}_2^p
\end{pmatrix}}_{\boldsymbol{N}}
\begin{pmatrix} \nu_1(k) \\ \nu_2(k) \\ \vdots \\ \nu_p(k) \end{pmatrix}
=
\begin{pmatrix} 1 \\ \xi_2(k) \\ \xi_2^2(k) \\ \vdots \\ \xi_2^p(k) \end{pmatrix}.
\tag{6.19}
$$

Note that

$$
\begin{aligned}
&\Xi \left(\boldsymbol{N} \otimes \boldsymbol{I} \right) \\
&= \left(\Xi(\mathrm{col}_1(\boldsymbol{N}) \otimes \boldsymbol{I}), \Xi(\mathrm{col}_2(\boldsymbol{N}) \otimes \boldsymbol{I}), \cdots, \Xi(\mathrm{col}_{p+1}(\boldsymbol{N}) \otimes \boldsymbol{I}) \right).
\end{aligned}
\tag{6.20}
$$

Therefore Eq. (6.18) can be rewritten as

$$
\Xi \left(\boldsymbol{N} \otimes \boldsymbol{I} \right) \left(\boldsymbol{\nu} \otimes \boldsymbol{I} \right) = \sum_{i=1}^{p+1} \nu_i \Xi(\mathrm{col}_i(\boldsymbol{N}) \otimes \boldsymbol{I}).
\tag{6.21}
$$

Based on Minkowski addition of two polytopes the equation

$$
\sum_{i=1}^{N} \mu_i(k) \boldsymbol{B}_i + \sum_{j=1}^{M} \nu_j(k) \boldsymbol{C}_j = \sum_{i=1}^{N} \sum_{j=1}^{M} \mu_i(k) \nu_j(k) (\boldsymbol{B}_i + \boldsymbol{C}_j),
\tag{6.22}
$$

holds, where $\boldsymbol{B}_i$ and $\boldsymbol{C}_j$ are the vertices of two individual polytopes and $\mu_i(k)$ and $\nu_j(k)$ are the non-negative parameters with $\sum_{i=1}^{N} \mu_i(k) = 1$ and $\sum_{j=1}^{M} \nu_j(k) = 1$.

Applying Minkowski addition on $\Xi(\mathrm{col}_i(\boldsymbol{N}) \otimes \boldsymbol{I})$ yields

$$\begin{aligned}\Xi(\mathrm{col}_i(\boldsymbol{N}) \otimes \boldsymbol{I}) &= \sum_{j=1}^{p+1} \boldsymbol{N}_{ji}\Xi_j \\ &= \sum_{i_0=1}^{p+1}\sum_{i_1=1}^{p}\cdots\sum_{i_p=1}^{1}\left(\mu_{i_0}^{(0)}\mu_{i_1}^{(1)}\cdots\mu_{i_p}^{(p)}\right) \\ &\qquad \left(\boldsymbol{N}_{1i}\Xi_0(i_0) + \boldsymbol{N}_{2i}\Xi_1(i_1) + \cdots + \boldsymbol{N}_{(p+1)i}\Xi_p(i_p)\right)\end{aligned} \tag{6.23}$$

Hence Eq. (6.21) can be rewritten

$$\begin{aligned}&\sum_{i=1}^{p+1} \nu_i \Xi(\mathrm{col}_i(\boldsymbol{N}) \otimes \boldsymbol{I}) \\ &= \sum_{i=1}^{p+1}\sum_{i_0=1}^{p+1}\sum_{i_1=1}^{p}\cdots\sum_{i_p=1}^{1}\left(\nu_i\mu_{i_0}^{(0)}\mu_{i_1}^{(1)}\cdots\mu_{i_p}^{(p)}\right) \\ &\qquad \left(\boldsymbol{N}_{1i}\Xi_0(i_0) + \boldsymbol{N}_{2i}\Xi_1(i_1) + \cdots + \boldsymbol{N}_{(p+1)i}\Xi_p(i_p)\right)\end{aligned} \tag{6.24}$$

Since

$$\begin{aligned}&\sum_{i=1}^{p+1}\sum_{i_0=1}^{p+1}\sum_{i_1=1}^{p}\cdots\sum_{i_p=1}^{1} \nu_i\mu_{i_0}^{(0)}\mu_{i_1}^{(1)}\cdots\mu_{i_p}^{(p)} = 1, \\ &\text{and} \quad \nu_i\mu_{i_0}^{(0)}\mu_{i_1}^{(1)}\cdots\mu_{i_p}^{(p)} \geq 0\end{aligned} \tag{6.25}$$

The polytopic representation of polynomials in Taylor Series expansion until order p for two-variable case is completed. It can be concluded that the total number of vertices by constructing the convex polytope in this way is

$$(p+1)^2 \prod_{q=1}^{p} i_q = (p+1)^2 p!. \tag{6.26}$$

Remark 6.1. From (6.26) it can be seen that the the total number of vertices is increased in a polynomial way with the increase of the order p. Compare with the result in [WL09c] also based on the Taylor Series expansion, where the number of the vertices is

$$\begin{cases} 2^{\frac{p-1}{2}}[(p+1)!!]^2 & p \text{ is odd} \\ 2^{\frac{p}{2}}[(p+1)!!]^2 & p \text{ is even.} \end{cases} \tag{6.27}$$

The number of vertices from [WL09c] will increase exponentially with the increase of the order p. It's clear that the result presented in this chapter needs much less computations.

6.2.2 Arbitrary Number of Variables

The construction rule presented for the two-variable case can be extended to the case with arbitrary number of variables in light of a proper recursion. Consider for instance the three-variable case with ξ_1, ξ_2, ξ_3. Based on the expansion of the Taylor Series at point 0 up to order p, in polynomials except the remainder there are the terms containing

only ξ_1 with power 0 i.e. ξ_1^0

only ξ_1 with power 1 i.e. ξ_1^1

...

only ξ_1 with power p i.e. ξ_1^p

Organize and group the terms according to the powers of ξ_1 so that $\xi_1^{p_l}$, $p_l = 0, 1, ..., p$ will be the common factor. Sorting out the common factor $\xi_1^{p_l}$ yields a polynomial with variables

$$\xi_2^{p_n}\xi_3^{p_m}, \quad 0 \le p_n, p_m \le (p - p_l), \quad p_l + p_n + p_m \le p. \tag{6.28}$$

Now the construction rule in two-variable case is applied to construct the polynomial with variables $\xi_2^{p_n}\xi_3^{p_m}$ as a polytope. A polytopic representation in the form of (6.24) can be derived. Based on recursion, the three-variable case can always be processed by using the approach in two-variable case. Analogically for a more variables case the recursive rule can always be established based on the two-variable case.

Remark 6.2. In fact the method presented in this section to convert any variable-dependent linear system into a polytopic linear representation can be applied to either discrete or continuous-systems. A standard polytopic description in form of Eq. (6.6) can be always obtained.

6.3 An Illustrative Example

In this section, an academic example is given to demonstrate the effectiveness of the proposed method with application in the stability analysis.

Consider the system

$$\boldsymbol{z}(k+1) = \begin{pmatrix} \xi_1\xi_2 & \xi_1^3 & \xi_2 \\ \xi_1^3 & \xi_2^3 & \xi_1^2 \\ \xi_2^2 & \xi_1^2\xi_2 & \xi_1\xi_2^2 \end{pmatrix} \boldsymbol{z}(k), \tag{6.29}$$

where the system matrix depends nonlinearly on the two time-varying uncertain but bounded variables ξ_1, ξ_2. Assume two cases for the uncertainty ranges of ξ_1, ξ_2

$$\begin{aligned} &\text{Case 1:} \quad \xi_1 \in [0.1, 0.85], \quad \xi_2 \in [0.1, 0.3] \\ &\text{Case 2:} \quad \xi_1 \in [0.1, 0.41], \quad \xi_2 \in [0.1, 0.76]. \end{aligned} \tag{6.30}$$

Generally for a time-varying system (6.1) even though at every step k the eigenvalues of system matrix $\boldsymbol{\Phi}(k)$ are inside unit circle, the stability of system (6.1) still can not be claimed. The stability can be checked by using switched parameter-dependent quadratic Lyapunov functions based on a polytopic representation in a form of (6.6). The stability criterion is cited from [IGL08].

Lemma 6.1 *The system* (6.1) *represented in form of* (6.6) *is stable if there exist positive definite symmetric matrices* $\boldsymbol{S}_i \in \mathbb{R}^{n\times n}$ *and symmetric matrix* $\boldsymbol{G} \in \mathbb{R}^{n\times n}$ *for all* $i = 1, 2, ..., M$ *and* $j = 1, 2, ..., M$ *such that the LMIs*

$$\begin{pmatrix} \gamma \boldsymbol{I} - \boldsymbol{S}_i & \boldsymbol{\Phi}_i \boldsymbol{G} & \boldsymbol{\Phi}_i \boldsymbol{G} \\ \boldsymbol{G}\boldsymbol{\Phi}_i^T & \boldsymbol{S}_j - 2\boldsymbol{G} & \boldsymbol{0} \\ \boldsymbol{G}\boldsymbol{\Phi}_i^T & \boldsymbol{0} & 2\boldsymbol{G} - \boldsymbol{I} \end{pmatrix} < 0 \tag{6.31}$$

are feasible $\forall i = 1, 2, ..., M$ *and* $\forall j = 1, 2, ..., M$ *with* $\|\boldsymbol{\Theta}^h\|_2^2 \le \gamma$.

Therein $\boldsymbol{\Phi}_i$ are the polytopic vertices, M is the number of the vertices, $\boldsymbol{S}_i$ and $\boldsymbol{G}$ are LMI matrix variables, $\boldsymbol{\Theta}^h$ is the remainder of the Taylor Series expansion calculated by

$$\begin{aligned} \boldsymbol{\Theta}^h &= \boldsymbol{f}(\xi_1, \xi_2, ..., \xi_l) - f(0) - \frac{\partial \boldsymbol{f}}{\partial \xi_1}\xi_1 - \frac{\partial \boldsymbol{f}}{\partial \xi_2}\xi_2 - \frac{\partial^2 \boldsymbol{f}}{2!\partial \xi_1^2}\xi_1^2 \\ &- \frac{\partial^2 \boldsymbol{f}}{\partial \xi_1 \partial \xi_2}\xi_1\xi_2 - \frac{\partial^2 \boldsymbol{f}}{2!\partial \xi_2^2}\xi_2^2 - \cdots , \end{aligned} \tag{6.32}$$

γ is the upper bound of the induced matrix norm of the remainder $\boldsymbol{\Theta}^h$. Usually γ in the principal diagonal will strongly affect, even sabotage, the system stability if its value is too large. However the value of γ can be influenced by the order p in Taylor Series expansion. Generally the higher the order p is, the smaller γ is [HWG+10]. However big p indicate high computation effort as shown in (6.26). A tradeoff between the requirement of computations and verification of stability through solving LMIs needs to be made. A simple rule is that the verification of stability is started from a small value of p. When the stability can be verified, the higher order p is not required anymore.

Consider the Taylor Series expansion up to order two and order three respectively. Arrange the variables in the Taylor Series into the following two cases:

Expansion to order two:

1) $1,\ \xi_1,\ \xi_1^2,$

2) $\xi_2,\ \xi_1\xi_2,$

3) $\xi_2^2.$

Expansion to order three:

1) $1,\ \xi_1,\ \xi_1^2,\ \xi_1^3,$

2) $\xi_2,\ \xi_1\xi_2,\ \xi_1^2\xi_2,$

3) ξ_2^2, $\xi_1 k_2^2$,

4) ξ_2^3.

Apply the approach presented in this chapter to construct the polytopic representation for both the order two and order three cases. Then use Lemma 6.1 to verify the stability based on obtained polytopic representation. The results are shown in Table 6.1. It can be seen that the upper bound γ of remainder $\mathbf{\Theta}^h$ decreases such that the stability can be verified when the approximation order increases. The dynamics of the systems (6.29)

p	Range of ξ_1	Range of ξ_2	Error γ	Verification
2	[0.1,0.41]	[0.1,0.76]	0.2276	fail
3	[0.1,0.41]	[0.1,0.76]	0.0322	stable
2	[0.1,0.85]	[0.1,0.3]	0.5056	fail
3	[0.1,0.85]	[0.1,0.3]	0.02348	stable

Table 6.1: the stability verification

subject to time-varying uncertainty in the system matrix are shown in Fig. 6.1 and 6.2 respectively. The initial states are chosen randomly in range $[-5, 5]$. The system behaves as verified that the states converge to equilibrium points.

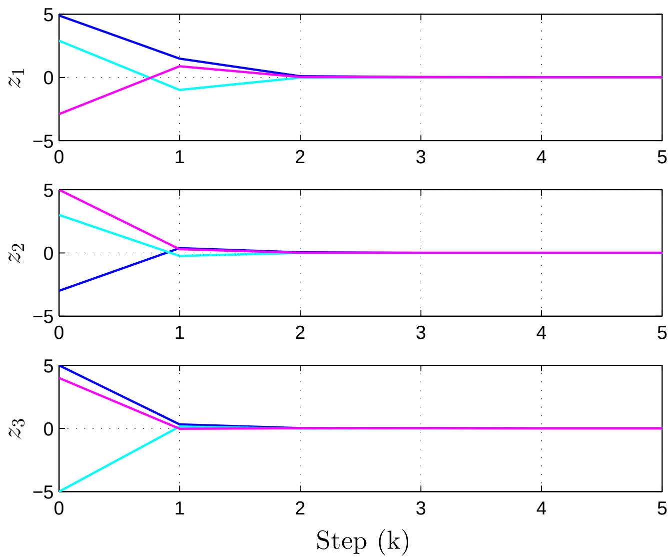

Figure 6.1: Transient dynamics of system (6.29) with three different initial values when $\xi_1 \in [0.1, 0.41]$ and $\xi_2 \in [0.1, 0.76]$

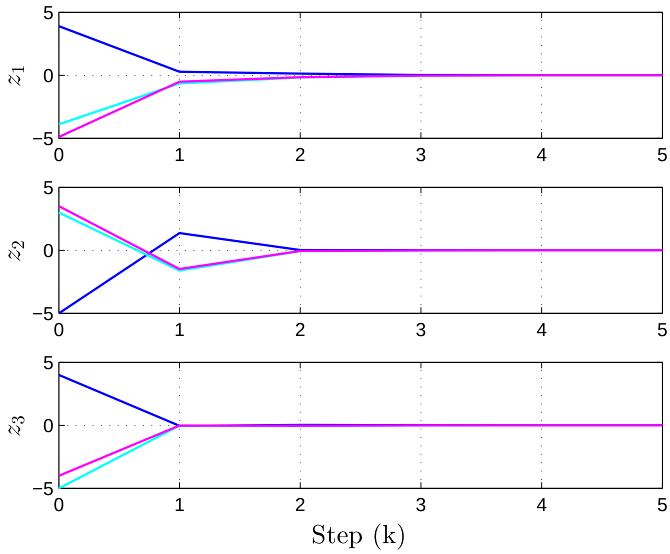

Figure 6.2: Transient dynamics of system (6.29) with three different initial values when $\xi_1 \in [0.1, 0.85]$ and $\xi_2 \in [0.1, 0.3]$

6.4 Conclusion

This chapter proposes an approach to construct a polytopic representation for the system subject to time-varying uncertainty in system matrix. Based on Taylor Series expansion approximation the approach can deal with any number of uncertain bounded variables. This generalizes the results in [HDI06] and [IGL08] which only consider one and two uncertain variables respectively. The approach improves also the work in [WL09c] such that less computation complexity and less conservativeness for approximation are achieved.

7 Conclusion and Future Work

Conclusion

Constructive event-triggered control designs for embedded control systems have been presented. The control designs have aimed at different control objectives. Chapter 2 addresses the event-triggered control in the frame of optimal control. The control performance is measured by the classic linear quadratic cost function. The event-triggering condition involving a user defined parameter influencing the communication rate is synthesized jointly with the controller design. Consequently the results in Chapter 2 are extended to the scheduling and control design for multiple embedded control systems in Chapter 5. The event-triggering conditions that function not only as a part of controller but also as a part of resource scheduler are utilized in scheduling algorithm. In parallel, the event-triggered control is designed for the system subject to actuator saturation in Chapter 3 and the system subject to bounded disturbance in Chapter 4 in order to serve different control objectives. All the presented results address the synthesized controller designs with a core consideration of ensuring stability. The implementation-aware feature is reflected in the low complexity of controller calculation and event-triggering condition verification. Obtaining the control gain can efficiently be accomplished off-line by using the toolbox in MATLAB.

A result about polytopic representation of time-varying uncertain systems is given in Chapter 6 with the purpose of linking the embedded control system to the robust control of polytopic systems. Less conservative results can be expected with the help of parameter dependent Lyapunov functions.

Realization, Applicability and Future Work

Purposefully the presented approaches can be applied in networked control system (see Fig. 7.1) to reduce the transmission traffic, which are in the controller-actuator channels or in sensor-controller channels and the actuation of actuator. One possible application can be found in suspension control systems of cars [GCK04, Aly12]. The event-triggering condition can be defined according to the requirement of passenger comfort. Increasing the passenger comfort requires more triggered events to damp the vibrations such that more actuation and more communications in the Controller Area Network (CAN) bus are demanded. Networked control systems are comprised of the system to be controlled and of actuators, sensors, and controllers whose operation is coordinated through some form of communication network [BA07]. The presented event-triggering condition is

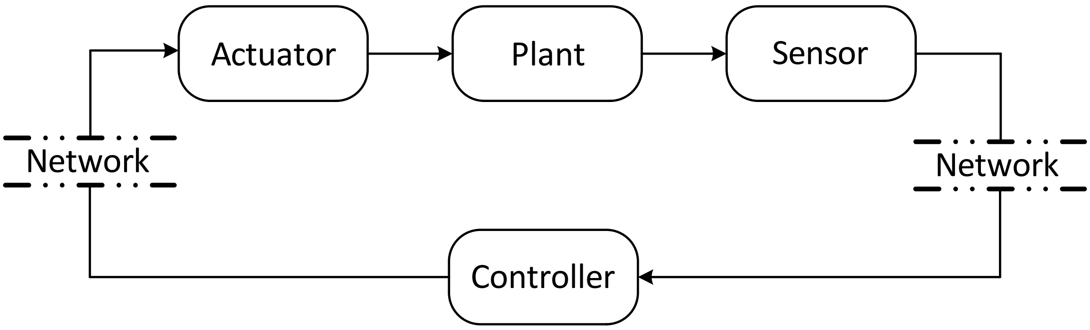

Figure 7.1: Networked control configuration

checked either in controller system or in sensor system such that a transmission decision is made. If the sensor node does not have the capacity for numerical computation such as checking the event-triggering condition, then the transmission of the state of the plant between sensor and controller is necessary. The transmission reduction can only occur in between controller and actuator. If the sensor as wireless nodes is instrumented in mobile device, where sensor data can be processed locally, the presented approaches can be applied for energy saving with the reduction of transmission, which can be very important for a mobile battery-powered equipment. One possible application can be found in the level and temperature control of thermofluid process in chemical industry [LL11b] with distributed sensor nodes. The energy saving can also be possibly achieved in the reduction of the numbers of actuation, where one application can be found in the mobile robot control [BGTT04].

One of the main characteristics from the presented approaches is the periodic measurement such that the control objectives and control performance can be achieved as expected in the control design. This periodic requirement can be easily realized in any kind of micro-controller with timer interrupt service routine. Nevertheless whether the digital signal can be transmitted periodically to the actuator depends on communication medium such as wired or wireless and communication protocol in the network. When the digital communication networks are shared by other applications the media access by the sensor that needs to transmit data may not be immediate and communication delays and packet losses may occur. One way to deal with the achievement of periodic communication goes to the information science [PSA97, GJJW00, CK03, CKL06, LLOC12]. From the control engineer standpoint for a given network a modelling of the delay by distinguishing the causes of the delay and quantifying the delay aroused in the network can be the starting step (for instance see Chapter 5). Coupling this model of delay with the control systems can be of significance for supplying a more realistic and accurate solution to the given problems.

Another characteristic of the presented approaches is the requirement of a full-state measurement that is used in checking the event-triggering condition and in state feedback controller. However in some control applications full state measurements may not be available, therefore observer-based event-triggered control needs to be considered. Combining the model of the observer in the controller synthesis is essential for the improvement of the presented approaches. Another point is how accurate the transmitted state information should be in order to guarantee a desired performance. Since the communication traffic can be alleviated by sending a relatively less accurate quantized state information, the trade-off between the control performance and the quantization of the state information can be an interesting topic. Under this circumstance how to design the event-triggered controller to compensate the inaccuracy from quantization of the output signal appears very appealing.

In event-triggered feedback the transmission of sampled measurement or actuation of an executive body is permitted by the fact that the novelty in the sensor information exceeds a specified threshold. In order to reduce the number of events a 'big' threshold could correspondingly accumulate a 'big' novelty, which is interpreted as a drastic operation in the actuating node. For instance a motor could output a big torque at this moment when an event is triggered. This behavior should be avoided especially in mechanic systems for increasing the lifespan. Therefore a suitable controller that is able to smooth the actuation should be considered. It is possible to supply a small variation of the control input value in the updating by considering the variation in the cost function and event-triggering condition.

Preliminarily Chapter 6 paves a path to the controller design for the time-varying uncertain systems. By employing parameter dependent Lyapunov function less conservative results could be achieved for robust stability analysis. Those techniques so far have not been embedded in the event-triggered control design. As a future work, relating the event-triggered control to the time-varying uncertain systems is a theoretical and practical interesting topic. It could easily find the application in the scheduling and control of networked embedded control systems.

8 Zusammenfassung

Ereignisbasierte Regelung linearer Systeme

mit Anwendung für eingebettete Regelungssysteme

Aufgrund der weitreichenden Verwendung in vielen Bereichen spielen eingebettete Regelungssysteme eine signifikante Rolle in unserer Gesellschaft. Solche Bereiche erstrecken sich von Verkehrsmitteln wie Kraftfahrzeuge, Schienenfahrzeuge oder Flugzeuge, über industrielle Anlagen, beispielsweise Fertigungsanlagen und verfahrenstechnische Anlagen, bis hin zu Infrastruktursystemen wie Energienetze oder intelligente Gebäude. Derzeit handelt es sich bei 98%.

Trotz der breiten praktischen Verwendung von eingebetteten Regelungssystemen ist die theoretische Basis dafür noch nicht vollständig. Meist werden die Regelungsentwürfe und Echtzeit Scheduling Verfahren in der Regelungstechnik beziehungsweise in der Informatik getrennt voneinander entwickelt.

Themen wie Funktionalität, Effizienz, Zuverlässigkeit und Sicherheit sind schwer in einem einheitlichen Rahmen mit der stark zunehmenden Komplexität zu behandeln. Die Komplexität ergibt sich im Rahmen der modernen Industrialisierung insbesondere durch zunehmende Verwendung von verdrahteten und drahtlosen Netzwerken zur Kommunikation. Dabei treten unvermeidlichen Herausforderungen wie Energie-, Rechen- und Kommunikationsbeschränkungen auf. Um theoretische Grundlagen für vernetzte Regelungssysteme aufzubauen ist daher eine Zusammenarbeit unterschiedlicher Fachrichtungen wie Mathematik, Informatik, Kommunikationstechnik und Regelungstechnik erforderlich.

Traditionell wird beim Echzeit-Scheduling angenommen, dass alle Regelungsaufgaben als periodische Aufgaben mit harten Deadlines dargestellt werden können, wobei durch das Scheduling Jitter auftreten kann. Die klassische Regelungstechnik hingegen nimmt an, dass die Regelungsaufgaben mit einer äquidistanten Abtastung und Aktuierung realisiert werden können, wobei eine konstante Ein-/Ausgangsverzögerung sichergestellt werden kann. Das Model, die Regelungsaufgabe als periodische Aufgabe zu betrachten, kann somit als Schnittstelle zwischen den beiden Sichtweisen verwendet werden.

Vom Standpunkt der Regelungstechnik ist die periodische Abtastung vorteilhaft, da für solche abgetastete Regelungssysteme fundierte Theorien in der Literatur vorhanden sind. Hingegen ist die periodische Aktualisierung der Stellgröße nicht immer erforderlich um eine gewünschte Performance zu erzielen, z.B. wenn keine Störung auf das System wirkt oder das System sich im stationären Endwert befindet. Die ereignisbasierte Regelung bietet eine gute Option den Kommunikations- und Aktuierungsaufwand im Vergleich zur periodischen Regelung zu reduzieren. Die ereignisbasierte Regelung basiert darauf, dass eine Versendung von Sensorsignalen beziehungsweise die Berechnung der Stellgröße durch ein Ereignis ausgelöst wird.

Dynamische Ressourcenzuweisung bei gemeinsamer Ressourcennutzung kann auch gut mit Hilfe der ereignisbasierten Regelungsarchitektur umgesetzt werden. Durch die Allokation der Ressourcen durch eine ereignisbasierte Regelungsstrategie kann durch Zulassung gewisser Verluste in der Regelgüte eine kosteneffiziente Lösung erreicht werden.

Diese Dissertation gibt einen Beitrag zur Forschung über ereignisbasierte Regelungsmethoden und ihre Anwendung in eingebetteten Regelungssystemen. Aus regelungstechnischer Sicht wird hier die Stabilität der zu regelnden Systeme als ein Hauptfokus gesehen. In sicherheitskritischen Echtzeit-Regelungssystemen, z.B. X-by-wire Systeme im Automobilbereich oder Avionikbereich, kann die Instabilität eines Systems katastrophalen Konsequenzen mit sich bringen. Daher muss die Stabilität als eine Grundanforderung in den Regelungsstrategien berücksichtigt werden. Dabei wird der Regler in einer Reglersynthese mit den Ereignisbedingungen für unterschiedliche Regelungsziele spezifisch entworfen. Im Hinblick auf die Regelung von mehreren Systemen mit begrenzten Rechen- und Kommunikationsressourcen ist ein effizientes und implementierungsbewusstes Scheduling erforderlich, welches die zeitliche Allokation der Regelungsaufgaben festlegt. Um eine bestimmte Regelgüte sicherzustellen ist ein gemeinsamer Regler- und Schedulerentwurf erforderlich.

Diese Dissertation hat das Ziel systematisch ereignisbasierte Regelungsstrategien als effiziente Alternative zur traditionellen periodischen Abtastregelung zu entwickeln. Das Auftreten der aperiodischen Regelung, was inhärenter Bestandteil der ereignisbasierten Regelung ist, wird durch die Ereignisbedingung bestimmt. Aufgrund dieser Charakteristik müssen hier Grundlagen geschaffen werden. Die Entwicklung eines Reglers zur Optimierung einer Regelgüte unter Berücksichtigung der Ereignisbedingung ist Kern des ereignisbasierten Reglerentwurfs. Bei diesem Entwurf muss die Gewährleistung der Stabilität des Regelungssystems mit allererster Priorität berücksichtigt werden. Im Hinblick auf unterschiedliche Regelungsziele wird diese im Verlauf des Reglerentwurfs berücksichtigt. Bei der Anwendung in eingebetteten Regelungssystemen ist zusätzliche eine effiziente Implementierung mit niedriger Komplexität erforderlich. Diese Dissertation zielt darauf ab einen Beitrag zu leisten um die ereignisbasierte Regelung zu komplettieren.

Im Einzelnen werden in der Dissertation folgende Punkte untersucht.

Kapitel 1 gibt einen Überblick über die Grundidee der ereignisbasierten Regelung basierend auf der Zustandsraumdarstellung. Dabei werden unterschiedliche Ereignisbedingungen diskutiert. Anhand von unterschiedlichen Regelungszielen, Vorgehensweisen und Anwendungen wird der Stand der Technik präsentiert.

Kapitel 2 fokussiert auf einen suboptimalen ereignisbasierten Regelungsentwurf für lineare Systeme mit einer Eingangsverzögerung. Als Performanceindex wird die linear quadratische Kostenfunktion zur Quantifizierung der Regelgüte und die durchschnittliche Ereigniszahl, d.h. die Anzahl der Ereignisse im Verhältnis zur Anzahl der Sensormessungen, zur Quantifizierung der Reduktion der Kommunikation betrachtet. Der Reglerentwurf wird unter Berücksichtigung der Ereignisbedingung als Optimierungsproblem beschrieben. Die Lösung des Optimierungsproblems geschieht offline zur Bestimmung der Reglerparameter. Der ereignisbasierte Regler, welcher durch ein praktisches Experiment verifiziert wird, zeichnet sich durch niedrige Komplexität aus und ist somit geeignet für eingebettete Echtzeit-Regelungssysteme.

Kapitel 3 befasst sich mit der ereignisbasierten Regelung für lineare Systeme mit Stellgrößenbeschränkung. Durch Einführung einer Hilfsmatrix lässt sich analysieren, ob ein gegebenes Ellipsoid kontraktiv invariant ist. Um die ellipsoidenförmigen kontraktiv invariante Menge zu maximieren wird eine Reglersynthese für die ereignisbasierte Regelung entwickelt. Somit wird der ereignisbasierte Regler als Optimierungsproblem formuliert in dem die Größe des Ellipsoids maximiert wird, wobei die Stabilität im Sinne von Lyapunov als Nebenbedingung berücksichtigt wird.

In Kapitel 4 wird ein ereignisbasierter Regler entworfen für zeitdiskrete Systeme, welche durch beschränkte Störungen beeinflusst werden. Das Hauptregelungsziel ist die Reduzierung des Einflusses der Störung bei einer Reduktion der Kommunikation durch die ereignisbasierte Regelung. Der Regler wird derart entworfen, dass die Konvergenz in eine ellipsoidenförmige positiv invariante Menge sichergestellt ist. Diese Menge wird als Abschätzung der Regelgüte für die Unterdrückung der Störung betrachtet. Um dies zu optimieren wird diese ellipsoidenförmige positiv invariante Menge in einer Reglersynthese minimiert unter Berücksichtigung der Ereignisbedingung. Das Ergebnis wird in einer praktischen Implementierung verifiziert.

In Kapitel 5 wird der Fall betrachtet, dass mehrere Regelungsaufgaben für unterschiedliche Strecken auf einem Prozessor realisiert werden. In diesem Szenario konkurrieren die Regelungssysteme um die begrenzten Ressourcen. Mit Hilfe eines gemeinsamen Scheduling- und Reglerentwurfs können durch dynamische Ressourcenzuweisung Vorteile gegenüber einer statischen Ressourcenzuweisung hinsichtlich der Regelgüte im Experiment erzielt werden. Dabei wird die Idee der ereignisbasierten Regelung als Hilfsmittel zur Ressourcenverteilung angewandt.

In Kapitel 6 wird die Modellierung von Systemen mit zeitvariablen Parametern untersucht. Die zeitvariablen Parameter sind durch Ober- und Untergrenzen beschränkt. In eingebetteten Regelungssystemen können beispielsweise Abtastzeit und Eingangsverzögerung zeitvariabel auftreten. Zur Modellierung solcher zeitvariabler Systeme wird hier die polytopische Darstellung verwendet. Diese Methode basiert auf einer Überapproximation der Taylor Reihe. Durch Iteration kann die Methode erweitert werden zur Behandlung von Systemen mit mehreren zeitvariablen Parametern.

Kapitel 7 fasst die Methoden und Ergebnisse der Dissertation zusammen. Zusätzlich wird die Realisierung und Anwendbarkeit der vorgestellten Methoden diskutiert und es werden Anregungen für weitere Untersuchungen gegeben.

A Supplementary Material

A.1 Stability Definitions

The stability and stabilization for event-triggered control systems can be investigated in the frame of non-autonomous systems since generally the initial states are unknown and the dynamics of the closed loop systems and the event-triggering conditions render a hybrid system [HDT13]. Thus, Lyapunov stability theory for discrete-time non-autonomous systems is reviewed first in the following.

Consider the discrete-time non-autonomous system

$$\boldsymbol{x}(k+1) = \boldsymbol{f}(\boldsymbol{x}(k), k), \quad \boldsymbol{x}(k_0) = \boldsymbol{x}_0, \tag{A.1}$$

where $\boldsymbol{x}(k) \in \mathbb{R}^n$ is the state vector, $k \in \mathbb{N}_0$ is the discrete time, $k_0 \in \mathbb{N}_0$ is the initial time and $\boldsymbol{f} : \mathbb{R}^n \times \mathbb{N}_0 \to \mathbb{R}^n$ is a generally nonlinear function. Assume that $\boldsymbol{x}_e = \boldsymbol{0}$ is an equilibrium point of (A.1), i.e. $\boldsymbol{f}(\boldsymbol{0}, k) = \boldsymbol{0}\ \forall k \in \mathbb{N}_0$. For a non-zero equilibrium point $\boldsymbol{x}_e$ by shifting the coordinate the stability analysis for the equilibrium point $\boldsymbol{0}$ can be reformulated. The stability of the equilibrium point $\boldsymbol{x}_e = \boldsymbol{0}$ in the sense of Lyapunov is characterized by the following

Definition A.1 *The equilibrium point $\boldsymbol{x}_e = \boldsymbol{0}$ of the discrete-time non-autonomous system* (A.1) *is*

- *stable at k_0 if for each $\varepsilon > 0$ there exists a $\delta = \delta(\varepsilon, k_0) > 0$ such that*

$$\|\boldsymbol{x}(k_0)\| \leq \delta \Rightarrow \|\boldsymbol{x}(k)\| \leq \varepsilon \quad \forall k \geq k_0, \tag{A.2}$$

- *uniformly stable if for each $\varepsilon > 0$ there exists a $\delta = \delta(\varepsilon, k_0) > 0$ independent of k_0 such that* (A.2) *is fulfilled,*

- *asymptotically stable at k_0 if it is stable and there exists a $\delta'(k_0) > 0$ such that*

$$\|\boldsymbol{x}(k_0)\| \leq \delta' \Rightarrow \lim_{k\to\infty} \|\boldsymbol{x}(k)\| = 0, \tag{A.3}$$

- *uniformly asymptotically stable if it is stable and there exists a $\delta' > 0$ independent of k_0 such that* (A.3) *is fulfilled uniformly in k_0, i.e. for each $\varepsilon' > 0$ there exists a $K = K(\varepsilon')$ independent of k_0 such that*

$$\|\boldsymbol{x}(k_0)\| \leq \delta' \Rightarrow \|\boldsymbol{x}(k)\| \leq \varepsilon' \quad \forall k \geq k_0 + K, \tag{A.4}$$

- *globally uniformly asymptotically stable if it is uniformly asymptotically stable for all* $\boldsymbol{x}(k_0) \in \mathbb{R}^n$,
- *unstable if it is not stable.*

Checking the conditions from the Definition A.1 for general discrete-time non-autonomous systems (A.1) is difficult and no universal methods exist. One important tool is the Lyapunov's direct method. The characteristics of Lyapunov functions are given as follows.

Definition A.2 *A function* $V : \mathbb{D} \to \mathbb{R}$ *is*

- *positive semidefinite in* $\mathbb{D} \subset \mathbb{R}^n$ *if*
  1. $V(\mathbf{0}) = 0$
  2. $V(\boldsymbol{x}(k)) \geq 0 \ \forall \boldsymbol{x}(k) \in \mathbb{D} \backslash \{\mathbf{0}\}$,
- *positive definite in* $\mathbb{D} \subset \mathbb{R}^n$
  1. $V(\mathbf{0}) = 0$
  2. $V(\boldsymbol{x}(k)) > 0 \ \forall \boldsymbol{x}(k) \in \mathbb{D} \backslash \{\mathbf{0}\}$,
- *negative definite (semidefinite) in* $\mathbb{D} \subset \mathbb{R}^n$ *if* $-V$ *is positive definite (semidefinite).*

Definition A.3 *A function* $V : \mathbb{D} \times \mathbb{N}_0 \to \mathbb{R}$ *is*

- *positive semidefinite in* $\mathbb{D} \subset \mathbb{R}^n$ *if*
  1. $V(\mathbf{0}, k) = 0 \ \forall k \in \mathbb{N}_0$
  2. $V(\boldsymbol{x}(k), k) \geq 0 \ \forall \boldsymbol{x}(k) \in \mathbb{D} \backslash \{\mathbf{0}\} \ \forall k \in \mathbb{N}_0$,
- *positive definite in* $\mathbb{D} \subset \mathbb{R}^n$ *if*
  1. $V(\mathbf{0}, k) = 0 \ \forall k \in \mathbb{N}_0$
  2. *there exists a positive definite function* $V_1 : \mathbb{D} \to \mathbb{R}$ *independent of* k *such that*

$$V_1(\boldsymbol{x}(k)) \leq V(\boldsymbol{x}(k), k) \quad \forall \boldsymbol{x}(k) \in \mathbb{D} \backslash \{\mathbf{0}\} \quad \forall k \in \mathbb{N}_0,$$

- *negative definite (semidefinite) in* $\mathbb{D} \subset \mathbb{R}^n$ *if* $-V$ *is positive definite (semidefinite),*
- *decrescent if there exists a positive definite function* $V_2 : \mathbb{D} \to \mathbb{R}$ *independent of* k *such that*

$$V(\boldsymbol{x}(k), k) \leq V_2(\boldsymbol{x}(k)) \quad \forall \boldsymbol{x}(k) \in \mathbb{D} \quad \forall k \in \mathbb{N}_0,$$

- *radially unbounded if there exists a positive definite function* $V_1 : \mathbb{D} \to \mathbb{R}$ *independent of* k *with* $V_1(\boldsymbol{x}(k)) \to \infty$ *as* $\|\boldsymbol{x}(k)\| \to \infty$ *such that*

$$V_1(\boldsymbol{x}(k)) \leq V(\boldsymbol{x}(k), k) \quad \forall \boldsymbol{x}(k) \in \mathbb{D} \quad \forall k \in \mathbb{N}_0.$$

Then Lyapunov's direct method can be formalized as

Theorem A.1 *If in a neighborhood* $\mathbb{D} \subset \mathbb{R}^n$ *of the equilibrium point* $\boldsymbol{x}_e = \mathbf{0}$ *of the discrete-time non-autonomous system* (A.1) *there exists a function* $V : \mathbb{D} \times \mathbb{N}_0 \to \mathbb{R}$ *such that*

1. $V(\boldsymbol{x}(k), k)$ *is positive definite*
2. $\Delta V(\boldsymbol{x}(k), k) = V(\boldsymbol{x}(k+1), k+1) - V(\boldsymbol{x}(k), k)$ *is negative semidefinite, then the equilibrium point is stable. If furthermore*
3. $V(\boldsymbol{x}(k), k)$ *is decrescent, then the equilibrium point is uniformly stable. If furthermore*
4. $\Delta V(\boldsymbol{x}(k), k) = V(\boldsymbol{x}(k+1), k+1) - V(\boldsymbol{x}(k), k)$ *is negative definite, then the equilibrium point is uniformly asymptotically stable. If furthermore* $\mathbb{D} = \mathbb{R}^n$ *and*
5. $V(\boldsymbol{x}(k), k)$ *is radially unbounded, then the equilibrium point is globally uniformly asymptotically stable.*

Proof. The proof can be deduced from the proof for continuous-time non-autonomous systems, see e.g [SL91, Section 4.2.1], [Vid02, Section 5.3] and [Mar03, Section 4.4]. See also [Vid02, Section 5.9] and [Mar03, Section 4.10] for a discussion on discrete-time non-autonomous systems (A.1). □

Remark A.1. Exponential stability is a stronger condition of uniform asymptotic stability. The definition can refer to [Vid02, Section 5.9].

A.2 Discretization of The Cost Function

This appendix addresses the discretization of the continuous-time cost function (2.5).

The cost function must be discretized over the discretization interval $t_k \leq t < t_{k+1}$ using ZOH. When selecting the time interval $h = t_{k+1} - t_k$, the cost function can be rewritten as

$$J = \sum_{k=0}^{\infty} \int_{t_k}^{t_k+h} \begin{pmatrix} \boldsymbol{x}(s) \\ \boldsymbol{u}(s-\tau) \end{pmatrix}^T \begin{pmatrix} \boldsymbol{Q}_c & \mathbf{0} \\ \mathbf{0} & \boldsymbol{R}_c \end{pmatrix} \begin{pmatrix} \boldsymbol{x}(s) \\ \boldsymbol{u}(s-\tau) \end{pmatrix} ds. \tag{A.5}$$

Substituting the solution of the continuous-time state equation (2.1) leads to

$$\begin{aligned} J = \sum_{k=0}^{\infty} \int_{t_k}^{t_{k+1}} & \left[\mathrm{e}^{\boldsymbol{A}(t-t_k)} \boldsymbol{x}(t_k) + \int_{t_k}^{t} \mathrm{e}^{\boldsymbol{A}(t-s)} \boldsymbol{B} \boldsymbol{u}(s-\tau) ds \right]^T \boldsymbol{Q}_c \\ & \left[\mathrm{e}^{\boldsymbol{A}(t-t_k)} \boldsymbol{x}(t_k) + \int_{t_k}^{t} \mathrm{e}^{\boldsymbol{A}(t-s)} \boldsymbol{B} \boldsymbol{u}(s-\tau) ds \right] + \\ & \boldsymbol{u}^T(t-\tau) \boldsymbol{R}_c \boldsymbol{u}(t-\tau) dt. \end{aligned} \tag{A.6}$$

Expanding (A.6), substituting the piecewise constant control vector, splitting the integrals and factoring out $\boldsymbol{x}(t_k)$, $\boldsymbol{u}(t_{k-1})$ and $\boldsymbol{u}(t_k)$ yields

$$J = \sum_{k=0}^{\infty} \left[I_1(k) + I_2(k) + I_3(k) + I_4(k) + I_5(k) \right] \tag{A.7}$$

with

$$\begin{aligned}
I_1(k) =& \int_{t_k}^{t_{k+1}} \left[\mathrm{e}^{\boldsymbol{A}(t-t_k)} \boldsymbol{x}(t_k) \right]^T \boldsymbol{Q}_c \left[\mathrm{e}^{\boldsymbol{A}(t-t_k)} \boldsymbol{x}(t_k) \right] dt \qquad \text{(A.8a)} \\
=& \boldsymbol{x}^T(t_k) \left[\int_0^h \left(\mathrm{e}^{\boldsymbol{A}t} \right)^T \boldsymbol{Q}_c \left(\mathrm{e}^{\boldsymbol{A}t} \right) dt \right] \boldsymbol{x}(t_k) \\
I_2(k) =& \int_{t_k}^{t_{k+1}} \left[\mathrm{e}^{\boldsymbol{A}(t-t_k)} \boldsymbol{x}(t_k) \right]^T \boldsymbol{Q}_c \left[\int_{t_k}^{t} \mathrm{e}^{\boldsymbol{A}(t-s)} \boldsymbol{B} \boldsymbol{u}(s-\tau) ds \right] dt \qquad \text{(A.8b)} \\
=& \int_{t_k}^{t_k+\tau} \left[\mathrm{e}^{\boldsymbol{A}(t-t_k)} \boldsymbol{x}(t_k) \right]^T \boldsymbol{Q}_c \left[\int_{t_k}^{t} \mathrm{e}^{\boldsymbol{A}(t-s)} \boldsymbol{B} \boldsymbol{u}(t_{k-1}) ds \right] dt + \\
& \int_{t_k+\tau}^{t_{k+1}} \left[\mathrm{e}^{\boldsymbol{A}(t-t_k)} \boldsymbol{x}(t_k) \right]^T \boldsymbol{Q}_c \\
& \qquad \left[\int_{t_k}^{t_k+\tau} \mathrm{e}^{\boldsymbol{A}(t-s)} \boldsymbol{B} \boldsymbol{u}(t_{k-1}) ds + \int_{t_k+\tau}^{t} \mathrm{e}^{\boldsymbol{A}(t-s)} \boldsymbol{B} \boldsymbol{u}(t_k) ds \right] dt \\
=& \boldsymbol{x}^T(t_k) \left[\int_0^\tau \left(\mathrm{e}^{\boldsymbol{A}t} \right)^T \boldsymbol{Q}_c \left(\int_0^t \mathrm{e}^{\boldsymbol{A}(t-s)} \boldsymbol{B} ds \right) dt \right] \boldsymbol{u}(t_{k-1}) + \\
& \boldsymbol{x}^T(t_k) \left[\int_\tau^h \left(\mathrm{e}^{\boldsymbol{A}t} \right)^T \boldsymbol{Q}_c \left(\int_0^\tau \mathrm{e}^{\boldsymbol{A}(t-s)} \boldsymbol{B} ds \right) dt \right] \boldsymbol{u}(t_{k-1}) + \\
& \boldsymbol{x}^T(t_k) \left[\int_\tau^h \left(\mathrm{e}^{\boldsymbol{A}t} \right)^T \boldsymbol{Q}_c \left(\int_\tau^t \mathrm{e}^{\boldsymbol{A}(t-s)} \boldsymbol{B} ds \right) dt \right] \boldsymbol{u}(t_k) \\
I_3(k) =& \int_{t_k}^{t_{k+1}} \left[\int_{t_k}^{t} \mathrm{e}^{\boldsymbol{A}(t-s)} \boldsymbol{B} \boldsymbol{u}(s-\tau) ds \right]^T \boldsymbol{Q}_c \left[\mathrm{e}^{\boldsymbol{A}(t-t_k)} \boldsymbol{x}(t_k) \right] dt \qquad \text{(A.8c)} \\
=& \int_{t_k}^{t_k+\tau} \left[\int_{t_k}^{t} \mathrm{e}^{\boldsymbol{A}(t-s)} \boldsymbol{B} \boldsymbol{u}(t_{k-1}) ds \right]^T \boldsymbol{Q}_c \left[\mathrm{e}^{\boldsymbol{A}(t-t_k)} \boldsymbol{x}(t_k) \right] dt + \\
& \int_{t_k+\tau}^{t_{k+1}} \left[\int_{t_k}^{t_k+\tau} \mathrm{e}^{\boldsymbol{A}(t-s)} \boldsymbol{B} \boldsymbol{u}(t_{k-1}) ds + \int_{t_k+\tau}^{t} \mathrm{e}^{\boldsymbol{A}(t-s)} \boldsymbol{B} \boldsymbol{u}(t_k) ds \right]^T \boldsymbol{Q}_c
\end{aligned}$$

$$
\begin{aligned}
&\left[\mathrm{e}^{\boldsymbol{A}(t-t_k)}\boldsymbol{x}(t_k)\right] dt \\
=&\boldsymbol{u}^T(t_{k-1}) \left[\int_0^\tau \left(\int_0^t \mathrm{e}^{\boldsymbol{A}(t-s)}\boldsymbol{B}ds\right)^T \boldsymbol{Q}_c \left(\mathrm{e}^{\boldsymbol{A}t}\right) dt\right] \boldsymbol{x}(t_k)+ \\
&\boldsymbol{u}^T(t_{k-1}) \left[\int_\tau^h \left(\int_0^\tau \mathrm{e}^{\boldsymbol{A}(t-s)}\boldsymbol{B}ds\right)^T \boldsymbol{Q}_c \left(\mathrm{e}^{\boldsymbol{A}t}\right) dt\right] \boldsymbol{x}(t_k)+ \\
&\boldsymbol{u}^T(t_k) \left[\int_\tau^h \left(\int_\tau^t \mathrm{e}^{\boldsymbol{A}(t-s)}\boldsymbol{B}ds\right)^T \boldsymbol{Q}_c \left(\mathrm{e}^{\boldsymbol{A}t}\right) dt\right] \boldsymbol{x}(t_k)
\end{aligned}
$$

$$
\begin{aligned}
I_4(k) =& \int_{t_k}^{t_{k+1}} \left[\int_{t_k}^t \mathrm{e}^{\boldsymbol{A}(t-s)}\boldsymbol{B}\boldsymbol{u}(s-\tau)ds\right]^T \boldsymbol{Q}_c \left[\int_{t_k}^t \mathrm{e}^{\boldsymbol{A}(t-s)}\boldsymbol{B}\boldsymbol{u}(s-\tau)ds\right] dt \qquad \text{(A.8d)} \\
=& \int_{t_k}^{t_k+\tau} \left[\int_{t_k}^t \mathrm{e}^{\boldsymbol{A}(t-s)}\boldsymbol{B}\boldsymbol{u}(t_{k-1})ds\right]^T \boldsymbol{Q}_c \left[\int_{t_k}^t \mathrm{e}^{\boldsymbol{A}(t-s)}\boldsymbol{B}\boldsymbol{u}(t_{k-1})ds\right] dt+ \\
& \int_{t_k+\tau}^{t_{k+1}} \left[\int_{t_k}^{t_k+\tau} \mathrm{e}^{\boldsymbol{A}(t-s)}\boldsymbol{B}\boldsymbol{u}(t_{k-1})ds + \int_{t_k+\tau}^t \mathrm{e}^{\boldsymbol{A}(t-s)}\boldsymbol{B}\boldsymbol{u}(t_k)ds\right]^T \boldsymbol{Q}_c \\
& \qquad \left[\int_{t_k}^{t_k+\tau} \mathrm{e}^{\boldsymbol{A}(t-s)}\boldsymbol{B}\boldsymbol{u}(t_{k-1})ds + \int_{t_k+\tau}^t \mathrm{e}^{\boldsymbol{A}(t-s)}\boldsymbol{B}\boldsymbol{u}(t_k)ds\right] dt \\
=&\boldsymbol{u}^T(t_{k-1}) \left[\int_0^\tau \left(\int_0^t \mathrm{e}^{\boldsymbol{A}(t-s)}\boldsymbol{B}ds\right)^T \boldsymbol{Q}_c \left(\int_0^t \mathrm{e}^{\boldsymbol{A}(t-s)}\boldsymbol{B}ds\right) dt\right] \boldsymbol{u}(t_{k-1})+ \\
&\boldsymbol{u}^T(t_{k-1}) \left[\int_\tau^h \left(\int_0^\tau \mathrm{e}^{\boldsymbol{A}(t-s)}\boldsymbol{B}ds\right)^T \boldsymbol{Q}_c \left(\int_0^\tau \mathrm{e}^{\boldsymbol{A}(t-s)}\boldsymbol{B}ds\right) dt\right] \boldsymbol{u}(t_{k-1})+ \\
&\boldsymbol{u}^T(t_{k-1}) \left[\int_\tau^h \left(\int_0^\tau \mathrm{e}^{\boldsymbol{A}(t-s)}\boldsymbol{B}ds\right)^T \boldsymbol{Q}_c \left(\int_\tau^t \mathrm{e}^{\boldsymbol{A}(t-s)}\boldsymbol{B}ds\right) dt\right] \boldsymbol{u}(t_k)+ \\
&\boldsymbol{u}^T(t_k) \left[\int_\tau^h \left(\int_\tau^t \mathrm{e}^{\boldsymbol{A}(t-s)}\boldsymbol{B}ds\right)^T \boldsymbol{Q}_c \left(\int_0^\tau \mathrm{e}^{\boldsymbol{A}(t-s)}\boldsymbol{B}ds\right) dt\right] \boldsymbol{u}(t_{k-1})+
\end{aligned}
$$

$$\boldsymbol{u}^T(t_k)\left[\int_{\tau}^{h}\left(\int_{\tau}^{t}\mathrm{e}^{\boldsymbol{A}(t-s)}\boldsymbol{B}ds\right)^T\boldsymbol{Q}_c\left(\int_{\tau}^{t}\mathrm{e}^{\boldsymbol{A}(t-s)}\boldsymbol{B}ds\right)dt\right]\boldsymbol{u}(t_k)$$

$$\begin{aligned}I_5(k) =& \int_{t_k}^{t_{k+1}}\boldsymbol{u}^T(t-\tau)\boldsymbol{R}_c\boldsymbol{u}(t-\tau)dt \\ =& \int_{t_k}^{t_k+\tau}\boldsymbol{u}^T(t_{k-1})\boldsymbol{R}_c\boldsymbol{u}(t_{k-1})dt + \int_{t_k+\tau}^{h}\boldsymbol{u}^T(t_k)\boldsymbol{R}_c\boldsymbol{u}(t_k)dt \\ =& \boldsymbol{u}^T(t_{k-1})\left[\int_0^{\tau}\boldsymbol{R}_c dt\right]\boldsymbol{u}(t_{k-1}) + \boldsymbol{u}^T(t_k)\left[\int_{\tau}^{h}\boldsymbol{R}_c dt\right]\boldsymbol{u}(t_k).\end{aligned} \tag{A.8e}$$

Substituting the augmented state vector $\boldsymbol{z}(k)$ according to (2.2), the discretization of cost function 2.5 can be achieved.

A.3 Proofs of Lemma 3.1 and Lemma 3.2

A.3.1 Proof of Lemma 3.1

In order to prove Lemma 3.1 the following Lemma is introduced.

Lemma A.1 *Let* $\boldsymbol{\mu}, \boldsymbol{\mu}_1, \boldsymbol{\mu}_2, ..., \boldsymbol{\mu}_p \in \mathbb{R}^n$ *and* $\boldsymbol{\nu}, \boldsymbol{\nu}_1, \boldsymbol{\nu}_2, ..., \boldsymbol{\nu}_l \in \mathbb{R}^m$*. If* $\boldsymbol{\mu} \in co\{\boldsymbol{\mu}_i : i \in \{1, 2, ..., p\}\}$ *and* $\boldsymbol{\nu} \in co\{\boldsymbol{\nu}_j : j \in \{1, 2, ..., l\}\}$*, then*

$$\begin{pmatrix}\boldsymbol{\mu}\\ \boldsymbol{\nu}\end{pmatrix} \in co\left\{\begin{pmatrix}\boldsymbol{\mu}_i\\ \boldsymbol{\nu}_j\end{pmatrix} : i \in \{1, 2, ..., p\}, j \in \{1, 2, ..., l\}\right\}. \tag{A.9}$$

Proof. From $\boldsymbol{\mu} \in \mathrm{co}\{\boldsymbol{\mu}_i : i \in \{1, 2, ..., p\}\}$ and $\boldsymbol{\nu} \in \mathrm{co}\{\boldsymbol{\nu}_j : j \in \{1, 2, ..., l\}\}$, there exist scalers $\alpha_i \geq 0$ and $\beta_j \geq 0$, $i = 1, 2, ..., p$, $j = 1, 2, ..., l$ such that

$$\sum_{i=1}^{p}\alpha_i = \sum_{j=1}^{l}\beta_j = 1, \quad \boldsymbol{\mu} = \sum_{i=1}^{p}\alpha_i\boldsymbol{\mu}_i, \quad \boldsymbol{\nu} = \sum_{j=1}^{l}\beta_j\boldsymbol{\nu}_j.$$

Therefore,

$$\begin{aligned}\begin{pmatrix}\boldsymbol{\mu}\\ \boldsymbol{\nu}\end{pmatrix} &= \begin{pmatrix}\sum_{i=1}^{p}\alpha_i\boldsymbol{\mu}_i\\ \sum_{j=1}^{l}\beta_j\boldsymbol{\nu}_j\end{pmatrix} = \begin{pmatrix}\sum_{i=1}^{p}\alpha_i\boldsymbol{\mu}_i\left(\sum_{j=1}^{l}\beta_j\right)\\ \sum_{j=1}^{l}\beta_j\boldsymbol{\nu}_j\left(\sum_{i=1}^{p}\alpha_i\right)\end{pmatrix} \\ &= \begin{pmatrix}\sum_{i=1}^{p}\sum_{j=1}^{l}\alpha_i\beta_j\boldsymbol{\mu}_i\\ \sum_{i=1}^{p}\sum_{j=1}^{l}\alpha_i\beta_j\boldsymbol{\nu}_j\end{pmatrix} = \sum_{i=1}^{p}\sum_{j=1}^{l}\alpha_i\beta_j\begin{pmatrix}\boldsymbol{\mu}_i\\ \boldsymbol{\nu}_j\end{pmatrix}\end{aligned}$$

Noting that

$$\sum_{i=1}^{p}\sum_{j=1}^{l}\alpha_i\beta_j = 1.$$

The proof is completed. □

Since $\|\boldsymbol{\nu}\|_\infty \leq 1$ yields $|\boldsymbol{\nu}_j| \leq 1, \forall j \in \mathbb{J}$, we can obtain

$$\text{sat}(\boldsymbol{u}_j) \in \text{co}\left\{\boldsymbol{u}_j, \boldsymbol{\nu}_j\right\}, \forall j \in \mathbb{J}$$

By applying Lemma A.1 inductively, we can obtain

$$\begin{aligned}
&\text{sat}(\boldsymbol{u}_1) \in \text{co}\left\{\boldsymbol{u}_1, \boldsymbol{\nu}_1\right\}, \\
&\text{sat}\left(\begin{pmatrix}\boldsymbol{u}_1\\ \boldsymbol{u}_2\end{pmatrix}\right) \in \text{co}\left\{\begin{pmatrix}\boldsymbol{u}_1\\ \boldsymbol{u}_2\end{pmatrix}, \begin{pmatrix}\boldsymbol{u}_1\\ \boldsymbol{\nu}_2\end{pmatrix}, \begin{pmatrix}\boldsymbol{\nu}_1\\ \boldsymbol{u}_2\end{pmatrix}, \begin{pmatrix}\boldsymbol{\nu}_1\\ \boldsymbol{\nu}_2\end{pmatrix}\right\}, \\
&\text{sat}\left(\begin{pmatrix}\boldsymbol{u}_1\\ \boldsymbol{u}_2\\ \boldsymbol{u}_3\end{pmatrix}\right) \in \text{co}\left\{\begin{pmatrix}\boldsymbol{u}_1\\ \boldsymbol{u}_2\\ \boldsymbol{u}_3\end{pmatrix}, \begin{pmatrix}\boldsymbol{u}_1\\ \boldsymbol{u}_2\\ \boldsymbol{\nu}_3\end{pmatrix}, \begin{pmatrix}\boldsymbol{u}_1\\ \boldsymbol{\nu}_2\\ \boldsymbol{u}_3\end{pmatrix}, \begin{pmatrix}\boldsymbol{u}_1\\ \boldsymbol{\nu}_2\\ \boldsymbol{\nu}_3\end{pmatrix}, \begin{pmatrix}\boldsymbol{\nu}_1\\ \boldsymbol{u}_2\\ \boldsymbol{u}_3\end{pmatrix}, \begin{pmatrix}\boldsymbol{\nu}_1\\ \boldsymbol{u}_2\\ \boldsymbol{\nu}_3\end{pmatrix}, \begin{pmatrix}\boldsymbol{\nu}_1\\ \boldsymbol{\nu}_2\\ \boldsymbol{\nu}_3\end{pmatrix}\right\}, \\
&\quad\vdots
\end{aligned} \tag{A.10a}$$

and finally,

$$\text{sat}(\boldsymbol{u}) \in \text{co}\big\{\boldsymbol{D}_i\boldsymbol{u} + \boldsymbol{D}_i^-\boldsymbol{\nu} : i \in \mathbb{I}\big\}.$$

The proof completes here.

A.3.2 Proof of Lemma 3.2

Let us describe the polyhedron $\mathcal{L}(\boldsymbol{H})$ in a more general way by a set of linear inequlities:

$$\mathcal{L}(\boldsymbol{H}) := \big\{\boldsymbol{x} \in \mathbb{R}^n : \boldsymbol{a}_j\boldsymbol{x} \leq 1, j \in \{1, ..., 2m\}\big\}, \tag{A.11}$$

where $\boldsymbol{a}_j = \boldsymbol{h}_j$ and $\boldsymbol{a}_{m+j} = -\boldsymbol{h}_j$, $j \in \{1, ..., m\}$. And given a symmetric and positive definite matrix $\boldsymbol{P} \in \mathbb{R}^{n\times n}$, there always exists nonsingular square matrix $\boldsymbol{B} \in \mathbb{R}^{n\times n}$, such that $\boldsymbol{P} = \boldsymbol{B}^T\boldsymbol{B}$. Without loss of generality we can assume that $\boldsymbol{B}$ is symmetric and positive definite by taking $\boldsymbol{B} = \boldsymbol{P}^{1/2}$. Define a new vector variable $\boldsymbol{y} = \boldsymbol{B}\boldsymbol{x}$. Then ellipsoid $\mathcal{E}(\boldsymbol{P}, \rho)$ can be represented as

$$\mathcal{E}(\boldsymbol{P}, \rho) = \left\{\boldsymbol{y} \in \mathbb{R}^n : \|\boldsymbol{y}\|_2^2 \leq \rho\right\}. \tag{A.12}$$

Thus $\mathcal{E}(\boldsymbol{P}, \rho) \subset \mathcal{L}(\boldsymbol{H})$ can be interpreted as

$$\begin{aligned}
\sup_{\|\boldsymbol{y}\|_2^2\leq\rho} \boldsymbol{a}_j\boldsymbol{B}^{-1}\boldsymbol{y} \leq 1, j \in \{1, ..., m\} &\Leftrightarrow \rho\|\boldsymbol{B}^{-1}\boldsymbol{a}_j^T\|_2 \leq 1, j \in \{1, ..., 2m\} \\
&\Leftrightarrow 1 - \boldsymbol{a}_j\left(\boldsymbol{P}/\rho\right)^{-1}\boldsymbol{a}_j^T \geq 0, j \in \{1, ..., m\}
\end{aligned} \tag{A.13}$$

By using the Schur complement and substituting $\boldsymbol{a}_j = \boldsymbol{h}_j$, $j \in \{1, ..., m\}$ back we obtain

$$\begin{pmatrix} 1 & * \\ \boldsymbol{h}_j^T & \boldsymbol{P}/\rho \end{pmatrix} \geq 0, \quad j \in \mathbb{J}. \tag{A.14}$$

The proof completes here.

A.4 Discretization of The System With Disturbance Term

In order to obtain a sampled-data system with respect to a certain sampling period h from a continuous-time system, the following procedures can be employed, especially for the disturbance term. The continuous-time system model is given by

$$\dot{\boldsymbol{z}}(t) = \boldsymbol{A}_c \boldsymbol{z}(t) + \boldsymbol{B}_c \boldsymbol{u}(t) + \boldsymbol{D}_c \boldsymbol{w}(t) \tag{A.15}$$

where $\boldsymbol{z}(t) \in \mathbb{R}^n$ is the state vector, $\boldsymbol{A}_c \in \mathbb{R}^{n\times n}$ is the system matrix, $\boldsymbol{B}_c \in \mathbb{R}^{n\times m}$ is the input matrix, and $\boldsymbol{u}(t) \in \mathbb{R}^m$ is the control signal, $\boldsymbol{D}_c \in \mathbb{R}^{n\times l}$ is the disturbance input matrix, and $\boldsymbol{w}(t) \in \mathbb{R}^l$ is the disturbance signal. The sampled-data system can be written

$$\boldsymbol{z}(k+1) = \boldsymbol{A}\boldsymbol{z}(k) + \boldsymbol{B}\boldsymbol{u}(k) + \boldsymbol{w}^*(k) \tag{A.16}$$

with

$$\begin{aligned} \boldsymbol{A} &= e^{\boldsymbol{A}_c h}, \qquad \boldsymbol{B} = \int_0^h e^{\boldsymbol{A}_c s} ds \boldsymbol{B}_c \\ \boldsymbol{w}^*(k) &= \int_0^h e^{\boldsymbol{A}_c s} \boldsymbol{D}_c \boldsymbol{w}((k+1)h - s) ds. \end{aligned} \tag{A.17}$$

When $\boldsymbol{w}(t)$ is constant during the time interval $[kh, (k+1)h]$, (A.17) yields

$$\boldsymbol{w}^*(k) = \int_0^h e^{\boldsymbol{A}_c s} ds \boldsymbol{D}_c \boldsymbol{w}(kh) \tag{A.18}$$

Therefore (A.16) can be rewritten

$$\boldsymbol{z}(k+1) = \boldsymbol{A}\boldsymbol{z}(k) + \boldsymbol{B}\boldsymbol{u}(k) + \boldsymbol{D}\boldsymbol{w}(k). \tag{A.19}$$

with $\boldsymbol{D} = \bar{d} \int_0^h e^{\boldsymbol{A}_c s} ds \boldsymbol{D}_c$ if $\|\boldsymbol{w}(t)\| \leq \bar{d}$. It means that the assumption (4.2) can be fulfilled for the sampled-data system (A.19). However if $\boldsymbol{w}(t)$ is time varying, unknown and only assumed $\|\boldsymbol{w}(t)\|_2 \leq \bar{d}$, in order to obtain the upper bound of $\|\boldsymbol{w}^*(k)\|_2$ we can make

$$\begin{aligned}\|\boldsymbol{w}^*(k)\|_2 &= \|\int_0^h e^{\boldsymbol{A}_c s}\boldsymbol{D}_c\boldsymbol{w}((k+1)h-s)ds\|_2\\ &\le \int_0^h \|e^{\boldsymbol{A}_c s}\boldsymbol{D}_c\|_2\|\boldsymbol{w}((k+1)h-s)\|_2 ds\\ &\le \bar{d}\int_0^h \|e^{\boldsymbol{A}_c s}\boldsymbol{D}_c\|_2 ds\\ &\le \bar{d}\|\boldsymbol{D}_c\|_2\int_0^h \|e^{\boldsymbol{A}_c s}\|_2 ds \end{aligned} \tag{A.20}$$

Because there exists non-singular matrix $\boldsymbol{P}$ such that

$$e^{\boldsymbol{A}_c s} = \boldsymbol{P}^{-1}e^{\boldsymbol{J}t}\boldsymbol{P},$$

where matrix $\boldsymbol{J}$ is the Jordan canonical form of matrix $\boldsymbol{A}_c$. $\boldsymbol{J}$ can be written in the form involving $r+1$ block matrices $\boldsymbol{J}_k, (k=0,1,...,r)$ along the diagonal:

$$\boldsymbol{J} = \begin{pmatrix} \boldsymbol{J}_0 & \boldsymbol{0} & \cdots & \boldsymbol{0}\\ \boldsymbol{0} & \boldsymbol{J}_1 & \cdots & \boldsymbol{0}\\ \vdots & \vdots & \ddots & \vdots\\ \boldsymbol{0} & \boldsymbol{0} & \cdots & \boldsymbol{J}_r \end{pmatrix} \tag{A.21}$$

where $\boldsymbol{J}_k \in \mathbb{C}^{n_k\times n_k}$. Here $\boldsymbol{J}_0 = \mathrm{diag}(\lambda_0, \lambda_1, ..., \lambda_p)$ are eigenvalues (not necessarily distinct) belonging to one-dimensional eigenspaces. To each $k = 1, ..., r$, there corresponds an eigenvalue λ_{p+k} and a generalized eigenspace of dimension $n_k \ge 2$. The corresponding Jordan block can be written

$$\boldsymbol{J}_k = \lambda_{p+k}\boldsymbol{I}_{n_k} + \boldsymbol{Z}_{n_k}, \tag{A.22}$$

where $\boldsymbol{I}_m$ is the $m\times m$ identity matrix and $\boldsymbol{Z}_m$ is an $m\times m$ nilpotent matrix of the form

$$\boldsymbol{Z} = \begin{pmatrix} 0 & 1 & \cdots & 0\\ \vdots & \vdots & \ddots & \vdots\\ 0 & 0 & \cdots & 1\\ 0 & 0 & \cdots & 0 \end{pmatrix} \tag{A.23}$$

The matrix $\boldsymbol{Z}$ has the properties that $\boldsymbol{Z}^k = 0, k \ge m$ whereas $\boldsymbol{Z}^k \ne 0$ for $k = 1, 2, ..., m-1$. Hence

$$e^{\boldsymbol{J}t} = \begin{pmatrix} e^{\boldsymbol{J}_0 t} & \boldsymbol{0} & \cdots & \boldsymbol{0}\\ \boldsymbol{0} & e^{\boldsymbol{J}_1 t} & \cdots & \boldsymbol{0}\\ \vdots & \vdots & \ddots & \vdots\\ \boldsymbol{0} & \boldsymbol{0} & \cdots & e^{\boldsymbol{J}_r t} \end{pmatrix} \tag{A.24}$$

Among the entries,

$$e^{\boldsymbol{J}_0 t} = \mathrm{diag}(e^{\lambda_0}, e^{\lambda_1}, ..., e^{\lambda_p}) \tag{A.25}$$

and for $k \geq 1$

$$e^{\boldsymbol{J}_0 t} = e^{(\lambda_{p+k}\boldsymbol{I}_{n_k}+\boldsymbol{Z}_{n_k})t} = e^{\lambda_{p+k}t}e^{\boldsymbol{Z}_{n_k}t}. \tag{A.26}$$

Due to the property of nilpotent matrix, an easy calculation gives

$$e^{\boldsymbol{Z}_m t} = \begin{pmatrix} 1 & t & \cdots & t^{m-1}/(m-1)! \\ 0 & 1 & \cdots & t^{m-2}/(m-2)! \\ \vdots & \vdots & \ddots & \vdots \\ 0 & 0 & \cdots & 1 \end{pmatrix} \tag{A.27}$$

Thus we have

$$\|e^{\boldsymbol{A}_c t}\|_2 \leq \|\boldsymbol{P}^{-1}\|_2\|\boldsymbol{P}\|_2(1+t+\cdots+t^{m_M-1}/(m_M-1)!)e^{\lambda_M t}, \tag{A.28}$$

where m_M is the dimension of the largest generalized eigenspace for all Jordan blocks and λ_M is the biggest eigenvalue. The computation of the form

$$\int_0^h (t^m/(m-1)!)e^{\lambda_M t}dt, \quad m \in \mathbb{N} \tag{A.29}$$

can be easily solved by using advanced mathematics. Therefore (A.20) can be upper bounded by

$$\|\boldsymbol{w}^*(k)\|_2 \leq \bar{d}\|\boldsymbol{D}_c\|_2\bar{c} \tag{A.30}$$

with $\int_0^h \|e^{\boldsymbol{A}_c s}ds\|_2 \leq \bar{c}$. After the approximation of the upper bound of the norm of the disturbance term $\boldsymbol{w}^*(k)$ sampled-data system (A.16) then can be approximately expressed as the form

$$\boldsymbol{z}(k+1) = \boldsymbol{A}\boldsymbol{z}(k) + \boldsymbol{B}\boldsymbol{u}(k) + \boldsymbol{D}\boldsymbol{w}(k), \tag{A.31}$$

where $\boldsymbol{D} = \bar{d}\|\boldsymbol{D}_c\|_2\bar{c}\boldsymbol{I}$ and $\boldsymbol{w}(k)$ satisfies the assumption (4.2). The possible over-approximation could introduce more conservativeness in the design of controller.

A.5 Tracking A Constant Reference Signal

Consider the discrete-time system

$$\begin{aligned} \boldsymbol{z}(k+1) &= \boldsymbol{\Phi}\boldsymbol{z}(k) + \boldsymbol{\Gamma}\boldsymbol{u}(k), \\ \boldsymbol{y}(k) &= \boldsymbol{C}\boldsymbol{z}(k) \end{aligned} \tag{A.32}$$

where $\boldsymbol{z}(k) \in \mathbb{R}^n$ is the state vector, $\boldsymbol{\Phi} \in \mathbb{R}^{n\times n}$ is the system matrix, $\boldsymbol{\Gamma} \in \mathbb{R}^{n\times m}$ is the input matrix, $\boldsymbol{u}(k) \in \mathbb{R}^m$ is the control signal, $\boldsymbol{y}(k) \in \mathbb{R}^l$ is the output and $\boldsymbol{C} \in \mathbb{R}^{l\times n}$ is the output matrix. For tracking a reference signal, the reference signal can be introduced with the feedback state [FPEN02, pp. 525-526]. A common tracking structure is shown in Fig. A.1, where $\boldsymbol{z}_r$ and $\boldsymbol{u}_{ss}$ are the desired final values of the state and the control

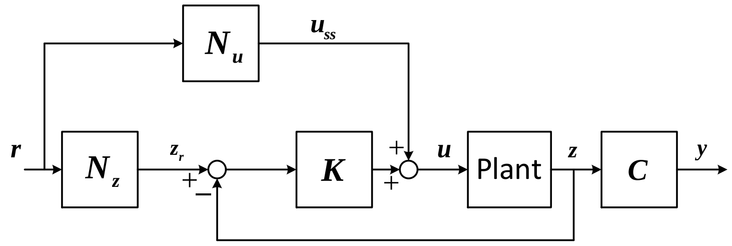

Figure A.1: Block diagram for introducing the reference input with full-state feedback

input, $\boldsymbol{N}_u$ is the matrix for the feed-forward signal to eliminate the steady-state errors, $\boldsymbol{N}_z$ is the matrix that transforms the reference signal r to a reference state and $\boldsymbol{K}$ is the state feedback gain. The matrices $\boldsymbol{N}_u$ and $\boldsymbol{N}_z$ are calculated by

$$\begin{pmatrix} \boldsymbol{N}_z \\ \boldsymbol{N}_u \end{pmatrix} = \begin{pmatrix} \boldsymbol{\Phi} - \boldsymbol{I} & \boldsymbol{\Gamma} \\ \boldsymbol{C} & \boldsymbol{0} \end{pmatrix}^{-1} \begin{pmatrix} \boldsymbol{0} \\ \boldsymbol{I} \end{pmatrix}. \tag{A.33}$$

For the DIC system (4.54) and (5.61) in the Section 4.4 and the Section 5.3 the matrix $\boldsymbol{N}_u$ is zero matrix. Matrix $\boldsymbol{N}_z = \begin{pmatrix} 1 & 0 \end{pmatrix}$ for system (4.54) in the Section 4.4 and Matrix $\boldsymbol{N}_z = \begin{pmatrix} 1 & 0 & 0 \end{pmatrix}$ for system (5.61) in the Section 5.3.

Bibliography

[ÅB99] K. J. Åström and B. Bernhardsson. Comparison of periodic and event based sampling for first order stochastic systems. In *Proceedings of 14th IFAC world conference*, 1999.

[ÅCES00] K. E. Årzén, A. Cervin, J. Eker, and L. Sha. An introduction to control and scheduing co-design. In *39th IEEE conference on decision and control*, 2000.

[AHT12] D. Antunes, W. P. M. H. Heemels, and P. Tabuada. Dynamic programming formulation of periodic event-triggered control: Performance guarantees and co-design. In *Proceedings of the 51st IEEE Conference on Decision and Control*, pages 7212–7217, 2012.

[Aly12] A. A. Aly. Car suspension control systems: basic principles. *International Journal of Control, Automation and Systems*, 1:41–46, 2012.

[Art06] Artemis. Tech rep, advanced research and technology for embedded intelligence and systems. Technical report, Strategic research agenda, 2006.

[Årz99] Karl-Erik Årzén. A simple event-based PID controller. In *Proceedings 14th World Congress of IFAC*, pages 423–428, 1999.

[Åst08] K. J. Åström. Event based control. In Alessandro Astolfi and Lorenzo Marconi, editors, *Analysis and Design of Nonlinear Control Systems: In Honor of Alberto Isidori*, pages 127–147. Springer, Berlin, 2008.

[ÅW90] K. J. Åström and B. Wittenmark. *Computer-Controlled Systems: Theory and Design*. Prentice-Hall, Englewood Cliffs, NJ, 2nd edition, 1990.

[BA07] J. Baillieul and P. J. Antsaklis. Control and communication challenges in networked real-time systems. *Proceedings of the IEEE*, 95:9–28, 2007.

[BC09] S. Bittanti and P. Colaneri. *Periodic Systems: Filtering and Control*. Springer, London, 2009.

[BCN91] S. Bittanti, P. Colaneri, and G. D. Nicolao. *The Riccati Equation, Communications and Control Engineering Series*, chapter 6, pages 127–162. Springer, Berlin, 1991.

[BD86] B. R. Barmish and C. L. DeMarco. A new method for improvement of robustness bounds for linear state equations. In *Proceedings of Conference on Information Sciences and Systems*, 1986.

[BGFB94] S. Boyd, L. E. Ghaoui, E. Feron, and V. Balakrishnan. *Linear Matrix Inequalities in System and Control Theory.* Philadelphia: SIAM, 1994.

[BGTT04] T. Butnaru, F. Gîrbacia, F. Tîrziu, and D. Talab. Mobile robot system controlled through mobile communications. *Product Engineering*, pages 433–442, 2004.

[Bla94] F. Blanchini. Ultimate boundedness control for uncertain discrete-time systems via set-induced lyapunov functions. *IEEE Transactions on Automatic Control*, 39:428–433, 1994.

[BLCA02] G. Buttazzo, G. Lipari, M. Caccamo, and L. Abeni. Elastic scheduling for flexible workload management. *IEEE transations on Computers*, 51:289–302, 2002.

[BM03] F. Blanchini and S. Miani. Stabilization of LPV systems: state feedback, state estimation, and duality. *SIAM Jounral of Control Optimization*, 42:76–97, 2003.

[BV04] S. Boyd and L. Vandenberghe. *Convex Optimization.* Cambridge University press, 2004.

[CA06] A. Cervin and P. Alriksson. Optimal on-line scheduling of multiple control tasks: A case study. In *Proceedings of the 18th Euromicro Conference on Real-Time Systems*, 2006.

[CEBÅ02] A. Cervin, J. Eker, B. Bernhardsson., and K. E. Årzén. Feedback-feedforward scheduling of control tasks. *Real-Time Systems*, 23:25–53, 2002.

[Cer03] A. Cervin. *Integrated control and real-time scheduling.* PhD thesis, Lund Institute of Technology, Sweden, 2003.

[CK03] Y. Choo and C. Kim. Periodic communication support in multiple access networks exploiting token with timer. *Information Networking Lecture Notes in Computer Science*, 2662:141–150, 2003.

[CKL06] D. M. Cuong, M. K. Kim, and H. C. Lee. Supporting hard real-time communication of periodic messages over switched ethernet. In *The 1st International Forum on Strategic Technology*, 2006.

[CMV+06] R. Castané, P. Martí., M. Velasco., A. Cervin., and D. Henriksson. Resource management for control tasks based on the transient ddynamic of closed-loop systems. In *18th Euromicro Conference Real-Time Systems*, 2006.

[Cog09] R. Cogill. Event-based control using quadratic approximate value functions. In *Proceedings of the 48th IEEE Conference on Decision and Control*, pages 5883–5888, 2009.

[CS11] J. Lunze C. Stöcker. Event-based control of nonlinear systems: An input-output linearization approach. In *Proceedings of the 50th IEEE Conference on Decision and Control and European Control Conference*, 2011.

[CTN07] D. Carnevale, A. Teel, and D. Nesic. A lyapunov proof of improved maximum allowable transfer interval for networked control systems. *IEEE Transactions on Automatic Control*, 52:892–897, 2007.

[CvdWHN09] M. B. G. Cloosterman, N. van de Wouw, W. P. M. H. Heemels, and H. Nijmeijer. Stability of networked control systems with uncertain time-varying delays. *IEEE Transactions on Automatic Control*, 54:1575–1580, 2009.

[CVMC11] A. Cervin, M. Velasco, P. Martí, and A. Camacho. Optimal online sampling period assignment: theory and experiments. *IEEE transactions on control systems technology*, 19:902–910, 2011.

[DB01] J. Daafouz and J. Bernussou. Stability analysis and control discrete-time systems with time varying parametric uncertainties. *System & Control Letters*, 43:355–359, 2001.

[DH12] M. C. F. Donkers and W. P. M. H. Heemels. Output-based event-triggered control with guaranteed l_∞-gain and improved and decentralised event-triggering. *IEEE Transactions on Automatic Control*, 57(6):1362–1376, 2012.

[DM09] S. Durand and N. Marchand. Further results on event-based PID controller. In *European Control Conference*, 2009.

[EDK10] A. Eqtami, D. V. Dimarogonas, and K. J. Kyriakopoulos. Event-triggered control for discrete-time systems. In *Proceedings of the 2010 American Control Conference*, pages 4719–4724, 2010.

[EDK11a] A. Eqtami, D. V. Dimarogonas, and K. J. Kyriakopoulos. Event-triggered strategies for decentralized model predictive controllers. In *Proceedings of the 18th IFAC World Congress*, 2011.

[EDK11b] A. Eqtami, D. V. Dimarogonas, and K. J. Kyriakopoulos. Novel event-triggered strategies for model predictive controllers. In *Proceedings of the 50th IEEE Conference on Decision and Control and European Control Conference*, 2011.

[EHÅ00] J. Eker, P. Hagander, and K. E. Årzén. A feedback scheduler for real-time control tasks. *Control Engineer Practice*, 8:1369–1378, 2000.

[FOSS12] A. Ferrara, A. N. Oleari, S. Sacone, and S. Siri. An event-triggered model predictive control scheme for freeway systems. In *Proceedings of the 51th IEEE Conference on Decision and Control*, 2012.

[FPEN02] G. F. Franklin, J. D. Powell, and A. Emami-Naeini. *Feedback control of dynamic systems*. Prentice hall, Upper Saddle River, NJ, 2002.

[Fra79] P. M. Frank. A continuous-time model for a PFM-controller. *IEEE Transactions on Automatic Control*, 25:782–784, 1979.

[Fri76] B. Friedland. Modeling systems for pulse-width modulated control. *IEEE Transactions on Automatic Control*, 21:739–746, 1976.

[Fuj08] H. Fujioka. Stability analysis for a class of networked/embedded control systems: A discrete-time approach. In *Proceedings of American Control Conference*, 2008.

[GA11] E. Garcia and P. J. Antsaklis. Model-based event-triggered control with time-varying network delays. In *Proceedings of the 50th IEEE Conference on Decision and Control and European Control Conference*, 2011.

[GAC96] P. Gahinet, P. Apkarian, and M. Chilaly. Affine parametric-dependent lyapunov functions and real parametric uncertainty. *IEEE Transactions on Automatic Control*, 41:436–442, 1996.

[GB08] M. Grant and S. Boyd. Graph implementations for nonsmooth convex programs. In *Recent Advances in Learning and Control*. Springer-Verlag Limited, 2008.

[GB13] M. Grant and S. Boyd. CVX: Matlab software for disciplined convex programming, version 2.0 beta. `http://cvxr.com/cvx`, sep, 2013.

[GCG93] F. Garofalo, G. Celentano, and L. Glielmo. Stability robustness of interval matrices via lyapunov quadratic forms. *IEEE Transactions on Automatic Control*, 38:281–284, 1993.

[GcH05] M. E. M. B. Gaid, A. Çela, and Y. Hamam. Optimal integrated control and scheduling of systems with communication constraints. In *44th IEEE Conference on Decision and Control and European Control Conference*, 2005.

[GcH09] M. E. M. B. Gaid, A. Çela, and Y. Hamam. Optimal real-time scheduling of control tasks with state feedback resource allocation. *IEEE Transactions on Control Systems Technology*, 17:309–326, 2009.

[GCK04] M. E. M. B. Gaid, A. Cela, and R. Kocik. Distributed control of a car suspension system. In *Eurosim 2004, COSI-ESEE*, 2004.

[GIL07] D. Görges, M. Izák, and S. Liu. Optimal control of systems with resource constraints. In *46th IEEE Conference on Decision and Control*, 2007.

[GJJW00] A. Garcia, L. Johansson, M. Jonsson, and M. Weckstén. Guaranteed periodic real-time communication over wormhole switched networks. In *Proceedings of ISCA 13th International Conference on Parallel and Distributed Computing Systems*, 2000.

[GOL09] R. Gielen, R. Olaru, and M. Lazar. On polytopic approximations of systems with time-varying input delays. *Nonlinear Model Predictive Control: Towards new challenging applications*, 384:225–233, 2009.

[Gör12] D. Görges. *Optimal Control of switched systems with application to networked embedded systems*. PhD thesis, University of Kaiserslautern, 2012.

[GSL+10] R. H. Gielen, S.Olaru, M. Lazar, W. P. M. H. Heemels, N. van de Wouw, and S. I. Niculescu. On polytopic inclusions as a modeling framework for systems with time-varying delays. *Automatica*, 46:615–619, 2010.

[HAPL04] D. Henrion, D. Arzelier, D. Peaucelle, and J. Lasserre. On parameter-dependent lyapunov functions for robust stability of linear systems. In *Proceedings of the 43rd IEEE Conference on Decision and Control*, 2004.

[HC05] D. Henriksson and A. Cervin. Optimal on-line sampling period assignment for real-time control tasks based on plant state information. In *44th IEEE Conference on Decision and Control and European Control Conference*, 2005.

[HC09] T. Henningsson and A. Cervin. Comparison of lti and event-based control for a moving cart with quantized position measurements. In *Proceedings of European Control Conference*, 2009.

[HDI06] L. Hetel, J. Daafouz, and C. Iung. Stabilization of arbitrary switched linear systems with unknown time-varying delays. *IEEE transactions on Automatic control*, 51:1668–1674, 2006.

[HDT13] W. P. M. H. Heemels, M. C. F. Donkers, and A. R. Teel. Periodic event-triggered control for linear systems. *IEEE Transactions on Automatic Control*, 58(4):847–861, 2013.

[HGvZ+99] W. P. M. H. Heemels, R. Gorter, A. van Ziji, P. van den Bosch, S. Weiland, W. Hendrix, and M. Vonder. Asynchronous measurement and control: a case study on motor synchronisation. *Control Engineer Practice*, 7:1467–1482, 1999.

[HJC08] T Henningsson, E. Johannesson, and A. Cervin. Sporadic event-based control of first-order linear stochastic systems. *Automatica*, 44:2890–2895, 2008.

[HLC02] T. Hu, Z. Lin, and B. M. Chen. Analysis and design for discrete-time linear systems subject to actuator saturation. *Systems & Control Letters*, 45:97–112, 2002.

[HSB08] W. P. M. H. Heemels, J. H. Sandee, and P. P. J. V. D. Bosch. Analysis of event-driven controllers for linear systems. *International Journal of Control*, 81:571–590, 2008.

[HWG+10] W. P. M. H. Heemels, N. Van De Wouw, R. Gielen, T. Donkers, L. Hetel, S. Olaru, M. Lazar, J. Daafouz, and S. Niculescu. A comparison of overapproximation methods for stability analysis of networked control systems. In *proceedings of the 13th International Conference on Hybrid Systems: Computation and Control*, 2010.

[IGL08] M. Izák, D. Görges, and S. Liu. Stability and control of systems with uncertain time-varying sampling period and time delay. In *Proceeding of the 17th IFAC Symposium on Automatic Control*, 2008.

[Joh99] M. Johansson. *Piecewise linear control systems*. PhD thesis, Lund Institute of Technology, 1999.

[KB06] E. Kofman and J. H. Braslavsky. Level crossing sampling in feedback stabilization under data-rate constraints. In *Proceedings of 45th IEEE Conference on Decision and Control*, 2006.

[Kha96] H. Khalil. *Nonlinear Systems*. Prentice-Hall, Upper Saddle River, NJ, 1996.

[KLJ12] G. A. Kiener, D. Lehmann, and K. H. Johansson. Actuator saturation and anti-windup compensation in event-triggered control. *Discrete Event Dynamic Systems: Theory and Applications*, 2012.

[KPK11] M. V. Khlebnikov, B. T. Polyak, and V. M. Kuntsevich. Optimization of linear systems subject to bounded exogenous disturbances: the invariant ellipsoid technique. *Automation and Remote Control*, 72:9–59, 2011.

[LÖ4] J. Löfberg. Yalmip : A toolbox for modeling and optimization in MATLAB. In *Proceedings of the 2004 IEEE International Symposium on Computer Aided Control Systems Design*, pages 284–289, 2004.

[LB02] B. Lincoln and B. Bernhardsson. Lqr optimization of linear system switching. *IEEE Transactions on Automatic Control*, 47:1701–1705, 2002.

[Lem10] M. Lemmon. Event-triggered feedback in control, estimation, and optimization. *Lecture Notes in Control and Information Sciences*, 406:293–358, 2010.

[LHJ13] D. Lehmann, E. Henriksson, and K. H. Johansson. Event-triggered model predictive control of discrete-time linear systems subject to disturbances. In *Proceedings of European Control Conference*, 2013.

[LJ12] D. Lehmann and K. H. Johansson. Event-triggered PI control subject to actuator saturation. In *IFAC Conference on Advances in PID Control*, 2012.

[LKJ12] D. Lehmann, G. A. Kiener, and K. H. Johansson. Event-triggered pi control: Saturating actuator and anti-windup compensation. In *Proceedings of the 51st IEEE Conference on Decision and Control*, 2012.

[LL10] J. Lunze and D. Lehmann. A state-feedback approach to event-based control. *Automatica*, 46(1):211–215, 2010.

[LL11a] D. Lehmann and J. Lunze. Event-based output-feedback control. In *Proceedings of 19th Mediterranean Conference on Control and Automation*, 2011.

[LL11b] D. Lehmann and J. Lunze. Extension and experimental evaluation of an event-based state-feedback approach. *Control Engineer Practice*, 19:101–112, 2011.

[LLOC12] F. Liu, C. Li, S. Ouyang, and L. Chen. Analysis and detection on long-time quasi-periodic communication behavior of network applications. *The Journal of China Universities of Posts and Telecommunications*, 19(Suppl. 2):80–85, 2012.

[LSCB00] X. Liu, L. Sha, M. Caccamo, and G. Buttazzo. Online control optimization using load driven scheduling. In *Proceedings of the 39th IEEE Conference on Decision and Control*, 2000.

[LX11] S. B. Li and B. G. Xu. Co-design of event generator and controller for event-triggered control system. In *Proceedings of the Chinese Control Conference*, pages 175–179, 2011.

[Mar03] H. J. Marquez. *Nonlinear Control Systems: Analysis and Design*. John Wiley & Sons, Hoboken, NJ, 2003.

[MAT10] M. Mazo, A. Anta, and P. Tabuada. An iss self-triggered implementations of linear controllers. *Automatica*, 46:1310–1314, 2010.

[MFFR02] P. Martí, J. Fuertes, G. Fohler, and K. Ramamritham. Improving quality-of-control using flexible timing constraint: Metric and scheduling issures. In *23rd IEEE Real-time systems symposium*, 2002.

[MH09] A. Molin and S. Hirche. On LQG joint optimal scheduling and control under communication constraints. In *Proceedings of the 48th IEEE Conference on Decision and Control held jointly with the 2009 28th Chinese Control Conference*, 2009.

[MH10] A. Molin and S. Hirche. Structural characterization of optimal event-based controllers for linear stochastic systems. In *Proceedings of the 49th*

IEEE Conference on Decision and Control, 2010.

[Mis06] M. Miskowicz. Send-on-delta concept: An event-based data-reporting strategy. *Sensors*, 6:49–63, 2006.

[MLB+09] P. Martí, C. Lin, S. A. Brandt, M. Velasco, and J. M. Fuertes. Draco: Efficient resource management for resource-constrained control tasks. *IEEE Transactions on Computer*, 58:90–105, 2009.

[MMDGC13] N. Marchand, J.J. Martinez, S. Durand, and J.F. Guerrero-Castellanos. Lyapunov event-triggered control: a new event strategy based on the control. In *9th IFAC Symposium on Nonlinear Control Systems*, 2013.

[Nai03] D. S. Naidu. *Optimal control systems.* CRC, 2003.

[NHT08] P. Naghshtabrizi, J. Hespanha, and A. Teel. Exponential stability of impulsive systems with application to uncertain sampled-data systems. *Systems & Control Letters*, 57:378–385, 2008.

[Nil98] J. Nilsson. *Real-Time Control Systems with Delays.* PhD thesis, Lund Institute of Technology, 1998.

[NR07] Ü. Nurges and E. Rüstern. Robust control via polytopic stability region approximations. In *Proceedings of Control & Automation*, 2007.

[NST96] S. R. Norsworthy, R. Schreier, and G. Temes. *Delta-sigma data converters.* IEEE Press, 1996.

[Obe05] R. Obermaisser. *Event-Triggered and Time-Triggered Control Paradigms.* Springer, 2005.

[OMT02] P. Otanez, J. Moyne, and D. Tilbury. Using deadbands to reduce communication in networked control systems. In *Proceedings of American Control Conference*, 2002.

[PANT11] R. Postoyan, A. Anta, D. Nesic, and P. Tabuada. A unifying lyapunov-based framework for the event-triggered control of nonlinear systems. In *Proceedings of the 50th IEEE Conference on Decision and Control and European Control Conference*, 2011.

[PNTN06] B. T. Polyak, A. V. Nazin, M. V. Topunov, and S. A. Nazin. Rejection of bounded disturbance via invariant ellipsoids technique. In *Proceedings of the 45th IEEE Conference on Decision and Control*, 2006.

[PPBSV05] L. Palopoli, C. Pinello, A. Bicchi, and A. Sangiovanni-Vincentelli. Maximizing the stability radius of a set of systems under real-time scheduling constraints. *IEEE Transactions on Automatic Control*, 50:1790–1795, 2005.

[PSA97] D. T. Peng, K. G. Shin, and T. F. Abdelzaher. Assignment and scheduling communicating periodic tasks in distributed real-time systems. *IEEE Transactions on Software Engineering*, 23:745–758, 1997.

[RJJ08] M. Rabi, K. H. Johansson, and M. Johansson. Optimal stopping for event-triggered sensing and actuation. In *Proceedings of the 47th IEEE Conference on Decision and Control*, 2008.

[RS00] H. Rehbinder and M. Sanfridson. Integration of off-line scheduling and optimal control. In *Proceeding of the 12th Euromicro Conference on Real-Time Systems,*, 2000.

[Sch99] C. W. Scherer. *Robust mixed control and LPV control with full block scalings*, chapter 10, pages 187–207. Springer-Verlag, 1999.

[SHHvdB07] J. Sandee, W. P. M. H. Heemels, S. Hulsenboom, and P. van den Bosch. Analysis and experimental validation of a sensor-based event-driven controller. In *Proceedings of American Control Conference*, 2007.

[SL91] J. E. Slotine and W. P. Li. *Applied Nonlinear Control*. Prentice hall, Englewood Cliffs, NJ, 1991.

[SLH10] J. Sijs, M. Lazar, and W. P. M. H. Heemels. On integration of event-based estimation and robust mpc in a feedback loop. In *Proceedings of the 13th ACM international conference on Hybrid systems: computation and control*, 2010.

[SLSS96] D. Seto, J. P. Lehoczky, L. Sha, and K. G. Shin. On task scheduability in real-time control systems. In *17th IEEE Real-Time Systems Symposium*, 1996.

[SP05] S. Skogestad and I. Postlethwaite. *Multivariable Feedback Control: Theory and Design*. Wiley, Chichester, 2005.

[SP11] A. Seuret and C. Prieur. Event-triggered sampling algorithms based on a lyapunov function. In *50th IEEE Conference on Decision and Control and European Control Conference*, 2011.

[SPTZ13] A. Seuret, C. Prieur, S. Tarbouriech, and L. Zaccarian. Event-triggered control with LQ optimality guarantees for saturated linear systems. In *9th IFAC Symposium on Nonlinear Control Systems*, 2013.

[Stu99] J. F. Sturm. Using SeDuMi 1.02, a MATLAB toolbox for optimization over symmetric cones (updated for version 1.3). *Optimization Methods and Software*, 11-12:625–653, 1999.

[Tab07] P. Tabuada. Event-triggered real-time scheduling of stabilizing control tasks. *IEEE Transactions on Automatic Control*, 52(4):1680–1685, 2007.

[Tsy84] Y. Z. Tsypkin. *Relay control systems*. Cambridge University press, 1984.

[TXB96] T. J. Tarn, N. Xi, and A. Bejezy. Path-based approach to integrated planning and control for robotic systems. *Automatica*, 32:1675–1687, 1996.

[vdWNCH10] N. van de Wouw, P. Naghshtabrizi, M. Cloosterman, and J. Hespanha. Tracking control for sampled-data systems with uncertain time-varying sampling intervals and delays. *International Journal of Robust and Nonlinear Control*, 20:387–411, 2010.

[VGH13] J. L. C. Verhaegh, T.M.P. Gommans, and W.P.M.H. Heemels. Extension and evaluation of model-based periodic event-triggered control. In *European Control Conference*, 2013.

[Vid02] M. Vidyasagar. *Nonlinear Systems Analysis*. Society for Industrial and Applied Mathematics (SIAM), Philadelphia, PA, 2nd edition, 2002.

[VK06] V. Vasyutynskyy and K. Kabitzsch. Implementation of pid controller with send-on-delta sampling. In *Proceedings of International Control Conference*, 2006.

[VMB09] M. Velasco, P. Martí, and E. Bini. On lyapunov sampling for event-driven controllers. In *Proceedings of the 48th IEEE Conference on Decision and Control held jointly with the 28th Chinese Control Conference*, 2009.

[WL08] X. Wang and M. Lemmon. Event design in event-triggered feedback control systems. In *Proceedings of the 47th IEEE Conference on Decision and Control*, 2008.

[WL09a] X. Wang and M. Lemmon. Self-triggered feedback control systems with finite-gain l_2 stability. *IEEE Transactions on Automatic Control*, 45:452–467, 2009.

[WL09b] X. Wang and M. D. Lemmon. Event-triggering in distributed networked systems with data dropouts and delays. *Hybrid Systems: Computation and Control Lecture Notes in Computer Science*, 5469(3):366–380, 2009.

[WL09c] W. Wu and S. Liu. An approach to reduce complexity in stability analysis for time-varying systems with polytopic uncertainties. In *IEEE Multiconference on Systems and Control*, 2009.

[WL11] X. Wang and M. D. Lemmon. Event-triggering in distributed networked control systems. *IEEE Transactions on Automatic Control*, 56:586–601, 2011.

Curriculum Vitae

Education

09/2004 – 12/2007	**Southern Yangtze University**
	Subject: Communication and control technology Specialization: Control theory and control engineering
	Degree: M. Sc.
	Thesis: The stability analysis of neural networks with delays (Excellent academic paper award)
09/2000 – 07/2004	**Nantong Institute of Technology**
	Specialization: Electrical engineering and automation
09/1997 – 07/2000	**Nanshi senior high school**
09/1994 – 07/1997	**Nanjing Lianyou Chang junior high school**
09/1988 – 07/1994	**Nanjing Lianyou Chang elementary school**

Professional Experience

03/2008 – 09/2014	**University of Kaiserslautern**
	Department of Electrical and Computer Engineering Institute of Control Systems